

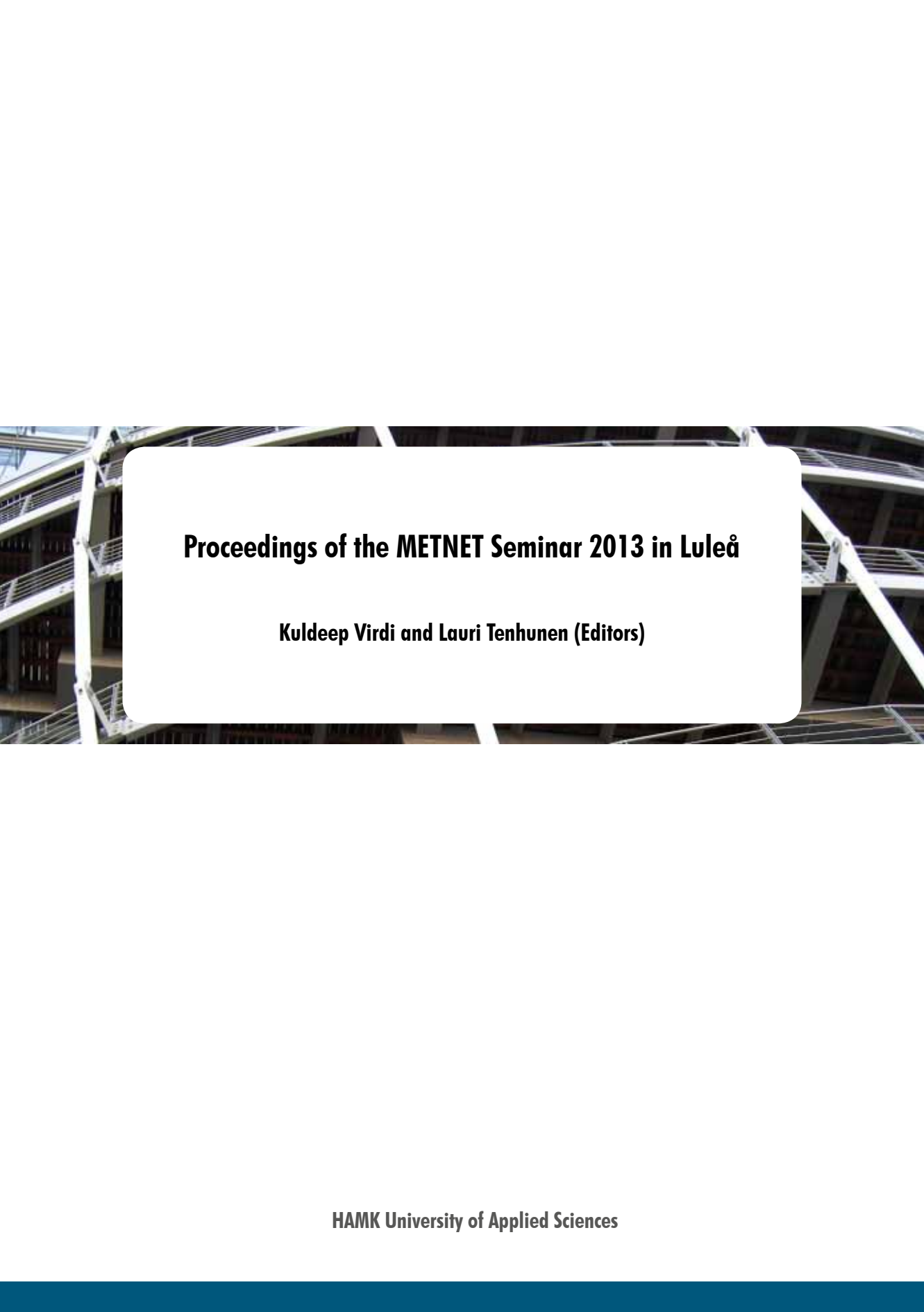
HAMK
UNIVERSITY OF APPLIED SCIENCES

Proceedings of the METNET Seminar 2013 in Luleå



Metnet Annual Seminar in Luleå, Sweden, on 22 – 23 October 2013

Kuldeep Viridi and Lauri Tenhunen (Editors)



Proceedings of the METNET Seminar 2013 in Luleå

Kuldeep Viridi and Lauri Tenhunen (Editors)

Editors:
Kuldeep Viridi, Aarhus University
Lauri Tenhunen, HAMK University of Applied Sciences

Proceedings of the METNET Seminar 2013 in Luleå

PRINTED

ISBN 978-951-784-641-7
ISSN 1795-4231
HAMKin julkaisuja 1/2014

ELECTRONIC

ISBN ISBN 978-951-784-642-4
ISSN 1795-424X
HAMKin e-julkaisuja 1/2014

© HAMK UAS and writers

PUBLISHER

HAMK University of Applied Sciences
PO Box 230
FI-13101 Hämeenlinna, FINLAND
tel. +358 3 6461
julkaisut@hamk.fi
www.hamk.fi/julkaisut

This publication has been produced in cooperation with ESF
partly funded EU project BOAT.

Hämeenlinna, January 2014



Index

PREFACE.....	6
CONNECTIONS AND MATERIALS.....	9
Michal Jandera and Lukas Ledecy <i>Czech Technical University in Prague</i> DESIGN OF LINER TRAY WITH DISTANCE SCREW CONNECTION IN THE NARROW FLANGE	10
Nikolay I. Vatin, Jarmo Havula, Lassi Martikainen, Alexey S. Sinelnikov, Anna V. Orlova and Stepan V. Salamakhin <i>Saint-Petersburg State Polytechnical University</i> <i>HAMK University of Applied Sciences</i> THIN-WALLED CROSS-SECTIONS AND THEIR JOINTS: TESTS AND FEM-MODELLING	13
Jukka Joutsenvaara <i>Kemi-Tornio University of Applied Sciences</i> FORMING LIMIT CURVE OF HIGH STRENGTH STEEL WITH THE HELP OF DIGITAL IMAGE CORRELATION	17
EXPERIMENTAL TECHNIQUES.....	33
Pavel Ryjáček and Miroslav Vokáč <i>Czech Technical University in Prague</i> MONITORING OF STEEL RAILWAY BRIDGE AND CONTINUOUS WELDED RAIL	34
P.A., Kuznetsov, O.V. Vasilyeva, I.V. Kudryavtseva and A.V. Tereschenko <i>FSUE CRISM "Prometey", Saint-Petersburg</i> LASER SYNTHESIS TECHNOLOGY FOR THE CREATION, RESTORATION AND REPAIR OF COMPLEX MACHINE PARTS	37
COMPUTATIONAL METHODS.....	43
Kristo Mela and Markku Heinisuo <i>Tampere University of Technology</i> WEIGHT AND COST OPTIMIZATION OF WELDED HIGH STRENGTH STEEL BEAMS	44

Teemu Tiainen, Kristo Mela, Timo Jokinen and Markku Heinisuo <i>Tampere University of Technology</i> HIGH STRENGTH STEEL IN TUBULAR TRUSSES.....	56
Markku Heinisuo and Timo Jokinen <i>Tampere University of Technology</i> TUBULAR COMPOSITE COLUMNS IN A NON-SYMMETRICAL FIRE	60
Michal Malendowski and Adam Glema <i>Poznan University of Technology</i> INFLUENCE OF NATURAL FIRE SCENARIO BY CFD AND FEM ANALYSIS COUPLING ONTO STEEL CONSTRUCTION STRUCTURAL RESPONSE	64
Alexander Tusnin and Olga Tusnina <i>Moscow State University of Civil Engineering</i> MEMBRANE STRUCTURES SUPPORTED BY A FRAME OF THIN-WALLED CLOSED SECTIONS.....	70
Olga Tusnina <i>Moscow State University of Civil Engineering</i> NUMERICAL STUDIES OF Z-PURLINS SUPPORTED BY SANDWICH PANELS	78
OPEN TOPICS	87
S.I. Matreninskiy, E.M. Chernyshov and V.Y. Mischenko <i>Voronezh State University of Architecture and Civil Engineering, Russia</i> PROBLEMS OF FUNCTIONING AND ELABORATION OF THE MASS HOUSING DEVELOPMENT AREAS OF THE CITIES AND SETTLEMENTS	88
Lauri Tenhunen and Arto Ranta-Eskola <i>HAMK University of Applied Sciences</i> <i>Rautaruukki Oyj</i> THE BLUE BOX AND THE TECHNOLOGICAL TRAJECTORIES IN CONTEXT OF UNIVERSITY-BUSINESS COOPERATION (UBC).....	100
Tarja Meristö and Jukka Laitinen <i>Laurea University of Applied Sciences</i> SUSTAINABILITY AS A BUSINESS OPPORTUNITY TODAY AND TOMORROW: TRIPLE HELIX PERSPECTIVE.....	111

Anatoly Perelmuter and Vitalina Yurchenko <i>Kyiv National University of Civil Engineering and Architecture</i> OPTIMIZATION OF STEEL TOWERS FOR LARGE WIND TURBINES	120
Olli Ilveskoski <i>HAMK University of Applied Sciences</i> STRUCTURAL BRACING – FORCES AND STIFFNESS.....	125
Hans-Albert Staedler <i>Alcoa Fastening Systems Industrial Products</i> INNOVATION IN MECHANICAL FASTENING TECHNOLOGY FOR MAINTENANCE-FREE JOINTS	143
Christine Heistermann, Anh Tuan Tran, Milan Veljkovic and Carlos Rebelo <i>Luleå University of Technology</i> <i>University of Coimbra</i> FLANGELESS CONNECTIONS IN STEEL TUBULAR WIND TOWERS	157

PREFACE

Some 40 universities, research institutes and enterprises have been cooperating from the year 2006 within Metnet network. They actively utilize their mutual connections, competitive strengths and the various cooperation possibilities. Metnet cooperation opens new options for universities and research organizations to customer- and needs-based product development, in collaboration with enterprises in construction and metal product industries in Europe. It makes it possible to foster innovative processes in partner organizations. Participating organizations learn from each other and exchange relevant pieces of information with target industries in Europe and beyond.

One of the outcomes of Metnet cooperation is the movement of researchers internationally from one organization to another. This clearly arises from the needs of increasing international presence of the metal industry. It also makes it possible for the mother organizations to broaden the scope of marketing and product development on larger geographical areas. Metnet partners help the transfer of qualified personnel to matching jobs where they can best utilize their abilities and to make the best use to their new working environment.

Metnet cooperation promotes regional innovation environments and strengthens their knowledge structures, especially in the involved European regions. Domestically, a participating partner organization represents its regional innovation environment but simultaneously is a partner of a larger and stronger international innovation world created by active cooperation between the institutes and enterprises.

The annual Metnet Seminar concentrates on presenting new research results in relevant scientific areas. In the Metnet Luleå Seminar, in October 2013, a new standard was brought about for the scientific and development papers. The presented papers covered a number of themes covering both experimental and numerical contributions.

The theme of computational mechanics included a paper on weight and cost optimisation of high strength steel beams. Another presentation was made on the optimisation of steel towers for large wind turbines. Experimental and computational results were the focus of a paper describing innovative flangeless connections for wind turbine towers. Two papers dealt with the fire limit state. In one paper, numerical results were presented on the increasingly important aspect of columns not exposed to fire on all four sides. As a step towards more realistic analysis of structures exposed to fire, a method was presented for the coupling of thermal response and the consequent mechanical response. Problems related to the use of new grades of steel such as S960 were discussed in another paper dealing with tubular trusses.

Thin walled sections were the topic of several papers. Finite Element analysis and test results were presented on thin walled cross-sections and their joints, on z-purlins, and on membrane structures supported by a frame of thin walled

boundary elements. One paper dealt with the influence of the spacing of screw connections on the design of liner trays.

Tests were described on the monitoring of a steel railway bridge, studying the influence of continuous welded rails, on the use of digital image correlation in formulating the stress-strain relationship for high strength steel, and on a technique for creating and repairing complex machine parts using 3-dimensional laser synthesis technology. Another presentation described recent developments on maintenance-free bolts.

METNET seminars deal with not only technical aspects of metal construction, but also issues of concern to industry on management, planning and sustainability of projects. Thus, one paper covered the topic of university and business co-operation and another on sustainability as a business opportunity.

Finally, a comprehensive technical note was presented on forces and stiffness issues relating to structural bracing.

Kuldeep Viridi

Lauri Tenhunen



CONNECTIONS AND MATERIALS

DESIGN OF LINER TRAY WITH DISTANCE SCREW CONNECTION IN THE NARROW FLANGE

Michal Jandera
Lukas Ledecny

Czech Technical University in Prague

The paper describes an experimental and numerical study on structural performance of cold-formed liner trays cladding system. In the described system, the outer sheeting is connected by distance screws to the narrow flanges of the liner tray profile. It allows additional thermal insulation between the liner tray and outer trapezoidal sheeting (see example on Figure 1). This is beneficial for the thermal insulation and acoustics performance of the system. As widely known and used in the current Eurocode (EN 1993-1-3 2006), when the narrow flange (restrained by the sheeting) is in compression, the resistance of the liner tray is influenced by the longitudinal spacing of fasteners supplying lateral restraint to the narrow flanges. In the design procedure described here, the length of the distance screw is also taken into account.

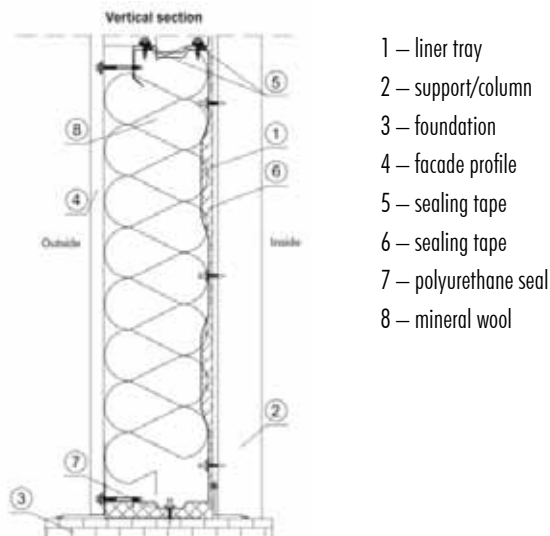


Figure 1. Liner tray wall system using distance screw.

Six bending tests of simply supported liner trays were carried out. For all of them, the narrow flange was in compression and distributed load was simulated by loads at four points of equal spacing. The width of the supports was designed so as not to affect the bending resistance. The liner tray profiles were 150 mm height and 600 mm width of the thickness 0.75, 0.88 and 1.0 mm. The screw provided 40 mm distance between the outer sheeting and the trays. Total depth of the system was then 190 mm. Spacing of the screws was 330 mm. Outer sheeting was made of 0.63 mm thick trapezoidal sheet. Failure occurred between the points of application of loads.

An FE model in software Abaqus was made, using GMNIA analysis. The model was validated using the experiment results. Despite some simplifications in the numerical model, the agreement was found to be very good. The resistance calculated by the model was, on average, about 2% lower with 4.8% standard deviation. The FE model failure mode was also found to correspond well with the test, as shown in Figure 2.

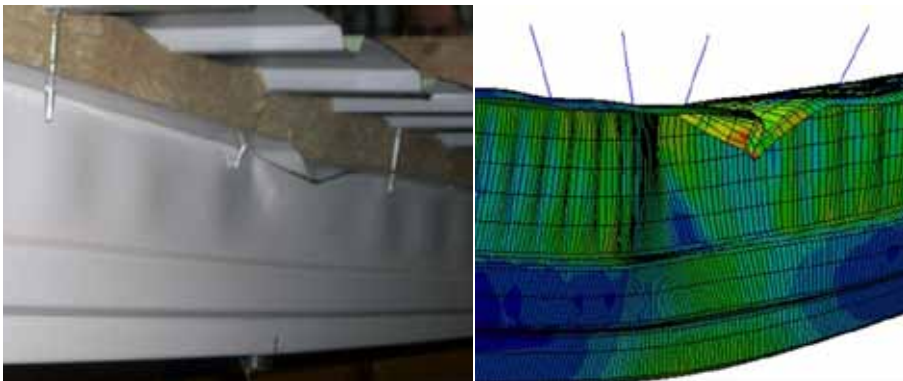


Figure 2. Failure mode of the test and FE model.

Later, based on the parametric study, a general design formula was developed. Material strength up to $f_y = 420$ MPa was considered. Liner tray profiles of height 100–150 mm and thickness 0.75–1.0 mm were used. The length of the distance screw (the gap between the liner tray and the outer sheeting itself) was considered as 0, 20, 40 and 60 mm. These parameters therefore set the limits of the proposed formula.

Variation in the spacing between the screws along the liner tray was also considered. The spacing was assumed between 165 mm (screw in each rib of the outer sheeting) and 660 mm. The influence of the spacing was retained as given by Eurocode (EN 1993-1-3 2006) by the correlation factor β_b . The design formula was finally obtained as follows:

$$M_{b,Rk} = \beta_p \frac{1.25}{h^{0.15}} M_{0,Rk} \quad (1)$$

where β_b is correlation factor:

$$\beta_p = 1.0 \text{ for } s_1 \leq 300 \text{ mm or}$$

$$\beta_p = 1.15 - \frac{s_1}{2000} \text{ for } 300 \text{ mm} < s_1 \leq 1000 \text{ mm, } s_1 \text{ is the screw spacing along the liner tray profile.}$$

The formula was designed to be safe in all cases. For the liner tray of 0.75 mm thickness Equation 1 under-predicts the resistance by approx. 5% on average. For liner trays of greater thickness, lower height, or lower yield strength than 420 MPa, the formula is even more conservative.

ACKNOWLEDGMENTS

The technical and financial support of RUUKKI CZ, namely Dan Marha and Jan Samec is gratefully acknowledged.

REFERENCES

EN 1993-1-3, 2006. Design of steel structures – Part 1–3: General rules – Supplementary rules for cold-formed members and sheeting. Brussels: CEN.

THIN-WALLED CROSS-SECTIONS AND THEIR JOINTS: TESTS AND FEM-MODELLING

Nikolay I. Vatin

Saint-Petersburg State Polytechnical University, vatin@mail.ru

Jarmo Havula

HAMK University of Applied Sciences, jarmo.havula@hamk.fi

Lassi Martikainen

HAMK University of Applied Sciences, lassi.martikainen@hamk.fi

Alexey S. Sinelnikov

Saint-Petersburg State Polytechnical University, alexey_sinelnikov@mail.ru

Anna V. Orlova

Saint-Petersburg State Polytechnical University, a_v_orlova@mail.ru

Stepan V. Salamakhin

Saint-Petersburg State Polytechnical University, ssalamakhin@gmail.com

This summary report describes the experimental and numerical research on a thin-walled cross-section's compression resistance and the shear strength of their joints. This work is continuation of an earlier paper (Vatin and Sinelnikov 2013). Current situation in the Russian market concerning the usage of cold-formed thin-walled cross-sections is aimed at starting up stipulation of such elements in the building industry.

In this area a number of Doctoral theses have been defended during recent years in Russia (Tusnin 2009, Belyy 1983, Astahov 2006). Theoretical research and laboratory tests were done only for specific types of thin-walled cross-sections. Jyrki Kesti contributed significantly to the development of local and distortional buckling of perforated steel wall studs. Today thin-walled cold-formed steel structures have a good presence in the Finnish building industry.

Steel galvanized C- and U-profiles and thermo-profiles are types of thin-walled cross-sections which are normally used in small house construction. Thermo-profiles have slots in webs that decrease the thermal flow through the web, but have a negative effect on the strength of the profiles.

Reticular-stretched thermo-profile, a new type of thin-walled cross-section, is the subject of research on reticular-stretched thermo-profiles and their joints. The following profiles are discussed:

1. Specimen S1 (stud) – АИ TCc 200-45-2,0;
2. Specimen S2 (rack) – АИ ПН 200-50-2,0.

Steel used for specimen production has the following parameters:

1. Steel grade S350GD (yield strength not less than 350 H/mm²);
2. Coating mass, 350 g/m²;
3. Coating thickness, 25 microns.

The research goal was to form the theoretical rationale for usage of the reticular-stretched thermo-profile including buckling and shear strength analysis based on the laboratory tests.

Tests were carried out in the Sheet Metal Centre at HAMK, using contemporary laboratory stand (Instron 3250).

First stage included preparation of specimen. Support blocks were placed inside the profile at the ends. The specimen was placed in vertical position in the test rig using level board (Stayer Standard 3460-150_z01).

Different boundary conditions were used for the two ends of the specimen. Three specimens had the following boundary conditions. Upper end of the specimen had a hinged support: the load of a hydraulic cylinder was applied through hinged block and then a thick steel plate was attached to the upper end of the specimen. Lower end of the specimen stood on the floor and was semi-rigid in nature.

Specimen S3 had hinged boundary conditions for both end of the specimen. Upper end of the specimen was like for other specimen described above. Lower end of the specimen had hinged support.

The specimen was compressed under various loads and deformations were recorded. To obtain the buckling force a load-deformation diagram was plotted and analyzed. From the load-deformation diagram it was determined that buckling failure was achieved at approximately 54 kN. The buckling mode was one half wave of the sinusoid. Some short downfall of the applied load was observed, demonstrating that first local buckling of the web takes place and then sudden overall buckling of the profile takes place.

The load-deformation pattern for self-drilling screws joint shows shear behavior through the following stages: First, all the clearances are closed; Second stage demonstrates elasto-plastic strain; Third stage is noted by the yield, strengthening, bearing failure of the sheet and achievement of the ultimate strength; and the Fourth stage – crushing of the joint. At the higher load level the end of the stud contacts the rack profile placed on a rigid base. The ultimate strength achieved was a force equal to 93 kN.

Numerical modeling of thin-walled cross-sections and their stud-to-rack joint was done with contemporary analysis software (SCAD Office and Lira)

using finite element method (FEM). FEM-models parameters were the same as for the tests described above. During the modeling process the thin-walled profile based on shell- and bar-elements and joint based on solid-elements were created and buckling/shear analysis tasks showed good results.

Point load (80kN) was applied to the flexural center (FC) and points nearby it to justify different type of profile deformation. It was shown that when the load point is situated before FC (6.0, 9.0 mm from the outside surface of the web) thin-walled profile bends inside itself. The differences between test and FEM-modelling results are equal to 0.33 and 3.75% accordingly.

When the load point is situated after FC (11.5 mm from the outside surface of the web). In this case the thin-walled profile bends outwards, which was different from the test result. The difference between test and FEM-modelling results is greater at 6.03%.

As for screw connection it was decided to model it using two-node FE with unilateral elastic constraint between nodes. Point load was applied to the flexural center (FC) step by step (5.0, 10.0, 15.0, 20.0, 25.0, 30.0 kN). Real bearing failure of the screw connection takes place due to crushing of the element material under a load of 25 kN. The FEM-model showed that the main stress of steel nearby connection place was approaching 335 MPa (more than the yield strength of the steel, accordingly to Table 3.1b Eurocode 3 Part 1–3). This is followed by large plastic deformations and round-form screw hole changes to oviform.

Results of experimental investigation into the behavior of thin-walled cross-sections by compression (buckling analysis) and shear strength of their joints have been reported. For both tests numerical analysis was carried out including bar/shell finite elements for compression and solid finite elements for shear strength analysis.

Compression bar buckling has resulted in the axial failure of profile specimens S3 at a buckling force 53.82 kN. Results of numerical analysis (shell finite elements) differ from compression tests by about 4%. When bar finite element are used, the results differed from the tests by about 22%. The analysis clearly demonstrated that existing Russian design guidelines for thin-walled cross-section modeling by bar finite elements is not exact and could be used only by taking into account an extra safety factor of 1.2.

Actual bearing failure the screw connection takes place due to crushing of the element material. Results of numerical analysis (solid finite elements) differ from shear strength tests by only about 2%.

The experimental work was commented upon by Arto Ranta-Eskola, Director of Research, Rautaruukki Oyj (Finland).

REFERENCES

Astakhov, I. V (2006). Prostranstvennaia ustoichivost' elementov konstruksii iz kholodnogutykh profilei, Dissertation, St.-Petersburg, 123 p.

Belyi, G. I (1983). Raschet uprugoplasticheskikh tonkostennykh sterzhnei poprostranstvenno-deformiruemoi scheme, Stroitel'naia mekhanika sooruzhenii: Mezhvuz. temat. sb. tr, LISI. №42, pp. 40–48.

Kesti, J (2000). Local and distortional buckling of perforated steel wall studs, Dissertation for the degree of Doctor of Science in Technology, Espoo, 101p. + app.19p

Tusnin, A. R (2009). Chislennyi raschet konstruksii iz tonkostennykh sterzhnei otkrytogo profilja, Moscow: Izd-vo ASV, 143 p.

Vatin, N.I. and Sinelnikov, A.S (2013). Strength and Durability of Thin-Walled Cross-Sections, Design, Fabrication and Economy of Metal Structures. International Conference Proceedings, 2013, Miskolc, Hungary, April 24–26, Miskolc, pp. 165–170

FORMING LIMIT CURVE OF HIGH STRENGTH STEEL WITH THE HELP OF DIGITAL IMAGE CORRELATION

Jukka Joutsenvaara

Kemi-Tornio University of Applied Sciences, Technology RDI Department,
Kemi 94600, Finland

ABSTRACT

Requirements for modern forming operations require in-depth knowledge of material behaviour in various stress-strain stages. Conventional method of evaluating material properties is the well documented and standardized uni-axial tensile test. The tensile test provides an easy way of comparing different materials. However, the test normally does not include data after the uniform elongation. The strain state after the uniform elongation transforms into diffuse necking and after that to a localized necking. In order to add more usability of acquired data it is often necessary to test material in various strain states even up to onset of localized necking. This is due the notion that most of the forming processes induce thinning to the part. The accuracy of estimations of thinning plays an important role in forming process design phase, e.g. in feasibility study. One way of acquiring such data is to define forming limit diagram (FLD) for the material. The forming limit diagram is constructed based on forming limit curve (FLC). The tests described here were made according to the current standard SFS-EN ISO 12004-2 with Erichsen Universal Sheet Metal Testing Machine, model 145-60. In conjunction, the GOM ARAMIS digital image correlation (DIC) system was used to measure the strain field over the whole visible area of the specimen during the test procedure. The tested steel sheet material for the following study was thermo-mechanically hot rolled, cold formable, structural steel with the minimum yield strength of 650 N/mm^2 and 3 mm in thickness. In addition to standardized test results, the strain rate in the A-geometry is observed in the presented paper for evaluation purposes. The usability of A-geometry strain data for a bulge stress analysis is also evaluated. The stress strain curves obtained from these various tests are then compared. Secondly, the strain rate of a standard tensile test specimen is compared with the strain rate of the FLC E-geometry specimen in major strain direction. This data is gathered for future use in research of the effect on results based on strain rates of different tests.

INTRODUCTION

Higher strengths of materials usually means lower formability. With modern steels it is possible to increase the formability by alloying or by novel production methods. The use of high strength steels instead of regular mild steels in construction and end products is one possibility to decrease the carbon foot print. The design and usage guidelines from the manufactures offer valuable information on how the material's potential is best utilized in a safe manner.

Complex forming problems, as typically found in automotive industry as well as in various other end products, require more detailed information of material behaviour during the forming process. Advanced forming methods, such as deep drawing or hydroforming, are processes that require more information than a standard tensile test can provide. A series of tests is made with variable geometry to better represent different strain stages that a material could exhibit during a forming process. The FLC specimen goes through the same elongation phases as in normal tensile test specimen, but with slightly different strains depending upon the biaxiality of the test and on the specimen geometry. In an FLC test the specimen is pushed out of plane by a spherical punch and the edges of the specimen are restrained by sheet holder. The specimen experiences elongation as well as displacement from its original position during the test due to the test set-up. After the uniform elongation is reached, diffuse necking can be clearly seen especially on narrower specimens as with the tensile test specimens. The diffuse necking in full round specimens are seen as a band of increased elongation around the dome at certain distance from assumed centre point.

As the forming process progresses the correct evaluation of thinning plays an important role. The thinning of the material determines the usability of the end product. For test purposes, the thinning in narrowest FLC specimen is similar to that in regular tensile test specimen. The difference in strain behaviour and evolution grows when testing wider specimens and eventually fully round specimen, namely A-geometry of the FLC specimens.

The forming limit is primarily material specific but also thickness of the specimen affects the position of the forming limit curve. Also, the conventional tensile test is widely used for comparison purposes, although the more in-depth analysis requires additional equipment and software, for instance, Digital image correlation (DIC) with automated strain analysis. Numerous studies have been made in recent years about the different formability tests in order to improve material models for the computational evaluation of forming processes. (Ghadbeigia et al. 2010, Kim et al. 2005)

In this study the formability of Class 650 high strength steel was investigated. The forming limit curve tests were carried out with Erichsen Universal Sheet Metal Testing Machine, model 145-60 according to SFS-EN ISO 12004-2 which is based on the Nakajima test set-up. The maximum sheet holder and drawing force of the test machine are 600 kN. Digital image correlation equipment was used for measurement and evaluation of surface strains on the specimens during the test. A continuous image acquisition during the test was needed for complete analysis, from start to failure of the specimen. From the selected specimens of the FLC test series additional analyses were made and the results were recorded. The strain evolution in different specimen geometries was also investigated in the major axis direction.

EXPERIMENTS

Material and Specimen Specifications

The tested material is single-phase carbon steel with minimum yield strength of 650 N/mm^2 . Adequate forming properties of the material are achieved by controlling the grain size during the manufacturing process. The controlled thermo-mechanical hot rolling process is also a key factor when determining the strength properties of the final product. Typically the rolling process is done below the re-crystallization temperature of that alloy in question. The use of this steel class, instead of regular constructional steel, could provide cost savings in materials for various constructions (Vierelä 2012).

The specimen geometries for determining the forming limit curve are shown in Figure 1. The dimensions are selected as appropriate for the Erichsen test machine. The specimens were cut from the sheets with laser. The rolling direction in the specimens is also determined by the used standard and it is visible in Figure 1. The test preparation phase of the specimens includes thorough cleaning of the surface with ethanol. The test area is then sprayed with an even coat of matt white finishing and on top of that a stochastic spray pattern is made with black paint. The analyser software requires the high-contrast stochastic pattern on the investigated surface.

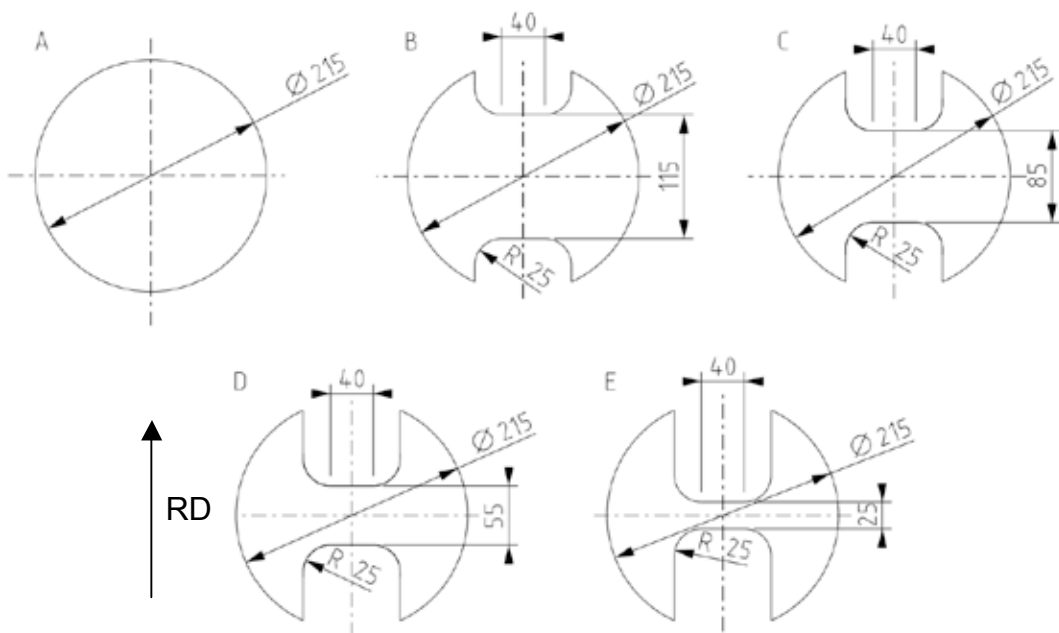
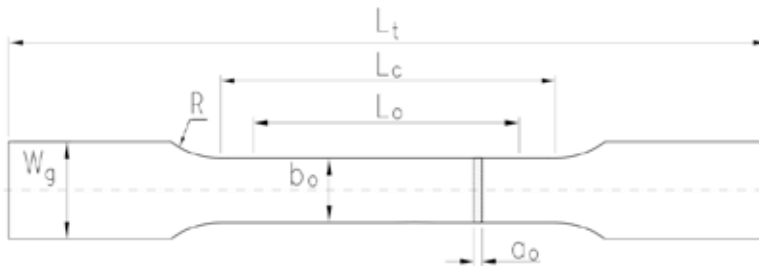


Figure 1. The FLC-specimen geometries with dimensioning.

In the other part of the test series, standard-sized tensile test specimens were used. The test series are partly based on the previous work of the author, so the tested material was high strength, single-phase, Class 650 steel with nominal thickness of 3 mm. The actual dimensions for the specimens are shown in Figure 2.



Specimen dimensioning

- a_0 —Thickness of specimen 3.04 mm
- b_0 —Width of gauge length 12.5 mm
- L_t —Total length of specimen 285 mm
- L_0 —Gauge length 80 mm
- L_c —Length of straight part 120 mm
- R —Radius of Fillet 37 mm
- W_g —Specimen width 30 mm

Figure 2. Dimensions of the tensile test specimen.

As with the previous tensile tests, the specimens had an extra thinning of 0.05 mm in the middle of the gauge length on both sides. The extra thinning was used in order to steer the deformation to the middle of the specimen during the tensile test. The predetermined location of maximum thinning helps the set-up phase of the optical measurement equipment for the test. The specimen preparation for the tensile test is the same as with FLC-specimens.

Use of digital image correlation as a tool for more in-depth research has been validated in numerous publications. Especially in formability evaluations, such as described here, Nakajima-test and others, computerization provides a substantial improvement on accuracy and on work load compared with, for instance, a manual measurement of strain field on a specimen. With the ARAMIS system, a stochastic pattern is used but in other commercial solutions prefabricated grids, namely square or circle, are used for strain analysis. (Banabic et al. 2010, Cordero et al. 2005, Yang et al. 2010)

Forming limit curve test

During the test, the specimen is punched out-of-plane with a spherical punch while the edges are locked with sheet holder. Drawbeads in the tooling can also be used to enhance the locking of the edges of the specimen. The tests were done at room temperature. Based on the standard, a single punch speed was used, namely 90 mm/min, or 1.5 mm/s, during the test. In order to accurately capture the ultimate or fracture strain on the specimen, a fast frequency of image taking is required. The standard suggests a minimum of 10 Hz image capture at the time of failure. Due to the memory limits of the DIC computer, the beginning of the test was recorded with lower frequency, namely 1.5 Hz. By minimizing the number of images, the processing time is also minimized. A schematic view of the set-up is shown in Figure 3.

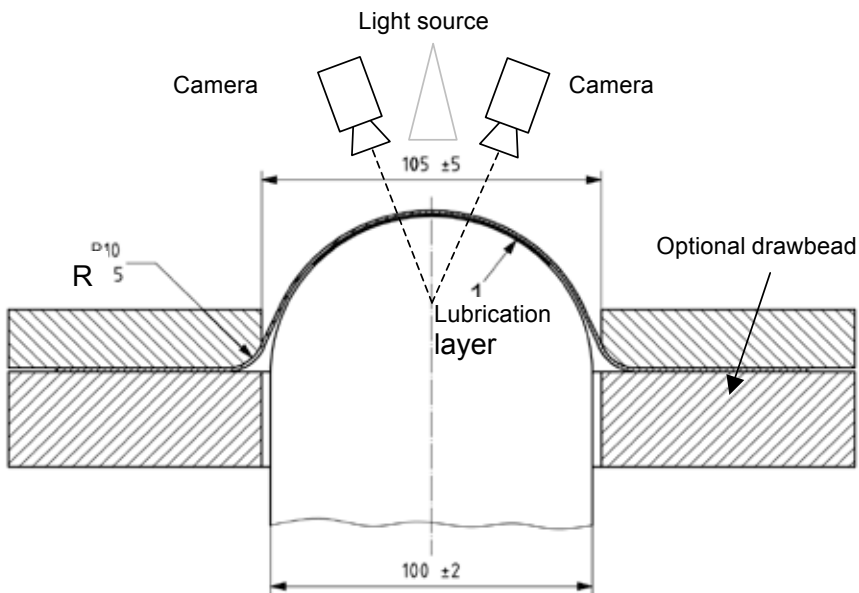


Figure 3. Schematic view of the FLC test set-up.

The ARAMIS camera system with 65 mm focal length lenses was used to capture the surface strains. The selected lenses were used due to the dimensions of the test crevice. The lighting for the test set-up was provided by a projector placed between the two cameras. The post-processing, i.e. strain analysis, of the images was done with the 3-D Analysis software ARAMIS from Gom gmbh (Germany). An actual test set-up is shown in Figure 4.



Figure 4. The test equipment.

Tensile Tests and Strain Measurements

A different test set-up of DIC equipment is required for the tensile test due to the proximity of the specimen. A 23 mm focal length lens with polarized filters and light sources were used for the test. The ARAMIS system was connected with the Zwick Roell 250 kN tensile test machine through I/O ports in order to get synchronised data from the load cell and extensometer during the test. The test speeds were matched with the strain rate from the FLC-test E-geometry. The equipment for tensile test is shown in Figure 5.

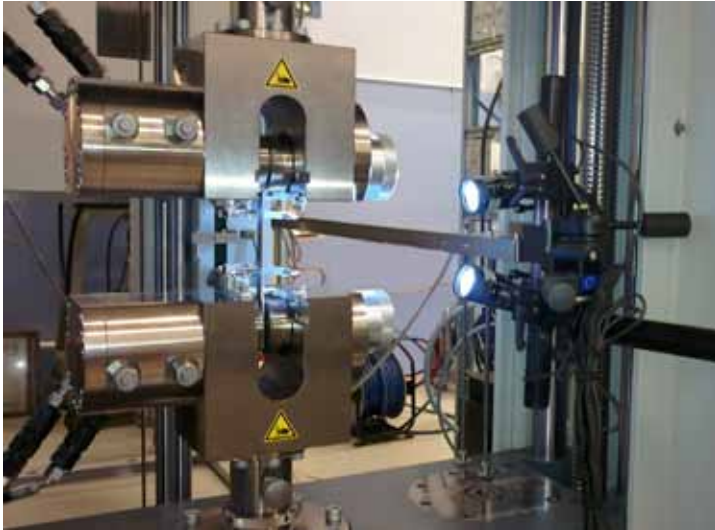


Figure 5. Set-up for the tensile test.

Images were recorded at two frequencies, namely 1.5 Hz and 10 Hz as with FLC-specimens. The resolution of images for the analysis was 2448×2048 pixels. The post-processing of the captured images was done with a 3-D Analysis software ARAMIS from GOM gmbh (Germany). After post-processing, the displacements and strain information of the whole visible surface of the specimen is acquired. The accuracy or level of detail, of the measurements depends also on the selected measuring volume which in turn is defined by the proper selection of lenses and their aperture values. (GOM gmbh 2008)

In the ARAMIS software, the same facet size was used for the both of the measurements. The facet size, i.e. the smallest software generated local extensometer, is also one of the factors that affect the scale of the results. The smaller facets provide more detailed information but also require more computational time in the main computer.

The DIC measurements have been widely used in various studies and research. Advances in photogrammetry equipment have also improved the quality of the data acquired from these measurements. The measurement procedure with non-contacting optical method provides faster testing with continuous, high resolution data. For instance, the scope of usage can be seen in various publications and conference proceedings. (Proulx 2013, Banabic 2010)

RESULTS

Curves from FLC-tests

The Forming Limit Diagram (FLD) is constructed based on the forming limit curve and corresponding strains in the two principal axes. The FLD describes

the material properties and behaviour in strain inducing forming processes. The acquired FLD is shown in Figure 6.

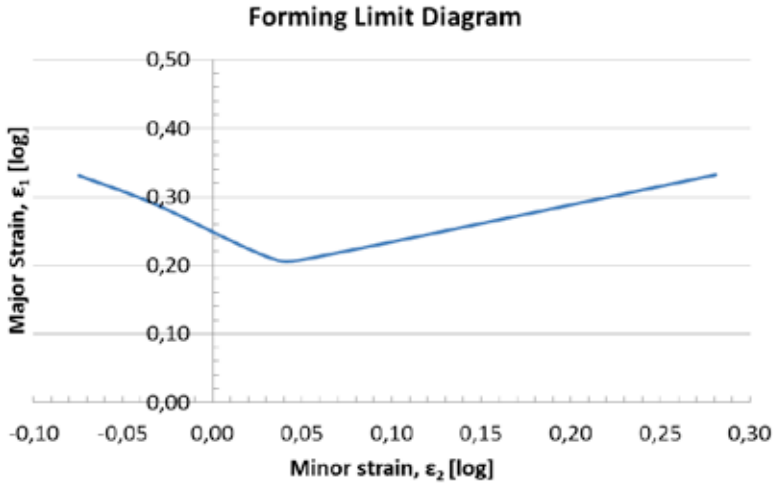


Figure 6. The Forming Limit Diagram of tested material.

Surface Strains and Strain Evolution in FLC-tests

With full-field optical analysis, it is possible to acquire surface strains of the visible surface. From that image sequence various data could be constructed depending on the research topic. The surface strains tell how the material behaves in particular forming process. For successive forming process, it is important to know the limits for safe and unsafe strain combinations in principal directions. When the strains supersede the forming limit curve, various failures are expected, for instance, wrinkling, excessive thinning, shearing. In Figures 7 and 8 can be clearly seen the evolution of surface strains.

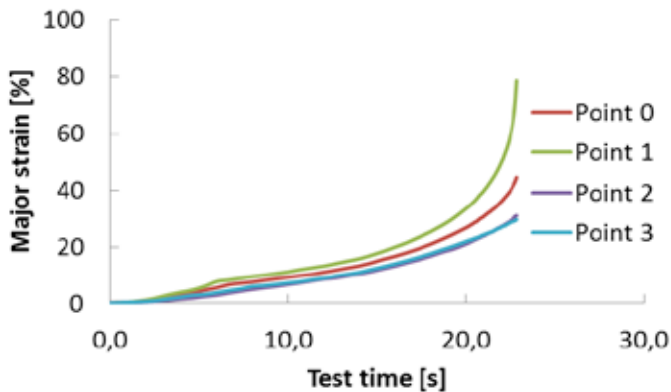


Figure 7. The major strain evolution of selected points on specimen surface.

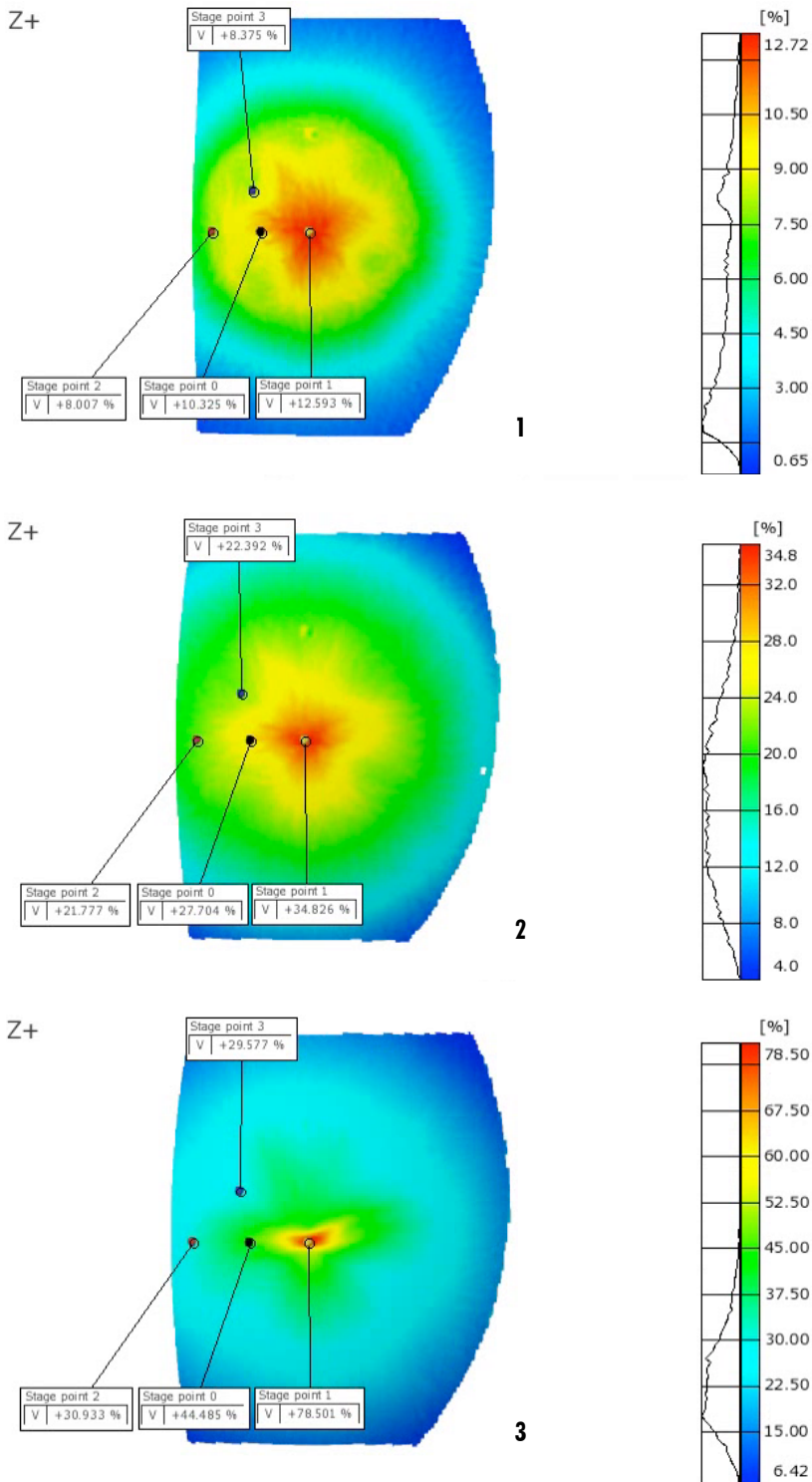


Figure 8. The surface strains of A-geometry specimen during the test.

The strain rate information is also easily acquired due to the combination of image acquisition and analysis equipment and software. In Figure 9 are shown the strain rates of selected points on the specimen surface during the test. As with any tests that evaluate the forming limits, the end of the test shows sharp changes in strain rate. This is closely related to the onset of the diffusion and local necking of the material. In the Figure 10 are shown few images of the analysed surface during the test overlaid with the strain rate information.

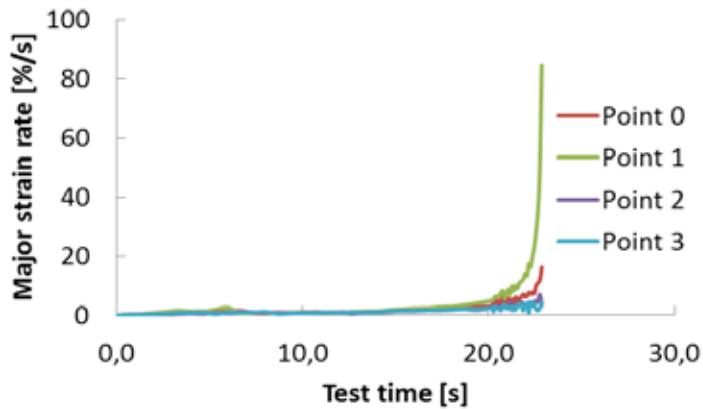


Figure 9. The major strain rate evolution during the test.

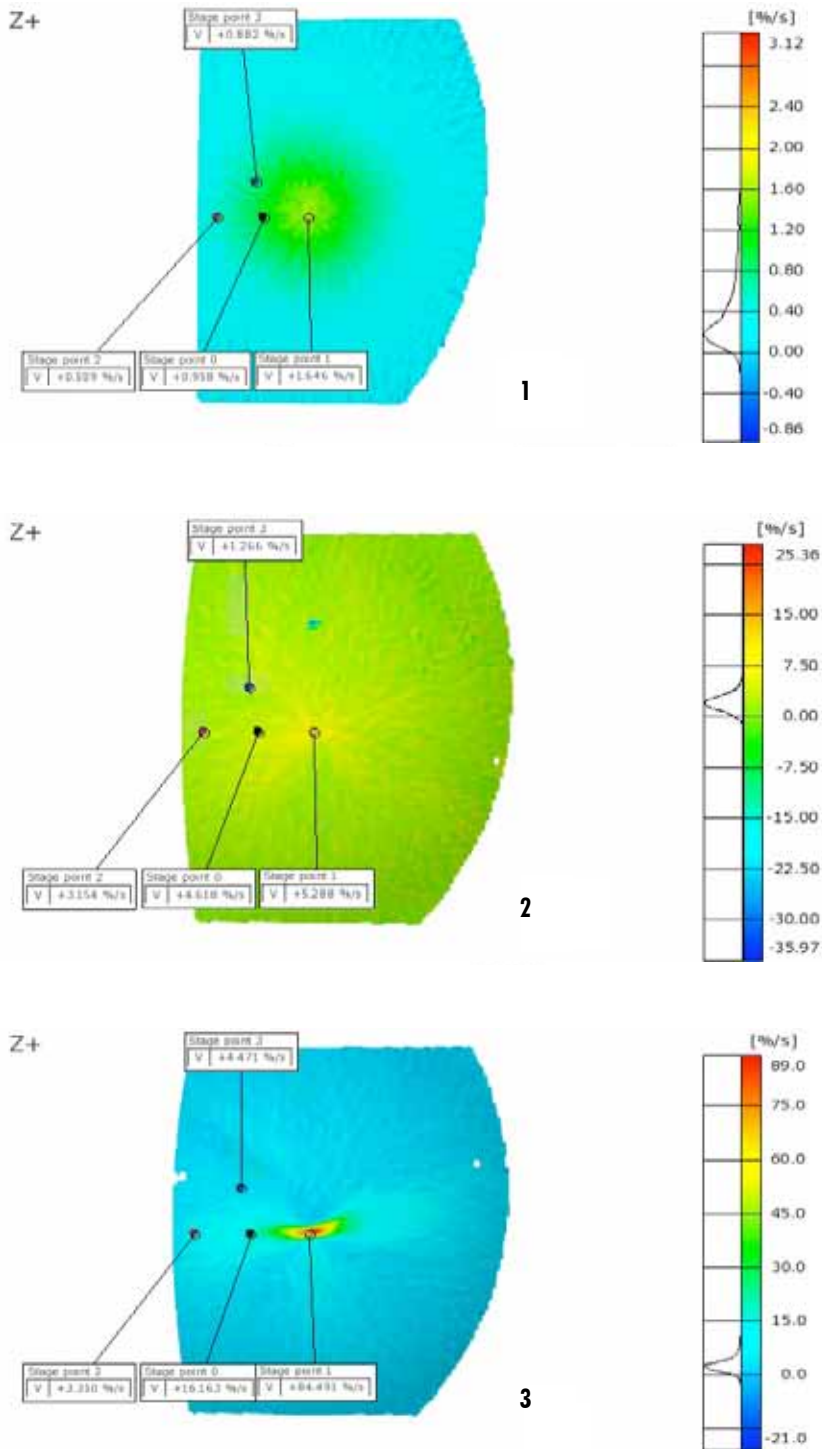


Figure 10. The variation of major strain rate of A-geometry specimen during the test (1–3).

Surface Strains and Strain Evolution in Tensile Tests

One of the most commonly used forms of data collected from a tensile test is a stress-strain curve. It holds information that is used to compare different materials or to determine their stress bearing capacity. The same surface parameters along with strain and other derivative data can be processed from the optically constructed surface analysis. For instance, a strain in different parts of the tensile test specimen can be easily viewed with the help of full-field analysis. Example views from standard tensile test are seen in Figure 11.

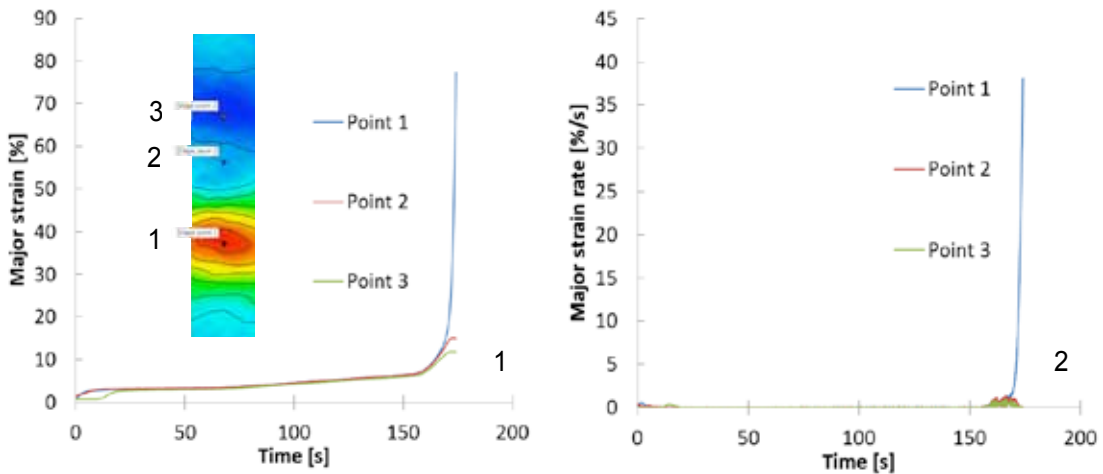


Figure 11. The major strain (1) and major strain rate (2) evolution during the tensile test.

Surface Strains and Strain Evolution in E-geometry of FLC-test

The E-geometry specimen of FLC-test series is the closest to a tensile test specimen, so it is used to evaluate the strain rate. From the analysis and by visual estimation, it is seen that the test speed resulting from FLC-testing would require tenfold increase in speed of the crosshead of the tensile test machine, in order to match the test time length. The major strain and major strain rate of two selected points on the E-geometry specimen's surface are shown in Figure 12.

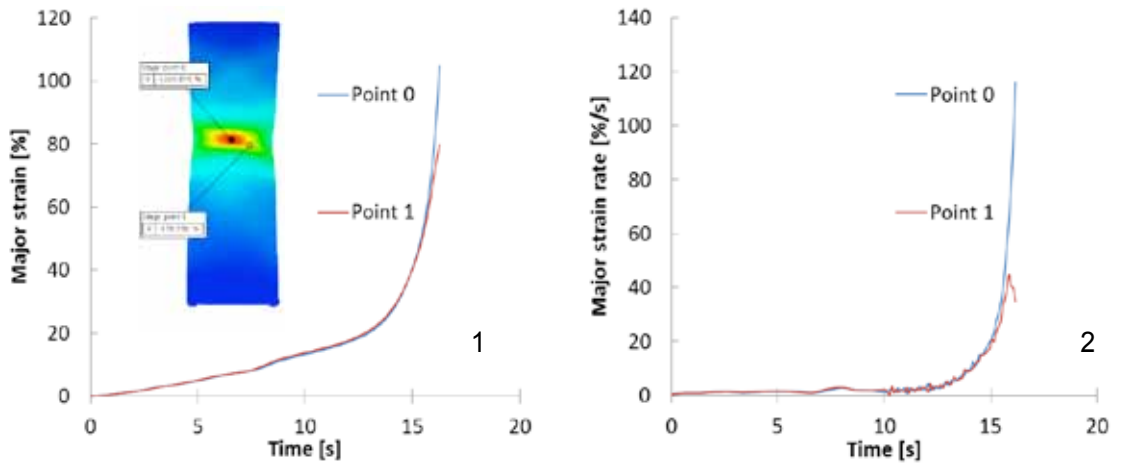


Figure 12. The major strain (1) and major strain rate (2) evolution on E-geometry specimen.

In addition to the surface strains shown in previous figures, side view of the recognized surface show clearly how the diffuse necking has evolved during the test. The curvature and evolution of strain localization is shown in Figure 13.

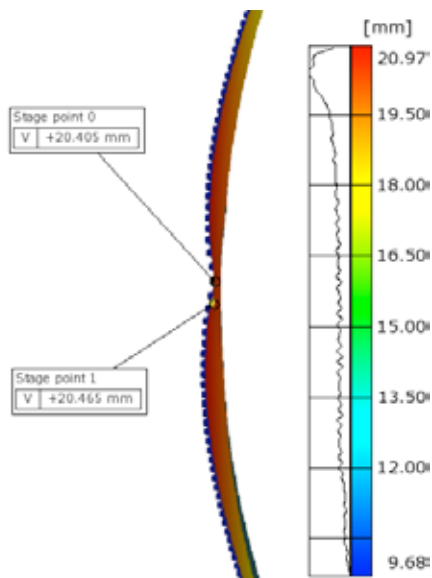


Figure 13. Curvature of the E-geometry specimen before failure.

Flow Stress Curve Based on FLC-test A-geometry

Normally, the flow stress is determined by hydraulically bulging of the specimen out of plane in a test rig. At the same time surface strains are obtained with non-contacting optical measuring system. The forming pressure is recorded by a pressure gauge. The momentary curvature of the surface is required to complete the equation for the flow stress. The curvature is acquired by using an analytical best-fit circle on the recognized surface. With the GOM ARAMIS system, the flow stress is obtained by executing analysis macro with some user interaction. A liquid forming medium is normally used for the test in order to eliminate the effect of friction that would normally occur when using solid, contacting punches and dies. (GOM gmbh 2008)

The FLC-tests described here were done with complex lubrication system which offers nearly frictionless conditions during the test. Therefore, the usability of full circle, A-geometry specimen with surface strains, curvature and punch force data is evaluated for flow stress estimation. With aforementioned analysis macro and the relation of bulge pressure and punch force from previous tests, a flow stress curve was obtained. The flow stress is shown in Figure 14 along with other stress strain curves obtained by the author in previous work. (Joutsenvaara 2012)

DISCUSSION AND CONCLUSIONS

In this paper, the forming limit diagram was constructed for the tested structural steel with the nominal yield strength of 650 N/mm^2 and 3 mm in thickness. The forming limit curve was made according to the current standard SFS-EN ISO 12004-2 with Erichsen Universal Sheet Metal Testing Machine, model 145-60. The test parameters were given in order to ensure similar conditions for future tests.

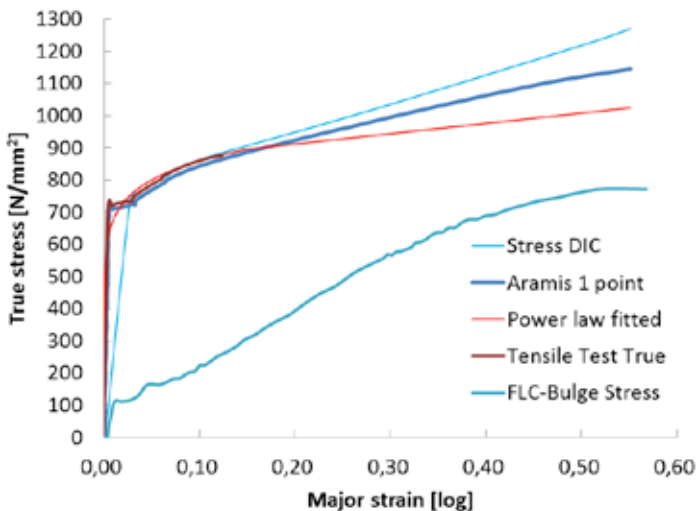


Figure 14. Comparison of various stress-strain curves obtained by the author.

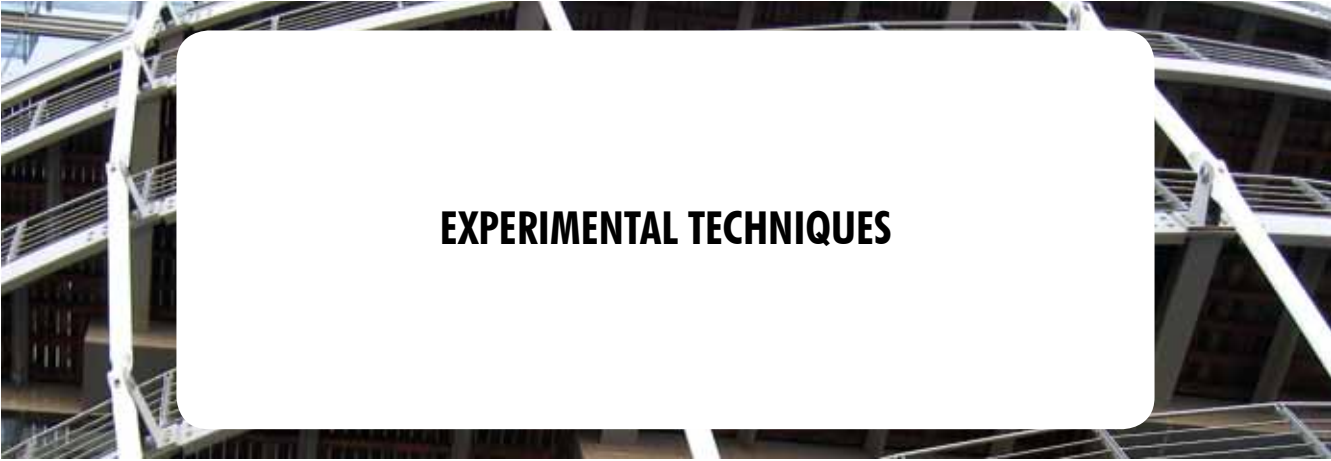
The strain values on the surface of the A-geometry were recorded as well as the strain rate during the whole test phase. To further clarify the strain evolution during the test phase, selected graphs and images were presented. In order to add comparison to a standardized tensile test, the strains on the tensile test and E-geometry specimen surface were presented. The strain rate is roughly three times higher in FLC E-geometry specimen compared to the tensile test specimen. In the case of the A-geometry, the major strain rate is roughly twice as high as in the tensile test specimen. For estimation purposes, the higher strain rates should indicate higher stresses and lower ultimate elongation. Based on the results presented here, the comparison of different material tests based on their strain rates is one of the future research topics. This requires also the evaluation for different kind of real forming processes with real products.

ACKNOWLEDGEMENTS

The author would like to acknowledge the financial support of Tekes – the Finnish Funding Agency for Technology and Innovation for their support for the METNET Network and “Osaamista ajoneuvoteollisuuden kanssa – ConceptCar” and MineSteel -projects. Research equipment mentioned in this paper at Kemi-Tornio University of Applied Sciences is partly funded by the Regional Council of Lapland (European Regional Development Fund).

REFERENCES

- Banabic D., Barlat F., Cazacu O., Kuwabara T., (2010) Advances in anisotropy and formability, *International Journal of Material Forming* , vol. 3, no. 3, pp. 165–189.
- Ghadbeigia H., Pinnaa C., Celottob S., Yatesa J.R., (2010). Local plastic strain evolution in a high strength dual-phase steel, *Materials Science and Engineering*, Vol. 527 pp. 5026–5032.
- Gom Hardware manual, (2008). Gom gmbh.
- Gom Software manual, (2008). Gom gmbh.
- Joutsenvaara, Jukka, (2012). Investigation of strain localization of high strength steel with the help of digital image correlation, *Proceedings of the METNET Seminar 2012 in Izmir*, pp. 19–30.
- Kim Hyoung Seop, Kim Sung Ho and Ryu Woo-Seog, (2005). Finite Element Analysis of the Onset of Necking and the Post-Necking Behaviour during Uniaxial Tensile Testing, *Materials Transactions*, Vol. 46 pp. 2159–2163.
- Proulx, Tom (Ed.), (2013). *Application of Imaging Techniques to Mechanics of Materials and Structures*, Volume 4.
- Vierelä Raimo, (2012). Edge formability research for hot-rolled steel Optim 650 MC.



EXPERIMENTAL TECHNIQUES

One of the most difficult problems during the bridge design was caused by the continuous welded rail. It was influenced by a number of complications:

- the small rail radius of the curvature, which resulted in the use of sleeper anchors;
- the combination of the ballasted bed and direct fastening;
- solving the transition from ballasted bed to direct fastening, including the barrier in the ballasted bed (see Fig. 2);
- long dilatation length, which had exceeded the standard limits.

The unusual solution of the CWR resulted in the necessity of establishing the long term monitoring of the CWR behaviour, including its interaction with the bridge. The monitoring started in summer 2010 and finished in October 2011. Thus, one full year was measured, including summer hot and winter cold temperatures.

The rail stress level was established for different temperatures. Extreme values were achieved over Pier 1, where the dilatation length is extreme. Interesting result is that the stress in the ballasted bed is higher than stresses reached on the direct fastening. It can be sometimes observed, that the stiffness of the ballast depends on the temperature. That dependence can be significant, when the water in the gravel freezes and increase its stiffness. To check that phenomenon on Kolín bridge, a total of 200 days were chosen in order to evaluate the influence of temperature on the longitudinal resistance, showing significant change of the bridge temperature had occurred.

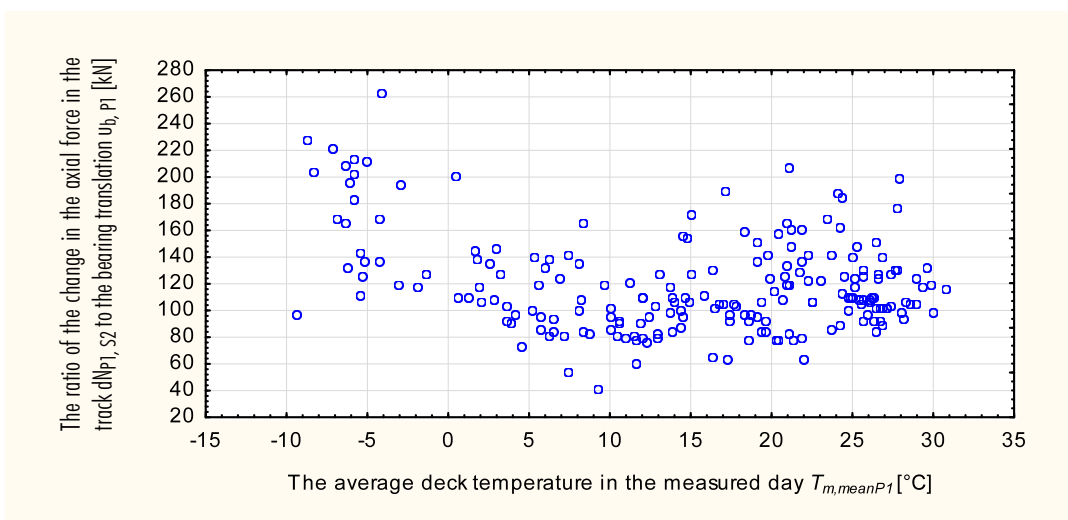


Figure 2. The ratio between the change in the axial force increment $\Delta N_{P1, S2}$ to the displacement $\Delta u_{b, P1}$, compared to the mean day temperature $T_{m, meanP1}$.

It is clear from Fig. 2, that the stiffness of the ballast is almost independent on the temperature. It means that the freezing of the ballast did not occur on that bridge, although a lot of snow was noticed during the monitoring.

The 3D FEM computer model in software Scia Engineer 2008 was created, in order to verify the experimental data and evaluate the longitudinal stiffness and resistance of the track. The model included the bridge structure and the adjacent 100m of the rail and substructure. The connection between the rail and the bridge was modelled with fictive stiff members with nonlinear stiffness in all directions, representing the vertical, transversal and longitudinal rail stiffness.

The relation between longitudinal resistance and the track/bridge displacement was established for the ballasted bed and also the direct fastening. The results were then compared with the experimental data. The longitudinal resistance function is shown in Fig. 3.

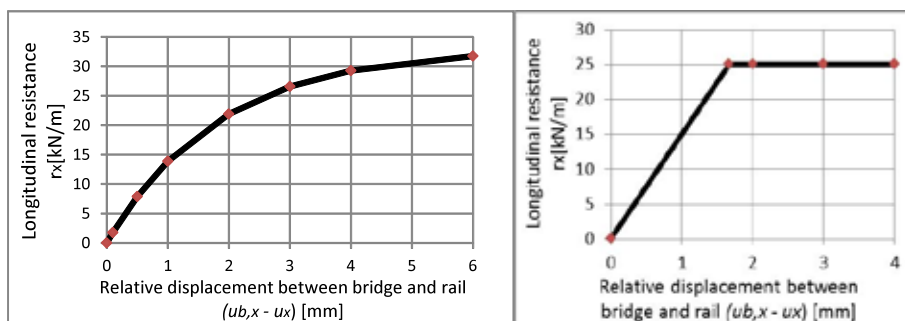


Figure 3. The relation between longitudinal track resistance on relative displacement for ballasted track and direct fastening.

The following conclusions emerged from the monitoring and the analysis of results:

- the coefficient of the equivalent thermal expansion were higher, than can be found in the literature,
- the functions of the longitudinal track resistance were evaluated, both for ballasted track and direct fastening,
- there were no signs of the temperature effect on the ballast stiffness,
- no significant impact of the ballast barrier on rail stresses was observed,
- the extreme stresses in the rail were found not on the direct fastening, but in the ballast.

Research reported in this paper was supported by Competence Centres program of Technology Agency of the Czech Republic (TA CR), project Centre for Effective and Sustainable Transport Infrastructure (no. TE01020168) and by TA CR 02031453.

LASER SYNTHESIS TECHNOLOGY FOR THE CREATION, RESTORATION AND REPAIR OF COMPLEX MACHINE PARTS

P.A., Kuznetsov, O.V. Vasilyeva, I.V. Kudryavtseva and A.V. Tereschenko

Department of Nano-structured Materials
FSUE CRISM "Prometey", 191017 Saint-Petersburg, Russia

ABSTRACT

Creation of new products and restoring worn items by traditional process is quite hard to perform and is expensive both in material and energy consumption, as also on time resources. The main objective of this study is to establish a technique and conduct repair of intricate parts with high surface hardness (up to 50–60 HRC). As a result, after the material selection, different brands of powders based on Fe, Ni, Co-Cr were tested. To find the optimum sintering and welding conditions in the process the following parameters were varied: laser power, the depth of sintered layers and the time of exposure to laser radiation. After selecting optimal operating system, restoration of a number of details was carried out. Results of hardness measurement of restored parts showed the correct level (about 53–55 HRC). The experimental results demonstrate that the technology of selective laser sintering and laser cladding allows obtaining products of a complex dimensional form with micro hardness parameters that approach the value characteristic of the products obtained by traditional methods.

METHODS AND MATERIALS

At the present time global market demands new approaches and technologies which allow creation of high quality goods and to reduce energy and material consumption. One of the most important tasks at present is the problem of hardening and recovery of heavy-duty parts and products in various fields of engineering, including arctic and agricultural machinery. For these purposes use is made of different technologies of cladding and surfacing. There is a number of cladding and surfacing technologies which may be used in different ways of energy supply to the base metal and using different powder materials. Most of the technologies have relatively low deposition locality energy input, resulting in a heat affected zone of great thickness. This, in turn, causes a significant reduction in the properties of the hardened layer. In addition, the hardened layer is subjected by internal stresses, resulting in deformities of the work pieces. The above mentioned causes significantly restrict the use of such surfacing technologies as plasma, arc and flame.

Today, technologies of producing complex parts and functional coatings from metal powder materials by laser radiation are developing rapidly. In order to

obtain functional coatings, creation and restoration of parts and products of complex geometry, including those damaged during operation, the technology of laser cladding and sintering of bulk objects is unique, allowing achievement of required operational characteristics, defined geometric dimensions of parts and coatings, as well as the opportunity to receive new composite materials, even from immiscible components. Relating to parts recovery technology and coatings processes technology from metal powders, laser bulk cladding is considered as a promising method. One such method is the LENS (Laser Engineered Net Shaping) technology.

In the schematic bulk laser cladding process, a high-power laser beam (Fig. 1) is focused on a metal surface that leads to formation of a local microscopic liquid melt bath. Inert carrier gas argon is injected into the melt bath portion of the metal powder. After laser beam exposure, the molten metal immediately solidifies, and by the addition of the powder into the molten bath the part surface thickness is increased. Thus, as a result of a systematic scanning of the surface of the part by a laser beam with simultaneous injection of powder are formed first and subsequent layers of the part which is being created. This method allows the use of almost any metal powder and alloy powder that can be melted by a laser beam without evaporation.

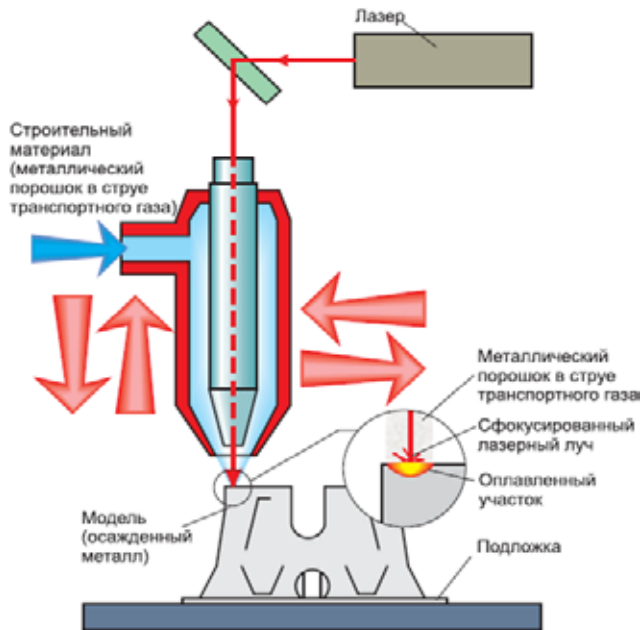


Figure 1. Scheme of LENS technology.

Due to ultrafast crystallization of the melting bath the building part has ultra-fine-grained or amorphous structure. According to the results of comparative tests on its mechanical properties, these parts in some cases become far superior than the parts obtained from similar alloys by traditional production methods (casting, stamping).

Table 1. Chemical composition of powders.

Element	R6M5	1560	PR-H30SRNDYU
Ni	-	73,3	1,46
Fe	80	3,7	55,1
Cr	3,5	14,8	32
B	-	3,1	1,9
Al	-	-	0,43
Si	-	4,3	3,6
V	1,7	-	-
W	7	-	-
Mo	6	-	-
C	-	0,8	4,9
Cu	-	-	0,48
Mn	-	-	1,2

For experiments on protective coatings deposition by bulk laser cladding, the following powders were selected: R6M5, 1560 Höganäs, PR-H30SRNDYU JSC "Polema". The chemical composition of the powders was investigated by the X-ray fluorescence analysis and results are presented in Table 1. Plates were made from steel 20 and were used as the substrates.

Table 2. Powders cladding conditions.

Powder	Laser power, W	Substrate scanning speed, m/s	Feed rate, g/s	Hatch, mm
R6M5	400	0,013	0,23	0,23
1560	320	0,015	0,18	0,23
PR-H30SRNDYU	350	0,015	0,20	0,23

Table 3. Results of Rockwell hardness measurements.

№ measurement	Powder		
	R6M5	1560	PR-H30SRNDYU
1	61,6	65,1	67,4
2	61,8	64,6	68,6
3	61,4	65,9	67,9
Average	61,6	65,2	68,0

RESULTS AND DISCUSSION

Selection of optimum modes is to choose the laser power, substrate scanning speed, powder feeding rate, and the distance between the laser beam passes. Based on the experience of working with similar chemical composition powders, LENS main parameters for each powder are summarized in Table 2. The results of Rockwell hardness measurements are summarized in Table 3. SEM graphs of the coatings prepared in transverse direction are presented on Figures 2–4.

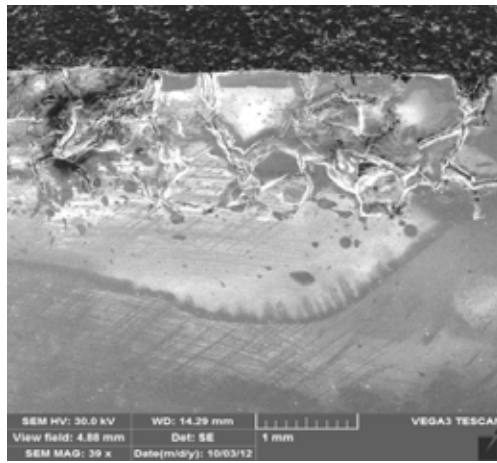


Figure 2. SEM graphs of the coating with JSC "Polema" powder.

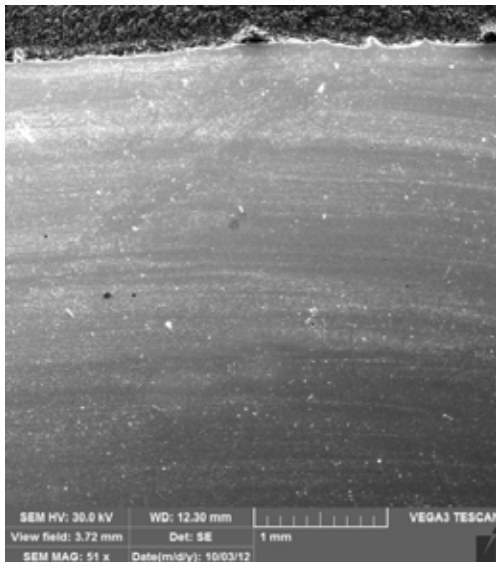


Figure 3. SEM graphs of the coating with 1560 powder.

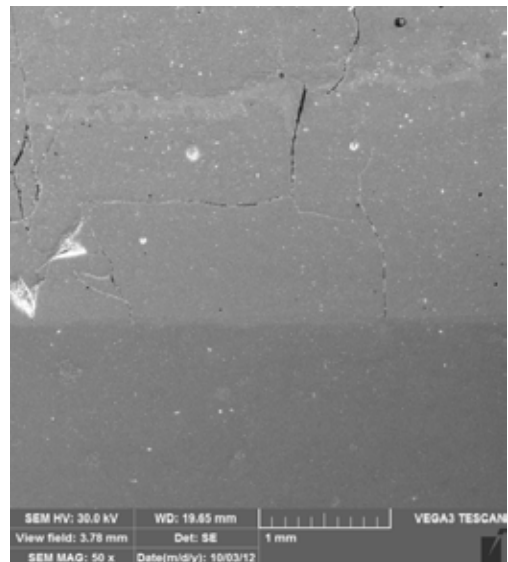


Figure 4. SEM graphs of the coating with R6M5 powder.

From the obtained results it is clearly seen that the coatings obtained with powders 1560 and PR-H30SRNDYU have the highest hardness but are fragile as evidenced by the cracks (Fig. 2 and 3). Their formation is explained as follows: cladding with the direct feed of powder in the area of laser radiation leads to the formation of large amount of carbide and boride compounds in the structure of coating. It affects the physical and mechanical properties of coatings. The formation of these compounds due to the presence in the chemical composition of powders carbide and boride generating elements confirms the tendency to cracking. Sample obtained from the powder brand R6M5 has stable hardness at all points of measurement and the absence in the chemical composition of carbide and boride generating elements reduced the risk of cracking to a minimum (Fig. 4).

SUMMARY

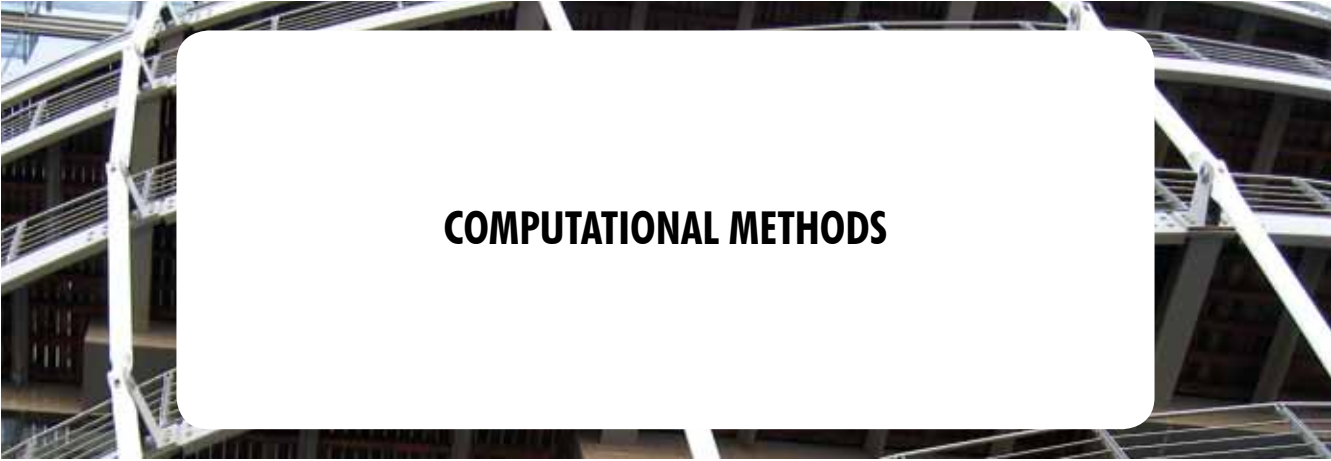
Analysis of the results leads to the conclusion that it is most appropriate to use laser cladding powder with low-carbide and boride generating elements (e.g., R6M5), giving a high surface hardness and a reduced tendency to cracking. Laser cladding technology LENS by high coating properties gives the prospect of increasing the resistance of the most heavily loaded local areas of different parts of the Arctic and agricultural equipment. In addition, the laser cladding can be successfully used for repair and rehabilitation of worn out sections of parts due to the high mechanical properties of the coating and the absence of deformation.

ACKNOWLEDGMENT

The work was done under a partnership agreement with Lappeenranta University of Technology "Development of materials and technologies for the Arctic" dated 02.01.2012.

REFERENCES

- [1] Shishkovsky I.V. "Lasersynthesis of functionally gradient mesostructures and bulk products" – Moscow: Fizmatlit, 2009 – p. 424.
- [2] Tereshchenko A.V., Bobyr V.V., Savin V.I., Kudryavtseva I.V., Vasilyeva O.V. Restoring a given geometry of machine parts and tools for technology selective laser sintering // Proceedings 14th International Scientific-Practical Conference "Technology of hardening, coating and repair: theory and practice" 17–20 April 2012 Abstracts. St. Petersburg. Part 1. – p. 178–181.
- [3] Tereshchenko A.V., Bobyr V.V., Savin V.I., Kuznetsov P.A., Kudryavtseva I.V. Creation of complex geometry parts by selective laser sintering of powder materials. // Proceedings of the 9th International Scientific and Technical Conference "Modern metal materials and technologies" on June 22–24, 2011. – St. Petersburg, 2011.



COMPUTATIONAL METHODS

WEIGHT AND COST OPTIMIZATION OF WELDED HIGH STRENGTH STEEL BEAMS

Kristo Mela
(kristo.mela@tut.fi)

Markku Heinisuo
(markku.heinisuo@tut.fi)

Tampere University of Technology
Department of Civil Engineering
P.O.Box 600, FI-33101 Tampere, Finland

ABSTRACT

Weight and cost optimization of welded beams in steel grades S355, S500 and S700 is considered in the paper. The aim is to study the utilization of high strength steels in welded geometrically double-symmetric I-beams by optimizing simply supported beams under uniform lateral load. The homogenous S355 profile works as the reference case. For higher steel grades, S500 and S700 are available. Shear and bending resistance are included, but lateral torsional buckling is neglected. Hybrid beams are also studied. In a hybrid cross-section, the steel grades of the flanges are higher than for the web. Cross-section class may vary from 1–4 following Eurocodes. The resistance rules of Eurocodes at room temperature are used as constraints in the problem when they are available. For hybrid cross-sections rules available in the literature are used to check the resistances. Weight and cost are used separately as optimisation criteria, such that each considered beam is optimized both for weight and cost. The geometries of the members are extremely simple and do not include any fittings or other features for joints. The costs include fabrication, transportation and erecting on site. The fabrication costs include materials, flame cutting, welding, sawing and painting with all costs needed in the workshop, such as real estate, energy, labor etc. The optimization is performed by the Particle Swarm Optimization method. The design variables are the cross-section dimensions of the members in the range which is typically used in practice, meaning discrete values. The results show that while significant weight reductions can be achieved by HSS, the cost savings remain moderate.

INTRODUCTION

High strength steels (HSS) are currently used in other applications than buildings. Nevertheless, HSS may be used cost effectively in buildings, as well. Proper information on the economy of HSS in building applications including not only material costs but also other costs, such as fabrication, transport and erecting on site is missing. The purpose of this paper is to provide insight on how to utilize the higher strength of available steels. This question is answered by finding the weight and cost optimal solutions for geometrically double-symmetric welded I-beam that is used as an example structure. By employing

optimization, the full potential of HSS can be discovered, as the solutions can be totally different from conventional designs.

For cost calculations, the method proposed in (Haapio, 2012) is used along with typical Finnish price levels. As publicly available experimental and measured data of fabrication cost is scarce, relative material cost data for different steel grades based on (Johansson, 2005) and cost factors for welding and sawing with relation to fabrication of S355 steel members are employed.

The beams made of S355 are used as a reference to which the solutions obtained by HSS are compared. S500 and S700 are chosen as the HSS grades. Hybrid beams are also considered, i.e. the flanges can be of different grade than the web. Furthermore, the top flange can be of different grade than the bottom flange.

The paper is organized as follows. First, the minimum weight and minimum cost optimization problems are formulated. This part consists of writing the expressions for the objective functions and introducing the constraints as well as the design variables. Then, the results of optimization are presented with discussion on the characteristics of the optimum designs. The paper ends with conclusions drawn from the study.

PROBLEM FORMULATION

The geometry of a simply supported beam under uniform later load considered for weight and cost minimization is shown in Figure 1. The beam is optimized for several loads and spans. The cross-section is geometrically double-symmetric I-profile.

Formulating an optimization problem requires identifying the design variables, the objective function and the constraints. In the present study, the design variables are the dimensions of the cross-section. The design variables are collected into a vector, denoted by (see Figure 1)

$$\mathbf{x} = \{bf \ tf \ hw \ tw\} \quad (1)$$

Variables tf and tb can take values from the discrete set T , which contains the following 19 elements:

$$T = \{5, 6, 8, 10, 12, 14, 15, 16, 18, 20, 22, 25, 30, 35, 40, 50, 60, 80, 100\} \text{ [mm]} \quad (2)$$

The flange width and web height are to be chosen from the discrete set of integer values ranging from 100 mm to 1000 mm in 10 mm intervals. That is $bf, hw \in B = \{100, 110, 120, \dots, 990, 1000\}$.

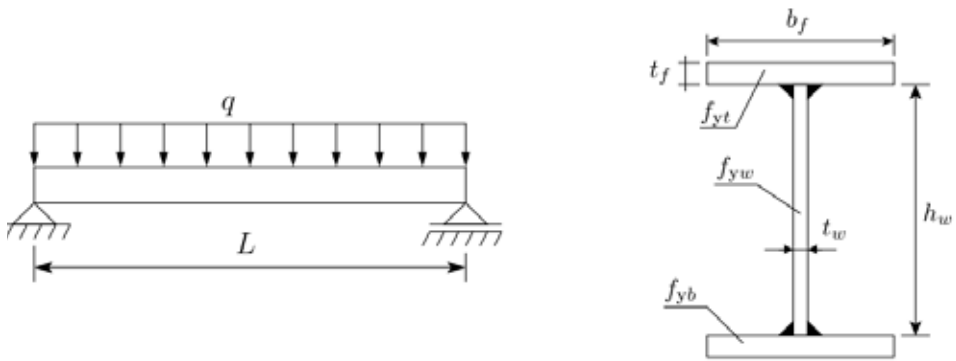


Figure 1. Simply supported beam to be optimized and the geometrically double-symmetric cross-section. Note that the yield strengths of the flanges need not be equal, i.e. $f_{yt} \neq f_{yb}$ is allowed.

Objective functions

In this study, both the weight and fabrication cost are chosen as objective functions. The weight is written as

$$W\mathbf{x} = \rho L 2A_f + A_w = \rho L 2b_f t_f + h_w t_w \quad (3)$$

where $\rho = 7850 \text{ kg/m}^3$ is the density of steel and L is the length of the beam.

The manufacturing cost function is based on the work of (Haapio, 2012). The manufacturing process is divided into cost centers, each containing a set of cost components such as labour, material, equipment, energy, and real estate. The main task is then to devise appropriate expressions for the cost components of every cost center. These expressions depend on the specific technologies used, and they contain many parameters that must be obtained by measurement. Unless otherwise stated, the default values found in (Haapio, 2012) are used for the parameters appearing in the cost function. Here, the parameter values are combined to single numbers, when possible.

The cost function can be written as

$$C\mathbf{x} = CM\mathbf{x} + CB\mathbf{x} + CC\mathbf{x} + CS\mathbf{x} + CW\mathbf{x} + CP\mathbf{x} + CT\mathbf{x} + CE(\mathbf{x}) \quad (4)$$

The material cost is

$$CM\mathbf{x} = c_M \rho L (c_{M,t} A_f \mathbf{x} + c_{M,w} A_w \mathbf{x} + c_{M,b} A_f \mathbf{x}) \quad (5)$$

where $c_M = 0.7 \text{ €/kg}$, and $c_{M,i}$ and A_i are the cost factor of the steel grade and the cross-sectional area of plate i . For S355, $c_{M,i} = 1.0$, for S500, $c_{M,i} = 1.15$ and for S700, $c_{M,i} = 1.30$.

The blasting cost depends on the number of plates and the length of the beam. It is

$$CB\mathbf{x} = 3 \cdot 3.6447 \cdot 10^{-4} L \quad (6)$$

The cutting cost can be expressed as

$$CCx=1.3227TNCu+TPCu x+TPCu x(cCCu x+ cEnCu) \tag{7}$$

where the non-productive time $TNCu=3.0$ min. Depending on the plate thickness, either flame cutting or plasma cutting is used. For plate thickness up to 30 mm, plasma cutting is used. The productive time is

$$TPCu x=LCu(x)8.9212t^2-486.87t+8115.8 \tag{8}$$

where t is the thickness of the plate. The cost of cutting consumables is $cCCu=0.38$ €/min and the cost of energy is $cEnCu=0.12$ €/min.

For flame cutting, productive time and cost of consumables are

$$TPCu x=LCu(x)-4.1939t+658.67 \tag{9}$$

$$cCu x=0.22+4.18(1\cdot 10^{-5}t^2+0.001t+0.0224) \tag{10}$$

whereas the torch's energy consumption is neglected, i.e. $cEnCu=0$.

The length of the cut is $LCu x=2(bf+L)$ for the flanges and $LCu x=2(hw+L)$ for the web.

The cost of welding the plates to form the actual beam can be expressed as

$$CWx=1.3627TNBW+TPBW x+TPBW x(cCBW+ cEnBW) \tag{11}$$

where $cCBW=0.08$ €/min and $cEnBW=1.36$ €/min. Furthermore, $TNBW=6.25$ min. The productive time is written as

$$TPBW x=7.85\cdot 10^{-6}Lwaw^{214}=7.85\cdot 10^{-6}LwCw^{214} \tag{12}$$

where $Lw=L$ is the length of the weld, and Cw is the weld size factor that depends on the grade of the web (Table 1). The expression of $Cw(x)$ is for welding of one flange. For the whole beam, both flanges need their own expressions. In order to take into account the expense of welding high strength steels, cost factors are introduced. These factors are given in Table 1.

Table 1. Cost parameters for different steel grades.

Grade	Cw	Welding factor	Sawing factor
S355	0.55	1.0	1.0
S500	0.80	1.25	1.15
S700	0.82	1.5	1.3

The sawing cost is written as

$$CSx=1.2013TNS+TPSx+TPSx(cCS(x)+ cEnS) \tag{13}$$

The non-productive time, $TNS=4.5+L/20000$ min, and the cost of energy is $cEnS=0.02$ €/min. The productive time depends on the position of the cross-section, when it is sawn. It is assumed that the geometrically double-symmetric profile is laid on its side such that the flanges are considered to be sawn vertically and the web horizontally. For taking into account the higher steel grades, cost factors are introduced to the productive time, see Table 1. The cost of consumables includes the wear of the saw blade. It depends on the plate thickness and on the productive time. For details of productive time and sawing consumables, see (Haapio, 2012, pp. 39–42).

The painting cost includes also the cost of drying and it can be written as

$$CPx=4.17 \cdot 10^{-6} LAu(x)+0.36L \cdot 1 \cdot 10^{-3} W_{Amin}x \cdot 1 \cdot 10^{-3} \quad (14)$$

where $Aux=3bf+4tf+2hw-2tw$ is the painted area per unit length, and $W_{Amin}x=bf$ is the smallest width dimension of the beam (it is assumed that $bf \leq hw$).

The transportation cost is expressed as

$$CTx=Vx0.0106dws+1.2729, \text{ if } W(x)/V(x) \leq 264Wx4 \cdot 10^{-5}dws+4.8 \cdot 10^{-3}, \\ \text{otherwise} \quad (15)$$

where $Vx=Lbf2tf+hw$ is the volume occupied by the beam and $W(x)$ is the weight of the beam. The conditional definition states that if the weight to volume ratio is below the given limit, then the transportation cost is determined by the volume of the beam. Otherwise, the cost will be determined by the weight.

Finally, the erecting cost of the beam can be written as

$$CEx=TEcLE+cEqEuE \quad (16)$$

where $cLE=3.1$ €/min is the cost of labor, $cEqE=1.3460$ €/min, and $uE=0.36$. The time needed for erecting the beam is

$$TE=L30000+Ls27+20.5nb-0.42+Ls36 \quad (17)$$

where $Ls=15$ m is the distance from the lifting area to the final position, and $nb=6$ is the number of bolts per joint. The erecting time consists of moving the main lift from one end to the other, lifting the beam, joining the beam to the main structure, and returning the hook to the lifting area. It is assumed that five workers are included in the erecting process, and that the beam is lifted by a crane with lifting capacity of 25 tons. It is assumed that the beam is lifted to 10 m. This is reflected in the equipment cost. Note that the erecting cost depends only on the length of the beam, as the number of bolts per joint and the capacity of the crane are fixed.

Constraints

The constraints of the optimization problems are derived from the Eurocodes (EN 1993-1-1, 2005; EN 1993-1-5, 2006). They ensure that the solution has sufficient moment and shear force resistance, and that the top flange does not buckle against the web. Finally, the displacement of the beam is limited.

The moment resistance constraint is

$$MRd(x) \geq MEd \quad (18)$$

If the cross-section belongs to Class 1 or 2, plastic design is applied and MRd is the plastic moment of the cross-section. If the web is in Class 3 and the top flange in Class 1 or 2, then the plastic moment of the cross-section with effective web is used. For Class 3, elastic bending resistance is used and for Class 4, effective cross-section is determined.

For elastic design of hybrid cross-sections, the partial plastification of the web is taken into account. In general, the minimum of the yield strengths of the flanges determines the maximum stress that can appear in the cross-section. For a linear stress distribution, it is common that the yield strength of the web is attained, and it will plastify in part. By allowing the web to plastify, the higher steel grades can be utilized better. For determining the plastified region of the web, it is assumed that the neutral axis is located at the centroid of the effective cross-section. This assumption leads to a small error in the force equilibrium of the cross-section, but it is considered negligible. Then, the location where the yield stress in the web is reached is determined from the linear stress distribution. The part of the web above this point yields. See (Ongelin and Valkonen, 2010, pp. 130–140) for more details.

The shear resistance constraint is

$$V_{c,Rd}(x) \geq VEd \quad (19)$$

Plastic shear resistance is employed and shear buckling is taken into account.

To prevent the top flange from buckling in the plane of the web, the following constraint is needed (EN 1993-1-5, Clause 8(1)):

$$hwtw \leq kE_{fyt}A_{wt,eff} \quad (20)$$

where $E=210000$ MPa, $A_w=hwtw$ is the area of the web, $A_{wt,eff}$ is the effective area of the top flange, and $k=0.4$ if plastic resistance is used and $k=0.55$ if elastic resistance is used.

The maximum displacement occurs at the midpoint of the span. The displacement constraint is written as

$$u_{max}(x) \leq u \quad (21)$$

where

$$u_{max} = 5384qSLSL4EIy(x) \quad (22)$$

is the displacement in the middle of the span and $u=L/200$ is the maximum allowed displacement. The load in service limit state, $qSLs=0.75q$.

Problem statement

The developments shown above can be combined to the following optimization problem

$$\begin{aligned} \min_x f(x) \text{ such} \\ \text{that } 1 - MRdxMEd \leq 0, 1 - Vc, RdxVEd \leq 0, hwtw - kEfytAwAyt, eff \leq 0, u_{max}(x) \\ u - 1 \leq 0, f, tw \in Tbf, hw \in B \end{aligned} \quad (23)$$

where f is either the weight, W or the cost C . Note that the constraints have been normalized and all terms are transferred to the right.

Both the minimum weight and minimum cost problems are nonlinear discrete optimization problems. With only four design variables and four constraints, the problems are small-scale, but the mathematical properties of the constraints makes finding the global optimum rather difficult. For example, when a cross-section is altered such that it goes from belonging to Class 2 to Class 3, the expression for moment resistance changes considerably. From a mathematical point of view, the moment resistance constraint is in general discontinuous in the regions where the cross-section class changes. This makes it difficult to apply classical methods of nonlinear discrete optimization that require continuity of the constraint and objective functions. On the other hand, heuristic, population-based algorithms can handle such problems. In this study, such an algorithm is used to solve the optimization problems at hand.

RESULTS OF OPTIMIZATION

Both the weight minimization and minimum cost problems were solved by the Particle Swarm Optimisation (PSO) algorithm (Kennedy and Eberhart, 1995; Poli et al., 2007). In the literature, many possibilities regarding the details of the algorithm are available. In this study, an implementation of the PSO method was produced, with chosen constraint handling mechanism, velocity update rules with inertia term, craziness effect and elite particle. Furthermore, whenever the best feasible solution was updated, a neighborhood search was performed, i.e. better solutions were searched in a neighborhood of the

solution. Detailed description of the algorithm is beyond the scope of this paper.

Three spans of 6 m, 8 m, and 10 m were considered with three different loads, $q=20$ kN/m, $q=60$ kN/m, and $q=100$ kN/m. For the three available steel grades, S355, S500, and S700, altogether 14 combinations could be formed for each span and load. The only restriction was that the grade of the web cannot be greater than the grade of either of the flanges.

Weight minimization

As a first step, it is interesting to compare the homogenous S500 and S700 cross-sections with the homogenous S355 profile, which works as the reference case. In Table 2, the ratios of the minimum weights of S500 to S355 and S700 to S355 are shown for different loads and spans. It can be seen that for the lowest load, $q=20$ kN/m, only marginal weight savings can be achieved by HSS. This is partly explained by the allowable plate dimensions, that are not favourable to HSS. On the other hand, the HSS solutions are mostly restricted by the displacement constraint where the higher strength does not play any role. For the S355 solution, the moment resistance constraint is dominant, even though the utilization ratio of the displacement constraint is also more than 90%.

For higher loads, weight savings provided by higher strength gets more significant. For the intermediate load $q=60$ kN/m, S500 gives a saving of about 15%, whereas S700 reduces the weight by about 25%. For the largest load, and largest span, the weight reductions are 23% for S500 and 35% for S700.

Table 2. Results of weight minimization. The numbers are the ratios W_{500^*}/W_{355^*} , and W_{700^*}/W_{355^*} , where W_{fy^*} is the minimum weight of the homogenous cross-section with yield strength f_y .

S500	Span (m)			S700	Span (m)		
Load	6	8	10	Load	6	8	10
20	0.98	0.97	0.90	20	0.98	0.97	0.90
60	0.85	0.84	0.84	60	0.76	0.74	0.73
100	0.84	0.84	0.77	100	0.71	0.67	0.65

Cost Minimization

For the results of cost optimization, it is again interesting to compare the homogenous S500 and S700 solutions with the S355 case. Also, it is interesting to see, how hybrid cross-sections perform in cost optimization. In Table 3 the relative cost optima of S500, S700 and the best solution compared to S355 are given. It can be seen that HSS solutions become beneficial only for the largest load. In most cases, the material and fabrication costs of HSS are too high compared with S355.

Table 3. Results of cost minimization.

S500	Span (m)			S700	Span (m)			Best	Span (m)		
Load	6	8	10	Load	6	8	10	Load	6	8	10
20	1.15	1.14	1.10	20	1.26	1.25	1.22	20	1	1	0.99
60	1.06	1.03	1.01	60	1.10	1.06	1.03	60	0.95	0.93	0.90
100	1.04	1.04	0.94	100	1.04	0.96	0.94	100	0.93	0.91	0.90

For the lowest load, the S355 solution is the most economical, except for the largest span. Then, the solution with both flanges of S500 and the web of S355 is more economical. With increased load, the hybrid cross-sections start to have a positive effect on the minimum cost. The cost savings vary from 5% to 10%. In all cases, the top flange is made of S700. The web is S355, except for the largest load and the largest span, in which case it is S500. The bottom flange is of S700, except for the case $q=60$ kN/m, $L=6$ m, where it is of S355.

The cost distribution of the minimum cost solution is shown in Figure 2. It can be seen that the material cost is 50% of the total cost. Erecting cost plays an important role with a 16% share. Beam welding and painting are also relatively important, with 11% share each. Sawing, blasting and transport contribute very little to the total cost.

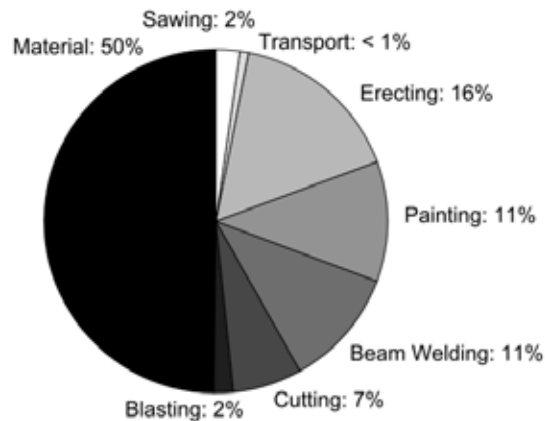


Figure 2. Cost distribution of the minimum cost beam. $q=60$ kN/m, L .

Discussion

In the above, the criterion values of the solutions were investigated. It is also interesting to study the actual designs that lead to the optimum solutions, i.e. to focus on the design space. A common feature of optimum designs is that the width of the flange is kept relatively low. The maximum flange width among the minimum weight solutions is 210 mm. Out of 126 cases, 83 solutions have flange width of 100 mm, i.e. the minimum value. Similarly, the thickness of the web is kept close to the minimum value of 5 mm. The maximum web thickness appearing in the minimum weight solutions is 8 mm and, in 99 of the 126 problems, the optimum web thickness is 5 mm. Thus, the strength and stiffness of the cross-section were increased mainly by increasing the web height and flange thickness. Consequently, the top flange was most often in Class 1 or 2, whereas the web is in Class 3 or 4. Similar behaviour is observed for the minimum cost designs.

In 68 of 126 cases, the minimum weight and minimum cost solutions coincide. There are also cases, where the minimum weight solution is more economical than the minimum cost solution and vice versa. This indicates, that the PSO was not able find the correct minimum cost or minimum weight solution. In all cases, the differences between the minimum cost and minimum weight solutions are very small.

On the other hand, for given load and span, the minimum weight and minimum cost solutions do not coincide in most of the cases, when comparing the different steel grade combinations. In Figure 3, the minimum cost and minimum weight solutions for $q=60$ kN/m, and $L=8$ m are depicted in the criterion space. It can be seen that the minimum cost solution is obtained in Case 4 (both flanges S700, web S355), and the minimum weight solution is obtained in Case 6 (flanges and web S700). The cost of the minimum weight solution is 556.55 €, whereas the minimum cost is 488.25 €. Thus, the minimum weight solution is 14% more expensive to manufacture. The minimum weight is 302.70 kg. The weight of the minimum cost solution is 317.14 kg, which corresponds to 4.7% increase. The solution of Case 5 (flanges S700, web S500) represents a compromise solution between minimum weight and minimum cost. The weight is 304.58 kg, which corresponds to only 0.6% increase from the minimum weight, whereas the cost 529.93 € corresponds to 4.8% decrease in manufacturing cost compared with the minimum weight design. Such trade-off information is useful, if there is uncertainty in the parameters of the cost function.

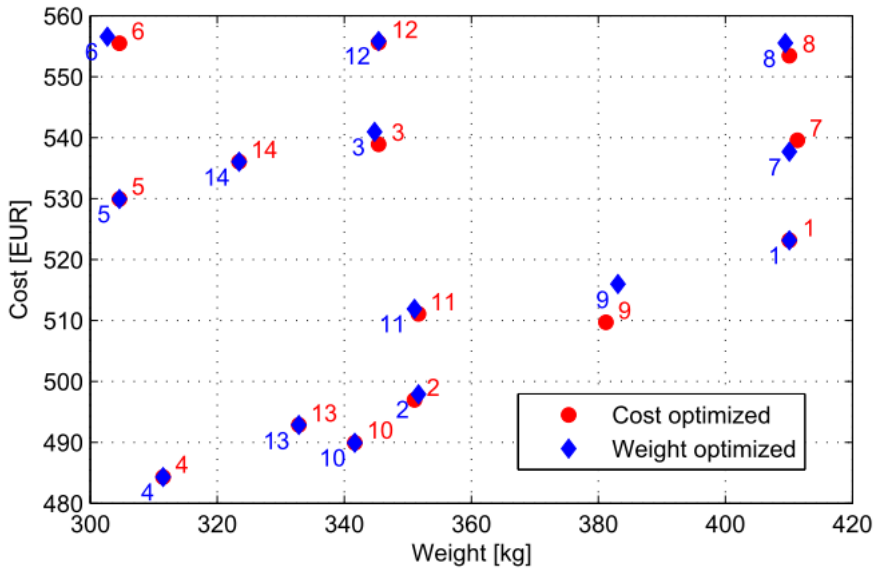


Figure 3. Minimum cost and minimum weight solutions of the WI-beam. $q=60 \text{ kN/m}$, $L=8 \text{ m}$.

CONCLUSION

The examples considered in the paper indicate that for geometrically double symmetric WI-beams under uniform lateral load, substantial savings in weight can be achieved by employing high strength steel. On the other hand, for smaller loads, the weight reduction can be relatively small, even marginal. With current material and fabrication costs, HSS tends to produce more expensive solutions than the conventional S355 cross-section for small loads. However, for larger loads, the cost difference is marginal (few percent), and for high loads and large spans, HSS solutions are more economical. Hybrid cross-sections can reduce the manufacturing cost up to 10% according to the case studies of this paper. In order to get real information on the cost savings provided by HSS it is essential to get measured up-to-date data of all actions needed in fabrication. The cost data used in this study is taken from (Haapio, 2012) and it is, in a way, mean data available for S355 steel. For HSS, this data is extrapolated using the given factors for material, welding and sawing costs.

The most economical combination of steel grades depends strongly on the load and span of the beam. It is normally very difficult to find the most economical solution by trial and error. For the designer, optimization provides an efficient way of obtaining good solutions quickly.

ACKNOWLEDGEMENTS

This study was carried out as part of a European research project RUOSTE, funded by the Research Fund for Coal and Steel.

REFERENCES

- Bernt Johansson. Buckling resistance of structures of high strength steel. In Hans-Peter Günther, editor, *Use and Application of High-Performance Steel for Steel Structures*, pages 120–128. IABSE, 2005.
- EN 1993–1–1. *Eurocode 3: Design of Steel Structures. Part 1–1: General rules and rules for buildings*. CEN, 2005.
- EN 1993–1–5. *Eurocode 3: Design of Steel Structures. Part 1–5: Plated structural elements*. CEN, 2006.
- Jaakko Haapio. *Feature-Based Costing Method for Skeletal Steel Structures Based on the Process Approach*. PhD thesis, Tampere University of Technology, 2012.
- James Kennedy and Russell Eberhart. Particle swarm optimization. In *IEEE International Conference on Neural Networks*, pages 1942–1948, 1995.
- Petri Ongelin and Ilkka Valkonen. *Welded profiles EN 1993-handbook*. Rautaruukki Oyj, 2010. In Finnish.
- Riccardo Poli, James Kennedy, and Tim Blackwell. Particle swarm optimization – an overview. *Swarm Intelligence*, 1:33–57, 2007.

HIGH STRENGTH STEEL IN TUBULAR TRUSSES

Teemu Tiainen

Kristo Mela

Timo Jokinen

Markku Heinisuo

Tampere University of Technology, Tampere, Finland

ABSTRACT

This paper deals with weight and cost optimization of Warren-type welded tubular roof trusses with and without verticals. Specially, the effect of steel grade is studied. The trusses are optimized being either S355, S500, S700 or hybrid solutions. Costs are calculated based on features of the trusses. The starting point is the exact geometry of the truss from which finite element analysis model is derived. This approach allows the resistance and other requirements of Eurocodes for both for the members and the joints to be used as constraints. Design variables are the height of the truss, the locations of the joints, gaps at the joints and the member sections (cold-formed square tubes). The resulting mixed-integer optimization problem is solved using the particle swarm optimization (PSO) algorithm. The results imply a significant saving in weight when using high strength steel. Cost reduction is smaller but existent. The results motivate the use and further research of high strength steels in building products.

INTRODUCTION

Tubular steel trusses are widely used in buildings to carry roof loads due to nice appearance, good economic and load bearing performance. Active research in the area has produced efficient and reliable analysis methods. The natural step after analysis is optimization. The three basic approaches found in structural optimization literature are sizing, shape and topology optimization [1] and this classification applies to trusses as well. In sizing optimization of a tubular truss, the design variables are the sections of each member. The problem can be formulated either continuous or discrete. For continuous design variables many optimization approaches have been proposed [1, 2]. However, in practical design problems the profile choice has to typically be made from steel supplier's catalogue resulting in discrete problem.

Truss optimization and cost analysis of steel structures have both been under active research work (see for example [3, 4, 5]). What the authors find missing so far in the literature is a consideration of using high strength steels (HSS) in tubular trusses. Therefore, the aim of this study is to find out by using optimization if the use of HSS in tubular steel trusses results in more economical solutions than with regular (S355) steel. When comparing trusses made of different steel grades it is essential to consider the costs, not only their weights. Steel grade has effect both on the material costs and on the fabrication costs. Weight affects transport and erection costs thus making it important as well.

In contrast with typical approaches, the starting point of the analysis is the parametric geometrical presentation of the truss. Sizing variables as well as geometrical dimension variables are present leading into mixed-integer problem. The example structures used are Warren type trusses with two possible layouts.

OPTIMIZATION FORMULATION

In this optimization formulation two types of Warren type tubular trusses (Fig. 1) are considered with Eurocode based constraints together with weight and cost as objective functions. Starting point of the optimization is the vector of design variables (19 or 23 elements) and other parameters that define the exact geometry of the truss. From this geometry, a finite element model using *Euler-Bernoulli* beam elements is derived. The braces of both models are aligned but in the finite element model brace elements are extended to point where two braces next to each other would intersect. In this case, a very rigid eccentricity element connects the braces to chord.

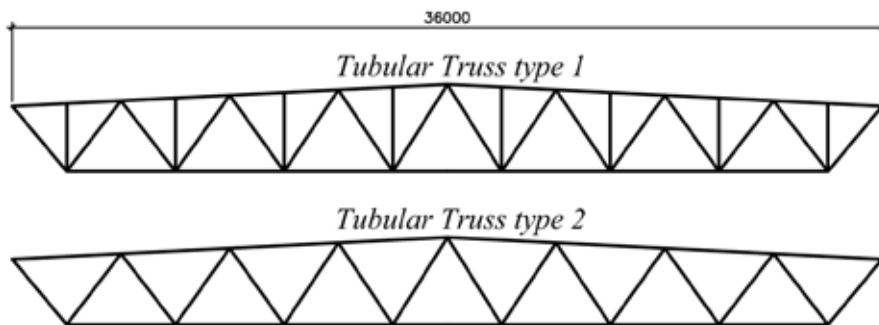


Figure 1. Two types of trusses considered.

From the finite element model, stress resultants N , Q_z and M_y are acquired and they are utilized to perform the resistance check of members and joints as required in standards EN 1993-1-1 [6] and EN 1993-1-8 [7] dealing with members and joints, respectively. For high strength steel and hybrid solutions some of the design had to be extrapolated in some cases giving very conservative results. In cost calculation, a very general method proposed by Haapio [8] is adopted.

The optimization problem of structural weight can be written as

$$\begin{aligned} \min f_{\mathbf{x}} &= \rho s i = 1 n m A i L i, g \\ \text{s. t. } \mathbf{x} &\in \Omega \end{aligned}$$

where, \mathbf{x} is the vector of design variables including both discrete sizing variables and continuous geometry variables and Ω is the feasible set; a set of solutions that comply all the constraints $g_i(\mathbf{x}) \leq 0$ derived from Eurocodes. The cost optimization problem has the same constraints as formulation 1 and can be written as

$$\begin{aligned} \min f_{\mathbf{x}} &= C S M + i = 1 n m (C B + C S + C W) + C P \\ \text{s. t. } \mathbf{x} &\in \Omega \end{aligned}$$

RESULTS

The optimization problem was solved with particle swarm optimization method. It is a heuristic method without rigorous mathematical basis and it usually yields good solutions but sometimes fails badly. The runs were repeated 10 to 20 times but still the results cannot be considered optimal but best found. The main findings can be seen in Figure 2 and 3 which present the best found weight and cost compared to those values of regular steel (S355) for types 1 and 2, respectively. It can be seen that weight reduction by using high strength steel is significant (20% to 30%). The costs are lower especially with the higher loading.

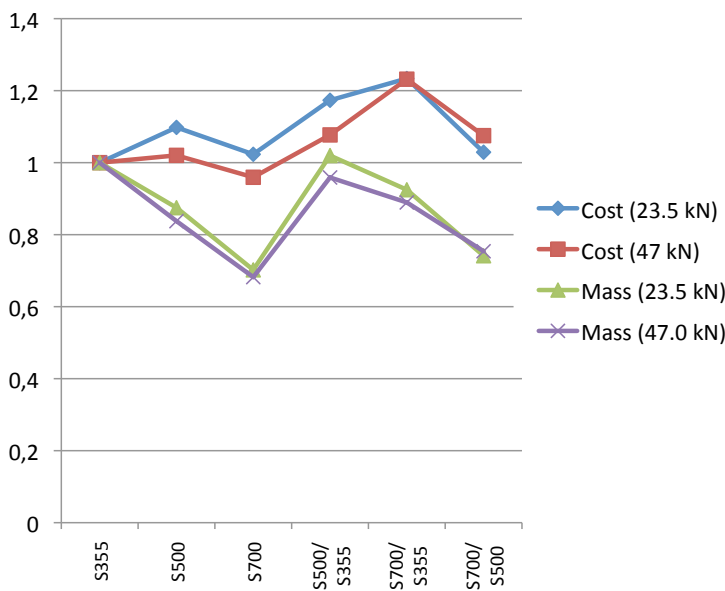


Figure 2. Type 1 truss results compared to S355/S355 solution.

CONCLUSIONS

The starting point of the optimization should be the geometrical presentation of the truss in order to check all requirements, such as geometrical rules of codes and correct structural analysis model with eccentricities. In sizing and shape optimization this will result in non-linear mixed-integer optimization for which heuristic methods can be used. As the problems are very demanding and the method does not include checks for optimality, the optimized results may need extra manual enhancement. Weight reductions compared to S355 trusses were of around 20% for S500 and 30% for S700. The cost reduction on the truss type Warren type truss without verticals performed better, at around 15%. Reductions for hybrid trusses were between these numbers, but for S700/S500 (chords S700, braces S500) the reductions were about the same as for S700/S700 trusses.

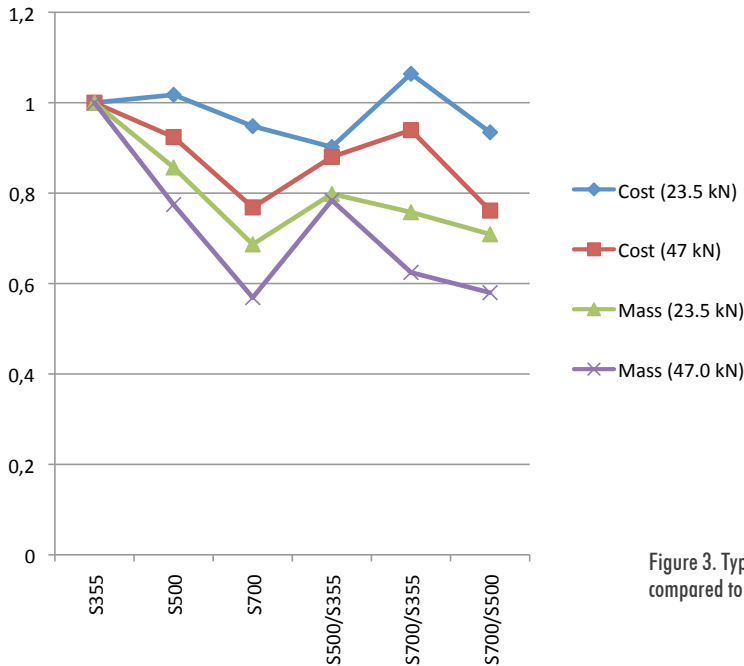


Figure 3. Type 2 truss results compared to S355/S355 solution.

The results demonstrate that the use of HSS is economical in tubular trusses applying the design rules of the present Eurocodes even though some of the rules “penalize” high strength steels. These issues should be solved in the future and the fabrication costs of HSS tubular trusses can be reduced and more savings achieved.

REFERENCES

- [1] Uri Kirsch. Structural optimization. Springer-Verlag, 1993.
- [2] Raphael T. Haftka and Zafer Gürdal. Elements of structural optimization. Kluwer academic publishers, 1992.
- [3] Jozsef Farkas and Károly Jármai. Analysis and Optimum Design of Metal Structures. A. A. Balkema, Rotterdam, 1997.
- [4] D. A. Nethercot. Towards a standardization of the design and detailing of connections. Journal of constructional Steel Research, 46:3–4, 1998.
- [5] L. Pavlovčič, A. Krajnc, and D. Beg. Cost function analysis in the structural optimization of steel frames. Structural and Multidisciplinary Optimization, 28:286–295, 2004.
- [6] CEN. EN-1993-1-1. Eurocode 3: Design of steel structures. Part 1–1: General rules and rules for buildings., 2006.
- [7] CEN. EN-1993-1-8. Eurocode 3: Design of steel structures. Part 1–8: Design of joints., 2006.
- [8] Jaakko Haapio. Feature-Based Costing Method for Skeletal Steel Structures based on the Process Approach. PhD thesis, Tampere University of Technology, 2012.

TUBULAR COMPOSITE COLUMNS IN A NON-SYMMETRICAL FIRE

Markku Heinisuo
(markku.heinisuo@tut.fi)

Timo Jokinen

Tampere University of Technology, Tampere, Finland

ABSTRACT

A considerable number of studies have been conducted worldwide on columns with fires that act on all four sides (symmetrical fire). In real buildings, columns are often embedded. Results of numerical analyses for reinforced concrete filled square steel tubes columns in non-symmetrical fires are presented for a total of 150 cases. An ISO 834 fire acts constant along the column on one, two adjacent or three sides. Three embedding systems are considered for the remaining sides: adiabatic, concrete wall and sandwich panel. When fire acted on one, two adjacent or three sides, the fire resistance times were on average about 3.4, 2 and 1.3 times longer than in a symmetrical fire. The final failure mode and corresponding resistance time depend on the direction of the initial bow imperfection. Experimental tests are needed to verify the results.

INTRODUCTION

Reinforced concrete filled tubular (CFT) columns combine the advantages of both steel and concrete materials, such as: attractive appearance, structural efficiency, fast construction technology and high fire resistance [1], [2]. A considerable number of numerical simulations and tests have been conducted worldwide on fires that act on all four sides of a column. These cases are used for the validation of the analysis models developed in this study. In [3] and related papers of the authors, composite W-shaped columns with different embedding systems are examined both experimentally and analytically. Likewise, in [4] concrete filled rectangular steel tubes in non-symmetrical fire are examined both experimentally and analytically. The paper excludes square columns and all columns are without reinforcement. Reference [4] reports that some columns finally collapsed towards the fire.

This paper presents results of numerical analyses for tubular composite columns in non-symmetrical fires. Reinforced concrete-filled square steel tubes of three sizes and two buckling lengths are considered at given central axial loads. The fire is assumed to be constant along the column length. The sides on which fire does not act are assumed to be embedded. Three different embedding systems are considered: adiabatic (see above), concrete wall, and steel-mineral wool-steel sandwich panel. Axial loads are defined so that they represent the maximum ultimate concentric loads for symmetrical cases with

respect to specified fire resistance times: 30, 60, 90 and 120 minutes. A total of 150 cases were analysed.

Thermal and mechanical analyses were conducted using the finite element software ABAQUS/Standard. Geometrically identical 3D finite element method (FEM) models were used both for thermal and mechanical analyses. The material models for steel tubes, reinforcement and concrete are presented in Eurocode 4 [5]. The effect of an initial bow imperfection is considered. The shape of the imperfection corresponded to the buckling mode of the column for the lowest buckling load in ambient conditions. All cases were analysed using an amplitude of span/666 for the imperfection towards the fire. Some cases were also studied with the initial imperfection away from the fire. All columns were hinge supported at both ends. The end nodes of the columns were fixed to the plane using the coupling command of ABAQUS in the mechanical analysis.

The reinforcement was modelled using one-dimensional stringer elements. 3D continuum finite elements were used both for the tube and the concrete. Thermal analysis was conducted first and the temperatures were stored. Then, mechanical analysis was done with a constant central axial load by increasing the temperatures inside the column according to the stored temperatures. Thermal analysis was done using a 3D continuum FE model for the entire column. To verify the numerical model, the temperatures and fire resistance times in the symmetrical fire were compared to results available in Reference [6] and [7]. Temperatures were also calculated using the Safir software [47]. In summary, the thermal analysis model seemed to work rather well in all cases considered.

Material models for concrete, tubes and reinforcement were taken from [5]. The Elastic and Plastic options of ABAQUS were used for steel. The Elastic and Concrete Sheared Cracking options of ABAQUS were used for concrete. Bi-linear and tri-linear stress-strain relationships, including those of [8], did not work properly, which led to convergence problems. Similar trials have been reported in [8]. Finally, a simple elastic stress-strain relationship was applied to concrete on the tension side. The resistance times were based on points in time when convergence was no longer reached using ABAQUS implicit and RIKS methods. The used model gives results which are close to [7] but for the smallest columns. Table 3 shows a comparison of fire resistance times between symmetric and non-symmetric fires.

Table 1. Ratios of fire resistance times for non-symmetric versus symmetric fires.

#	CFT column	Target	Load [kN]	Ratio to 4S case [-]									
				4S	3S	2S	1S	C3S	C2S	C1S	S3S	S2S	S1S
1	150x150, 2m	R30	476	1.00	1.43	1.85	3.56	1.52	2.37	4.12	1.35	1.73	3.45
2	150x150, 2m	R60	174	1.00	1.37	1.73	2.68	1.50	2.36	3.24	1.30	1.68	2.60
3	150x150, 3m	R30	303	1.00	1.23	1.43	3.73	1.20	1.42	3.56	1.22	1.39	2.89
4	150x150, 3m	R60	110	1.00	1.00	1.49	2.92	1.07	1.91	3.30	0.99	1.43	2.53
5	250x250, 3m	R30	1975	1.00	1.53	2.49	4.63	1.51	2.26	5.97	1.51	2.35	5.14
6	250x250, 3m	R60	1094	1.00	1.44	2.51	4.22	1.54	3.15	4.22	1.41	2.42	4.18
7	250x250, 3m	R90	728	1.00	1.29	2.08	2.81	1.33	2.70	2.81	1.28	2.07	2.81
8	250x250, 3m	R120	443	1.00	1.19	1.95	2.01	1.23	2.01	2.01	1.17	1.90	2.01
9	250x250, 5m	R30	1171	1.00	1.50	1.94	2.89	1.47	1.72	3.13	1.47	2.14	2.89
10	250x250, 5m	R60	634	1.00	1.17	2.54	3.65	1.15	2.29	4.26	1.17	2.27	3.65
11	250x250, 5m	R90	406	1.00	1.33	2.51	2.68	1.19	1.89	2.68	1.15	2.40	2.68
12	250x250, 5m	R120	233	1.00	1.15	1.89	1.89	1.53	1.89	1.89	1.14	1.87	1.89
13	400x400, 3m	R30	8031	1.00	1.27	2.05	4.60	1.30	2.11	4.99	1.26	2.01	-
14	400x400, 3m	R60	5942	1.00	1.18	2.23	4.31	1.23	2.34	4.31	1.15	2.09	-
15	400x400, 3m	R90	4868	1.00	1.05	2.24	3.11	1.03	2.40	3.11	1.18	2.14	-
16	400x400, 3m	R120	4053	1.00	0.93	2.37	2.62	0.93	2.57	2.62	1.08	2.24	-
17	400x400, 6m	R30	5624	1.00	1.46	2.72	3.69	1.37	3.26	4.41	1.44	2.59	-
18	400x400, 6m	R60	3564	1.00	1.50	3.17	4.36	1.76	3.99	4.36	1.46	3.06	-
19	400x400, 6m	R90	2625	1.00	1.60	3.18	3.18	1.74	3.18	3.18	1.57	3.17	-
20	400x400, 6m	R120	2045	1.00	1.53	2.35	2.35	1.55	2.35	2.35	1.50	2.35	-

The main conclusions from this study are that composite tubular columns resisted the same axial load longer in non-symmetric fires than in symmetric fires. If a column is embedded in concrete on three sides (fire acts on one side), fire resistance time increases 2.7-fold, in the case of two adjacent embedded sides it increases 1.4-fold, and with one embedded side 1.1-fold compared to a symmetric fire. In the case of embedding with sandwich panels, the fire resistance times did not increase as much as with concrete embedding. The increase is about the same as in the adiabatic case. Slender columns tended to collapse towards the fire, stocky columns finally collapsed away from the fire. It is recommended that initial bow imperfection should be considered in directions both away from and towards the fire. Tests are needed to verify the calculations.

ACKNOWLEDGMENTS

CSC Oy deserves special thanks for providing ABAQUS license, computing time and general assistance. The financial support of Seinäjoen Seudun Elinkeinokeskus (SEEK) is also gratefully acknowledged.

REFERENCES

- [1] Espinos A., Romero M., Hospitaler A. Advanced model for predicting the fire response of concrete filled tubular columns, *Journal of Constructional Steel research*, 66(8–9), pp. 1030–1046, 2010.
- [2] Ding J., Wang Y.C. Experimental study of structural behavior of steel beam to concrete filled tubular column assemblies with different types of joints, *Engineering Structures*, 29(12), pp. 3485–3502, 2007.
- [3] Pires T., Correia A., Rodrigues J. Silva J., CHS and partially encased columns subjected to fire, *Proceedings of EUROSTEEL 2011 6th European Conference on Steel and Composite Structures, ECCS, Brussels*, pp. 1569–1574, 2011.
- [4] Yang H., Liu F., Zhang S. Fire performance of CFST columns in non-uniform fire, *Proceedings of EUROSTEEL 2011 6th European Conference on Steel and Composite Structures, ECCS, Brussels*, pp. 1563–1568, 2011.
- [5] EN 1994-1-2 – Eurocode 4: Design of composite steel and concrete structures – Part 1–2: Structural fire design, CEN, Brussels, p. 110, 2006.
- [6] CIDECT, Improvement and extension of the simple calculation method for fire resistance of unprotected concrete filled hollow columns, Saint-Remy-les-Chevreuse, France, CTICM, CIDECT research project 15Q-12/03, 101 p, 2004.
- [7] TRY, Betonit ytteisen ter sliittopilarin suunnitteluohje, Julkaisumonistamo Etel ranta Oy, Helsinki, 2004. (in Finnish)
- [8] Hong, S., Varma, A., Analytical modeling of the standard fire behavior of loaded CFT columns, *Journal of Constructional Steel Research*, 65(1), pp. 54–69, 2009.

INFLUENCE OF NATURAL FIRE SCENARIO BY CFD AND FEM ANALYSIS COUPLING ONTO STEEL CONSTRUCTION STRUCTURAL RESPONSE

Michał Malendowski
(michal.malendowski@put.poznan.pl)

Adam Glema
(adam.glema@put.poznan.pl)

Institute of Structural Engineering
Poznan University of Technology, Poznan, Poland

ABSTRACT

The problem of numerical analysis of steel structure under natural fire is considered. The emphasis is put on the importance of coupling between computational fluid dynamics (CFD) and finite element analysis (FEA) codes with respect to proper calculation of temperature field inside the structural members. Models preparation, simulation analysis and results verification precede research on comparing of computations of structural analysis within steel construction. Computations consist of two sequential numerical simulations: CFD analysis of fire evolution with the use of FDS software, introducing temperature and heat flux to thermo-mechanical part of structure respond with the use of ABAQUS finite element system. Behaviour of the steel construction under fire is comprehensively discussed to get a safe design with the checks of ultimate limit state. The main goal of the paper is to analyse different fire scenarios within the building by taking into account, for example, fire load size and placement, and its influence on the fire development, temperature and heat distribution, as well as history and state of deformation and stresses in steel structure. A set of numerical examples is selected and computed for a range of representative fire scenarios. Conclusions are formulated to present the ability to control the structure under the fire accident and give directions for designing of safe construction.

INTRODUCTION

Nowadays the usage of natural fire approach for the design of new structures is gradually rising. In this paper the most general type of this approach is considered, namely designing using coupled CFD-FEA procedures. Difficulties are caused especially in the translation of heat condition resulted from CFD fire analysis into solid mechanics boundary conditions, when the model differences between those two codes are significant. Therefore, to study the influence of fire scenario onto the structural response of structures under natural fire, the coupling procedure and boundary conditions translation method is developed.

In this work firstly the standard approaches used in current fire engineering practice are briefly introduced. Then the theoretical background of the heat transfer problem is invoked as the base for the development of further translation method. Finally the description of proposed method, implementation, its verification and a test case of steel structure under different natural fire scenarios is discussed.

THEORETICAL BACKGROUND OF THE HEAT TRANSFER PROBLEM

Calculation of heat transfer at the interface between solid and gas phase needs to take into consideration two main and inseparable, in that sense, heat transfer sources: convective and radiative heat flux. The net heat flux into the unit surface is the algebraic sum of incoming heat fluxes by convection and radiation, and can be expressed by the well know expression:

$$q_{net} = q_{con} + q_{rad} \quad (1)$$

As far as the two incoming heat quantities are inherent for the general definition of the boundary conditions in heat transfer problem consideration, they two different physical phenomena and from the mathematical point of view can be derived separately.

CONVECTIVE HEAT FLUX

The convective heat flux is basically proportional to the difference between the gas and surface temperatures at the interface between solid and gas phase, and is usually expressed as:

$$q_{con} = \alpha \theta_g - \theta_s \quad \text{Wm}^2 \quad (2)$$

Where α , θ_g , and θ_s are respectively the coefficient of heat transfer by convection [$\text{W}/\text{m}^2 \text{K}$], gas and solid surface temperatures [K].

RADIATIVE HEAT FLUX

From the structural point of view, the radiative heat flux into the solid phase corresponds to the absorbed radiation resulted from the incident radiation coming into the solid surface. From the point of view of CFD field modelling, the constitutive radiative heat transfer equation can be obtained from the equilibrium of intensity change in a particular direction across elemental volume of fluid medium.

Finally, the radiant incoming heat flux vector $q_{rad,inc}$ can be calculated as an integral from the incident intensity over the spherical domain of interest. The net radiant heat flux absorbed by the solid body q_{rad} can be then calculated as a difference between the incident ($q_{rad,inc}$) and outgoing heat, using the well known equation for the surface radiation:

$$q_{rad} = q_{rad,inc} - \varepsilon \sigma \theta_s^4 \quad (2)$$

where ε is the emissivity of solid surface and σ is the Stephan-Boltzmann constant.

HEAT FLUX AND SECTION TEMPERATURES CALCULATION METHOD

In the proposed approach, the section temperature calculation takes into account both convective and radiative heat fluxes facing the particular section surfaces. As long as convective heat flux is dependent only on the constant coefficient of the heat transfer by convection and fluid-surface temperature difference, calculation of temperature does not cause problems. This means that special attention must be paid for the proper recognition of radiation's directions. To do that, authors introduce the definition of face view angles as lower and upper limit of radiation direction that can reach particular point on the section surface (Fig. 1).

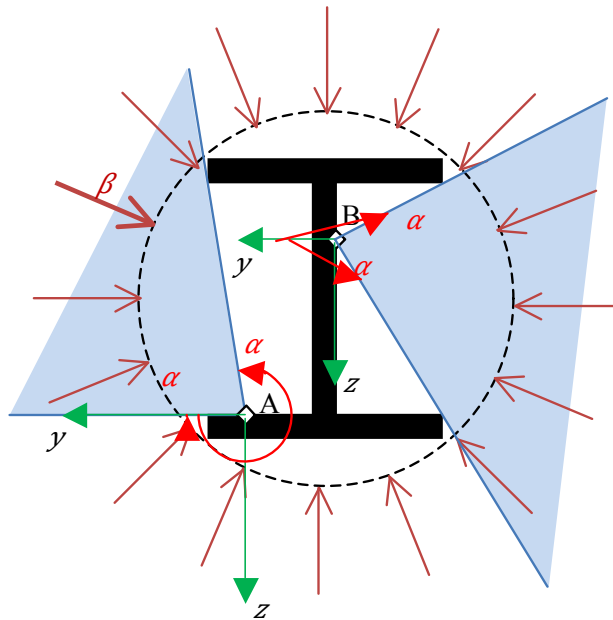


Figure 1. Geometrical visualization of view angles α_1 and α_2 for points A and B and corresponding angle of radiation vector β .

HEAT TRANSFER FROM AMBIENT BOUNDARY INTO THE SECTION

The above approach is useful for the derivation of boundary conditions at the section's surface. Assuming that the net stored heat is equal to the net received heat, the relevant partial differential equation can be reduced to a zero-dimensional case and becomes an ordinary differential equation with only time dependence:

$$q = hc\rho d\theta dt \quad (3)$$

where q is the net heat flux coming into the element and h , c , and ρ are the thickness of section's wall, specific heat and density, respectively.

IMPLEMENTATION

Implementation of the proposed approach is made by coupling the CFD code called FDS McGrattan et al. [1] and FEM program Abaqus [2]. The formulation is appropriate for sequential incremental coupling. However, single boundary transfer is considered in the following investigations.

COUPLING METHOD

When the structural elements are not present in the CFD model, the coupling must be arranged in such a way, so as to provide sufficient information for external calculation of section temperatures. This means that even if elements themselves are not a part of CFD analysis, their position must be somehow marked in that model. The idea is then to represent the existence of structural member into the CFD model by introduction of the output request in the point corresponding to the real position of the member.

BEAM FINITE ELEMENTS

Since the main goal of most structural engineering studies within the field of fire engineering is the proper prediction of structural response in fire, the approach taken is to use beam finite element throughout applying the above procedure for the beam's integration points.

COMPUTATIONAL EXAMPLE

The structure under consideration is a single-compartment frame structure with dimensions 8m by 20 m, height equal to 3,20 m at the ridge and 2,50 m at the eaves. The geometry of that structure comes from the natural fire full scale test conducted by Pyl et al. [3].

The structure is a standard steel assembly for small halls. All columns, girders and purlins are made from I-sections: IPE140, IPE160, IPE120, respectively. The distance between frames is equal to 5,0 m.

LOADS

Two contrasting fire scenarios are considered: a localized fire in the middle of the compartment and a uniformly distributed fire load spread throughout the floor. The fire is described by given heat release rate per unit area. The mechanical load is primarily reduced to dead load only (taking into account 0,3 kN/m² of cladding system), which corresponds to the experimental conditions (no snow and wind) and favours the goals of this contribution. Finally also three additional load cases are introduced, to check the structural behaviour of construction in more severe conditions.

RESULTS

The results are obtained both for thermal and mechanical data comparison between two selected fire scenarios. A special emphasis is also made to verify the coupling method used for translation of heat condition between FDS and Abaqus.

According to simulations, structure lasts more than 60 minutes, when no other dead load acts on the frame. When mechanical load increases, fire resistance time decreases, which is to be expected. In accordance with the limited number of test cases, no pattern of dependence between mechanical load and fire resistance time was observed for both fire scenarios. A summary of results is presented in Table 1.

Table 1. Comparison between fire resistance times for different fire scenarios.

	fire resistance time (minutes)			
	1,0 dead load	1,5 dead load	2,0 dead load	2,5 dead load
Pool	> 60	> 60	54	22
distributed	> 60	60	29	15
pool and distributed	-	-	1.86	1.47

CONCLUSIONS

Development of contemporary structural engineering design standards, like Eurocodes, gives engineers more and more possibilities for evaluation of structural safety in fire. Nevertheless, it is still a major issue to examine, assuming certain level of accuracy, whole building or assembly in natural fire simulation using 3D approaches. The proposed method is a flexible tool responding to the need for incorporating natural 3D fire simulations for the evaluation of structural safety.

The heat transfer analysis on the interface between solid and fluid phase are formulated in the paper and simplified, but take into account both radiative and convective heat fluxes and temperatures as well, at specific points on the section surface. The results obtained show significant difference in fire resistance time between pool fire scenario and uniformly distributed fire. The simulations show that distributed fire scenario is more severe for the structure than a local fire, even if the local fire per unit area power is approximately four times greater.

The next step in implementation of the method is to extend scripts and run more exact calculations of heat transfer coefficients for convection on the fluid-solid interface and to take into account the radiation in section's cavities with the view factors application. Special laboratory tests of different structural elements under natural fire wait to be performed for experimental validation of the method under investigation.

REFERENCES

- [1] McGrattan, K., Hostikka, S. and Floyd, J., *Fire Dynamics Simulator (Version 5) – Technical Reference Guide*, NIST Special Publication 1018–5, 2010.
- [2] McGrattan, K., Hostikka, S. and Floyd, J., *Fire Dynamics Simulator (Version 5) – User's Guide*, NIST Special Publication 1019–5, 2010.
- [3] Pyl, L., Schueremans, L., Dierckx, W., Georgieva, I., *Fire safety analysis of a 3D frame structure based on a full-scale fire test*, Thin-Walled Structures, 61, pp. 204–212, 2012.

MEMBRANE STRUCTURES SUPPORTED BY A FRAME OF THIN-WALLED CLOSED SECTIONS

Alexander Tusnin
Professor, Dr. Sc.

Olga Tusnina
PhD Student

Moscow State University of Civil Engineering (MGSU), Moscow, Russia

ABSTRACT

In the paper the work of membrane structures on the rectangular plan with plane support contour when membrane eccentrically fastened is considered. Features of strain-stress state of the membrane structure with support contour made of closed section profiles are studied. An analysis of the differential equation of the twist angles of the contour has allowed to establish behaviour of the system when membrane is fastened eccentrically to support contour. This is defined by the relations that include the pure and restraint torsional stiffness of the contour, span, thickness and elastic modulus of the membrane, eccentricity of its fastening to contour and a sectorial coordinate of the membrane edge. Test numerical analyses of the membrane models validated the derived laws.

INTRODUCTION

Membrane structures are widely used as roofing elements in many kinds of buildings [4, 8, 9]. Typically, a membrane structure is the thin metal shell (membrane) fastened to the support boundary. Supports can be made of steel, reinforced concrete or concrete-filled steel tubular members. In the membrane structures with spans 6–18 m supports are often made of thin-walled welded closed profiles. For simplification the membrane structure can be fastened to the edges of the rectangular boundary frame (Fig. 1). In this case, because of the eccentrically applied membrane forces, the frame begins to twist.

Many researchers are involved in studies of membrane structures [5, 7]. A study of the behaviour of membrane structures with thin-walled support frames of closed profile experiencing restrained torsion is of considerable practical interest.

THEORETICAL CONSIDERATIONS

Torsion of closed thin-walled rectangular profiles is accompanied by their cross-sectional warping. With the restraining of free warping (in the places of fastening and connections with other members), additional normal stresses occur in thin-walled profile and its torsional stiffness increases.

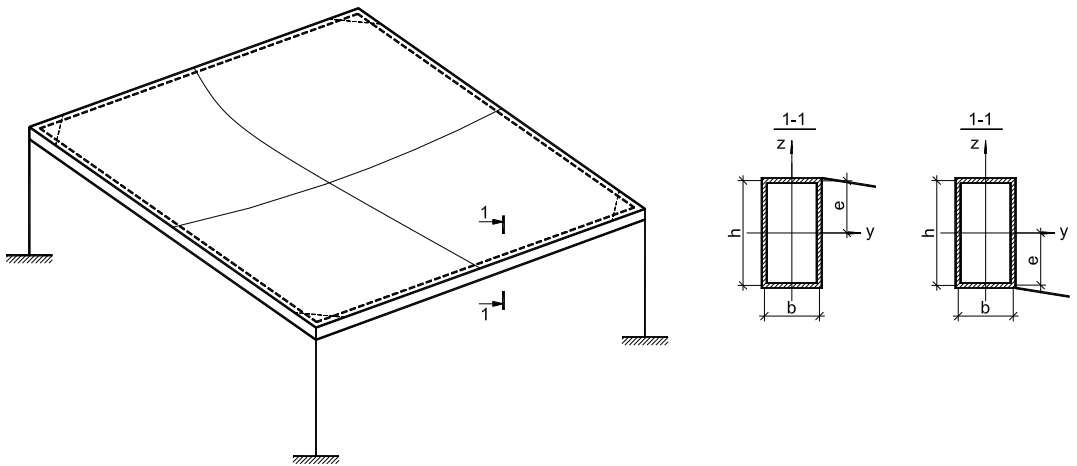


Figure 1. View of membrane covering. Schemes of the membrane sheet fastening to support boundary frame of closed profile.

For the analysis of thin-walled open profile rods the well-known Vlasov theory is successfully applied [10]. Analogous to the theory used for thin-walled beams with open profile for beams with a close profile, the warping stiffness of the beam is introduced in addition to the pure torsion stiffness. The deformations of the supporting frame need to be taken in consideration when analysing thin-walled closed profile beams, especially when the membrane is connected to the support boundary with eccentricity. The interaction of twisted thin-walled support frame with the membrane has some special features and requires a further study.

METHODS

The simple model is studied with the aim of determination the main parameters influenced on the work of the system. The system consists of contour beam with the span $2a$ with fixed edges (constraints are set on the linear displacements in the plane perpendicular to the contour and on the angles of rotation) and flat membrane with the sizes $2a \times a$ and thickness t (fig. 2).

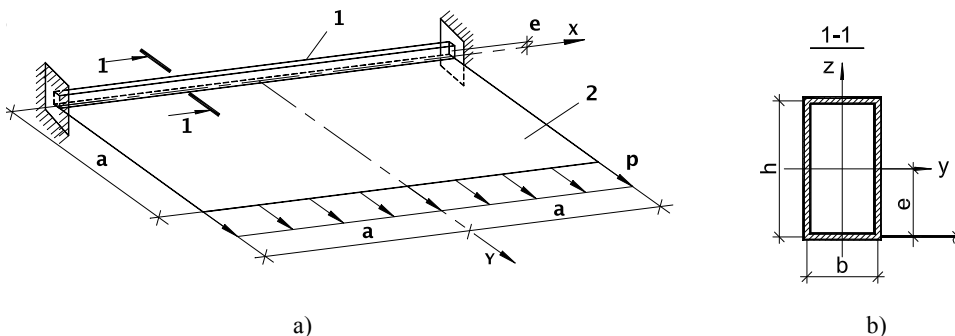


Figure 2. The studied system, a) general view; b) cross-section of the contour.

The sheet is fastened with eccentricity e at the height of the boundary beam. The uniformly distributed load p acts on the free edge of the sheet with the coordinate $y=a$. Numerical studies have been carried out using the program MSC NASTRAN. The analysis is carried out for half of the structure taking into account symmetry of the system by the introduction appropriate constraint at the axis of symmetry.

Initially, the problem was solved with the use of BEAM finite elements for the modelling of support boundary excluding torsional restraint. The steel membrane was modelled as PLATE finite elements (mesh 20×20) with thickness of 1 mm. The connection between the boundary beam and the membrane was modelled by using bars of high stiffness, with the eccentricity of membrane fastening. The size $a=6$ m, the load is $p=120$ kN/m, cross-section of boundary beam is $200 \times 100 \times 6$ mm. The design scheme of the considered membrane model is shown in Fig. 3. With the use of this model, the following results were obtained. The displacement of the membrane edge in the middle of contour beam in the direction of the Y-axis is equal to 17.5 mm, and the angle of rotation of the Boundary beam about its longitudinal axis (X-axis) is 0.526° .

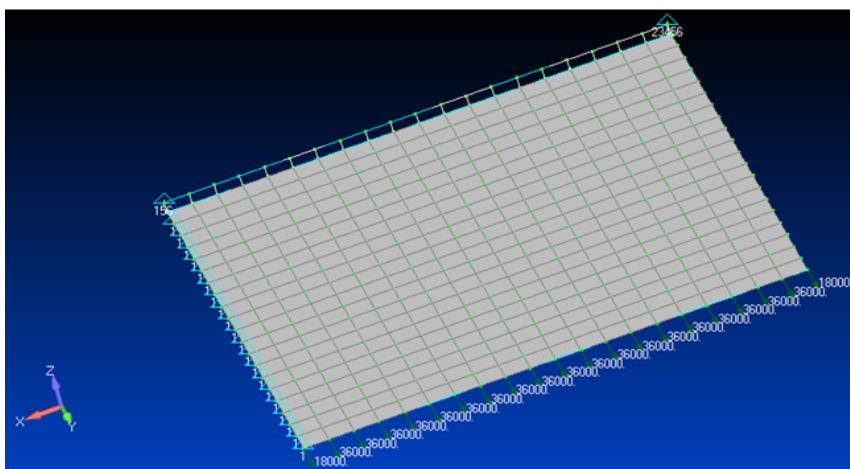


Figure 3. The numerical model when contour is modelled by BEAM finite elements.

The same membrane system with the same sizes and loads but with the boundary beam modelled using PLATE finite elements were analysed. The design scheme for this case of contour modeling is represented on the Fig. 4.

For the midspan of a boundary beam, the following results were obtained in this case. The displacement of the membrane edge in the Y-axis direction is 24 mm. The angle of rotation about the longitudinal axis is 0.0498° .

A comparison of the results for these two models allowed us to make following conclusions. Twist angle of the beam for the first model (0.526°) exceeds twist angle in the second model (0.0498°) more than 10 times. Displacements for the first model (17.5 mm) are smaller than for the second model (24 mm) by 27%.

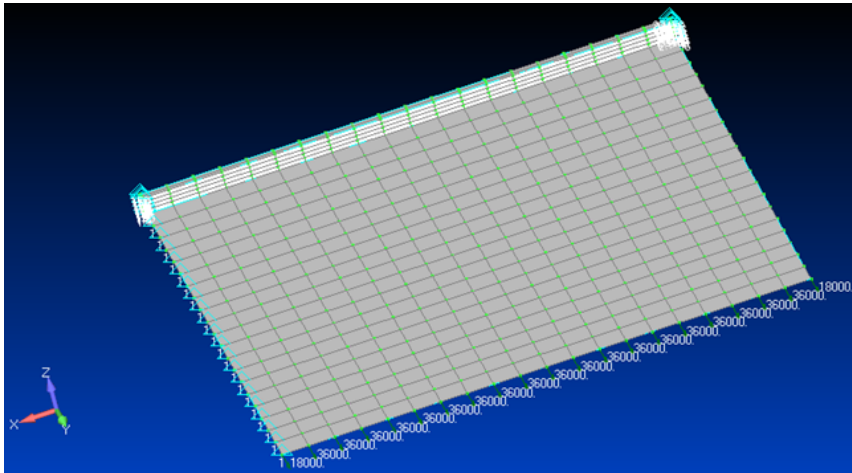


Figure 4. The numerical model when the boundary is modelled using PLATE finite elements.

Thus, required accuracy of the analysis is not achieved when use simple BEAM elements for modelling the support beams. Because of inability of the beam finite elements for the boundary, its interaction with the membrane need to be studied and the basic parameters influencing on the behaviours of structure need to be derived.

Let us consider the differential equation of the twist angles of thin-walled closed profile support beam about its longitudinal axis which is generally represented in the same view as for thin-walled open profile section [9]:

$$(GI_t)_k \frac{\partial^2 \theta}{\partial x^2} - (EI_\omega)_k \frac{\partial^4 \theta}{\partial x^4} + m - \frac{\partial b}{\partial x} = 0, \quad (1)$$

where, GI_t – the stiffness of the support contour on the pure torsion; EI_ω – contour sectorial stiffness; θ – twist angel of the contour; m - intensity of the distribution of torque; b – intensity of the distribution of bi-moment.

Equation (1) is valid in the absence of the bending of the beam. For this problem:

$$m = N_y e \cos \theta, \quad N_y = \frac{E_m t_m}{1 - \mu^2} \left(\frac{\partial v}{\partial y} + \mu \frac{\partial u}{\partial x} \right), \quad (2)$$

$$b = N_{xy} \omega, \quad N_{xy} = \frac{E_m t_m}{2(1 + \mu)} \left(\frac{\partial v}{\partial x} + \frac{\partial u}{\partial y} \right),$$

where, E_m , t_m – Elastic modulus and the thickness of the membrane; μ – Poisson ratio; u and v – the displacements of membrane through its fastening to a contour parallel to the axes X and Y respectively; e – the eccentricity of the membrane fastening to contour on the vertical; ω – the sectorial coordinate

of cross-section of the contour where the membrane is fastening, N_y – the normal force per unit length in membrane acting along Y-axis in the place of contour with membrane interface; N_{xy} – the shear force per unit length in membrane in the place of contour-membrane interfacing.

Given the well-known dimensionless parameters [6]:

$$\bar{u} = \frac{u a}{t^2}, \quad \bar{v} = \frac{v a}{t^2}, \quad \bar{\xi} = \frac{x}{a}, \quad \bar{\eta} = \frac{y}{a}, \quad (3)$$

Using relations (2), equation (1) can be represented as follows:

$$\bar{m} \frac{\partial^2 \bar{v}}{\partial \bar{\xi}^2} - \bar{m}_\omega \frac{\partial^4 \bar{v}}{\partial \bar{\xi}^4} + \frac{1}{1 - \mu^2} \left(\frac{\partial \bar{v}}{\partial \bar{\eta}} + \mu \frac{\partial \bar{u}}{\partial \bar{\xi}} \right) - \frac{\bar{\omega}}{2(1 + \mu)} \left(\frac{\partial^2 \bar{v}}{\partial \bar{\xi}^2} + \frac{\partial^2 \bar{u}}{\partial \bar{\xi} \partial \bar{\eta}} \right) = 0, \quad (4)$$

where, $\bar{m} = \frac{GI_t}{E_m t_m a e^2}$ – the relative stiffness of the contour on pure torsion;

$\bar{m}_\omega = \frac{EI_\omega}{E_m t_m a^3 e^2}$ – the relative sectorial torsional stiffness of the thin-walled

open profile contour; $\bar{\omega} = \frac{\omega}{a e}$ – the relative sectorial coordinate of the membrane edge.

In the derivation of equation (4) it is assumed that $\cos \theta = 1$ (for the twist angles $\theta \leq 18^\circ$ the error does not exceed 5%), and relative twist angle is equal to $\bar{\theta} = \frac{v}{e}$.

The relations include torsional stiffness of the contour, span, thickness and Elastic modulus of the membrane, eccentricity of its fastening to contour determine the behaviour of the system. Relative values m , m_ω and ω do not change with changing of absolutely values of the contour span, thickness, Elastic modulus of the membrane and contour, eccentricity of the membrane fastening etc. Given the above a simplified method of the analysis of membrane structures can be developed. In the frame of this method, the values of relative parameters will determine stresses and displacements occurring in the structure. The productivity of such an approach is proved by practice of design [8, 9]. The aim of this paper is to confirm the validity of the equations derived for the relative parameters (m , m_ω and ω).

For the thin-walled support contour of the closed rectangular profile [8] the following expressions are valid:

$$\text{The inertia moment on the pure torsion} - I_t = \frac{2b^2h^2t_k}{(h+b)},$$

$$\text{section inertia moment} - I_\omega = \frac{b^2h^2t_k(h-b)^2}{24(h+b)},$$

$$\text{section coordinate of the membrane edge} - \omega = \frac{hb \cdot (h-b)}{4 \cdot (h+b)}.$$

In the expressions for the inertia moments and section coordinate, the following symbols are used: t_k – the thickness of the contour wall, b and h – the width and the height of the profile on the middle surface of the cross-section.

Taking this into account the relative parameters of the membrane structure

for thin-walled closed profile contour with eccentricity $\dot{a} = \frac{h}{2}$ are equal:

$$\bar{m} = \frac{8Gb^2t_k}{E_m t_m a(h+b)}, \quad \bar{m}_\omega = \frac{Eb^2t_k(h-b)^2}{6E_m t_m a^3(h+b)}, \quad \bar{\omega} = \frac{b \cdot (h-b)}{2 \cdot (h+b) \cdot a}.$$

The correctness of these relations for the generalized parameters is confirmed by the results of numerical studies of the modelling of boundary by the PLATE finite elements. The validity of the approach was confirmed by the analysis of structures with the eccentric fastening of the membrane to the boundary with pure torsion [3]. In addition to the above derived relations the well-known generalized parameters for the bending stiffness of the contour in the plane of membrane [8, 9]:

$$\bar{n} = \frac{EI_k}{E_m t_m a^3}.$$

RESULTS

The numerical studies were carried out with constant values of generalized parameters but various geometric sizes and characteristics of the structure and the values of the load. The boundary was modelled using PLATE finite elements (Fig. 4).

The forces and displacements for the middle of the boundary span can be expressed as follows:

$$M_{sp} = \beta_1 \frac{pa^2}{6}; \quad B_{sp} = \beta_2 \frac{pI_\omega}{t_m \cdot a^2};$$

$$v = \gamma_1 \frac{pa^4}{24EI_k}; \quad \theta = \gamma_2 \frac{pea^2}{(GI_t)_k},$$
(5)

where, correction factors $\beta_1, \beta_2, \gamma_1, \gamma_2$ depends only on the generalized parameters. In equation (5), M_{sp} – bending moments in the contour in the plane of membrane of the span; B_{sp} – flexural-torsional bi-moment in the beam; v and θ – horizontal displacement and twist angle of the beam. In Table 1, the results of numerical analyses are represented. Geometrical sizes of the beam cross-section, loads, thickness and span of membrane were varied and the generalized parameters were constant. The results represented for two cases of membrane structure – in first case the cross-section of beam is $200 \times 100 \times 6$ mm, and in the second – $400 \times 200 \times 12$ mm.

Analysis of the data in Table 1 obtained with varying torsional stiffness of the contour, span and thickness of the membrane shows that at constant values of generalized parameters m, m_ω, n and ω the values of correction factors in Equation (5), (maximum error doesn't exceed 5.3%) do not depend on the span and thickness of membrane, stiffness characteristics of the beam and load. Consequently, the generalized parameters m, m_ω, n and ω really characterize the behaviour of the system when the membrane eccentrically fastened to the thin-walled closed profile support beam.

Table 1. Parameters of the stress-strain state of the membrane model.

Parameter		1 case	2 case	Error, %
\bar{n}		$3.249 \cdot 10^{-5}$		-
\bar{m}		0,1		-
\bar{m}_ω		$1.543 \cdot 10^{-6}$		-
$\bar{\omega}$		0.00278		-
a, m		6	12	-
t_m, m		0.001	0.002	-
t_k, mm		0.006	0.012	-
$p, kN/m$		120	240	-
$GI, kN \cdot m^2$		1250	20000	-
$EL, kN \cdot m^2$		2.29	73.2	-
Beam bending moment	$M_{sp}, kN \cdot m$	0,741	6.009	-
	β_1	$1.029 \cdot 10^{-3}$	$1.042 \cdot 10^{-3}$	1.3
Flexural-torsional bi-moment in the beam	$B_{sp}, kH \cdot m$	0,057	0,456	-
	β_2	1539.15	1538.81	0.022
Deformation of the beam	v, mm	24.0	48,4	-
	γ_1	$5.356 \cdot 10^{-3}$	$5.385 \cdot 10^{-3}$	0.54
	θ, rad	$8.692 \cdot 10^{-4}$	$9.18 \cdot 10^{-4}$	-
	γ_2	$2.512 \cdot 10^{-3}$	$2.653 \cdot 10^{-3}$	5.3

CONCLUSIONS

On the basis of the numerical analyses presented, it is shown that the redistribution of stresses in the structure depended on its geometrical characteristics. Twisting of contour beam leads to the irregular displacements of the membrane edge along the length of beam when membrane is fastened eccentrically to the beam. This causes redistribution of the normal forces in membrane through its interface with the boundary beam. In the middle of the span forces perpendicular to the beam decrease and on the edges of the boundary beam, they increase. Tangential forces occurred along the membrane edge. Redistribution of forces in the membrane is reflected in the stress-strain state of the beam: the bending moments decreases and additional compression occurs.

REFERENCES

1. Brudka Ya., Lubinski M. 1974 *Legkie stalnye konstrukcii (Light steel structures)*. Moscow: Stroizdat, 125 p.
2. Bychkov D.V. 1948 *Raschet balochnykh I ramnykh system iz tonkostennykh elementov*. Moscow: Stroizdat, 208 p.
3. Ereneyev P.G., Tusnin A.R. 1990 *Vliyaniye excentrichnogo krepleniya membrani k opornomu konturu na perepaspredeleniye usilii v sisteme* // *Stoitelnaya mekhanika I raschet sooruzhenii* No.1, 8–13 pp.
4. Farfel M.I. 2009 *Razrabotka I issledovanie konstrukcii dushkatnogo bloka iz membrannich panelei* Moscow, 176 p.
5. Hideki Magara, Kiyochi Okamura, Mamory Kawaguchi 1984 *An analysis of membranes structures engineering*. London, 1–12 pp.
6. Kornishin M. S. 1968 *Nelineinye zadachi teorii plastin I pologih obolochek I metody ih resheniya* Moscow: Nauka, 191 p.
7. Taylor R.L., Oriate E., Ubach P. 2005 *Finite element analysis of membrane structures* // *Computational methods in applied sciences* Vol. 3, 47–68 pp.
8. Trofimov V.I., Ereneyev P.G. 1990 *Membrannie konstrukcii zdaniy I sooruzhenii. Chast 1*. Moscow: Stroizdat, 248 p.
9. Trofimov V.I., Ereneyev P.G. 1991 *Membrannie konstrukcii zdaniy I sooruzhenii. Chast 2*. Moscow: Stroizdat, 198 p.
10. Vlasov V.Z. 1961 *Thin-Walled Elastic Beams*. Israel Program for Scientific Translations, Jerusalem, 493 p.

NUMERICAL STUDIES OF Z-PURLINS SUPPORTED BY SANDWICH PANELS

Olga Tusnina
PhD Student

Moscow State University of Civil Engineering, Moscow, Russia

ABSTRACT

In this paper numerical analysis of thin-walled Z-purlins in the cladding of buildings made of sandwich panels are considered. The software used is MSC NASTRAN. The influence of the mesh of elements on the results of calculations is studied. The results of numerical analyses allowed developing the method for determining the stiffness of the connection of the purlin with the sandwich panels.

INTRODUCTION

Nowadays Z-, C- and Σ -purlins are widely used as supporting elements in roof coverings of modular buildings based on the light steel skeletons. Sandwich panels are used to cover the building envelope. A purlin-sheeting interaction plays a significant role in the performance of these types of structures.

When loading the structure by distributed loads, the thin-walled cold-formed purlin undergoes a restrained torsion because of the eccentric load application. The sheeting does not allow free rotation of the purlin and its supports. The bearing capacity of the purlin is significantly different for cases when purlin is considered as a free beam and as a beam which is attached to sheeting because of complex interaction of the purlin with sheeting. This is the reason the purlin cannot be considered separately from the sheeting fastened to it.

The type of fasteners also plays a role in the behaviour of the system. Today, screws are used as fasteners of the sheeting to purlin as a rule. Alternatively, rivets can be used as fasteners. Screws are installed through the thickness of the sandwich panel (Figure 1). Rivets, however, form the connection between the bottom flat sheet of the sandwich panel and the flange of the purlin (Figure 2).

The investigation of the complex behaviour of such systems may be performed experimentally or theoretically. One of the way of the implementation of theoretical studies is to use numerical analysis. In this paper the results of the numerical analysis of the system are presented.

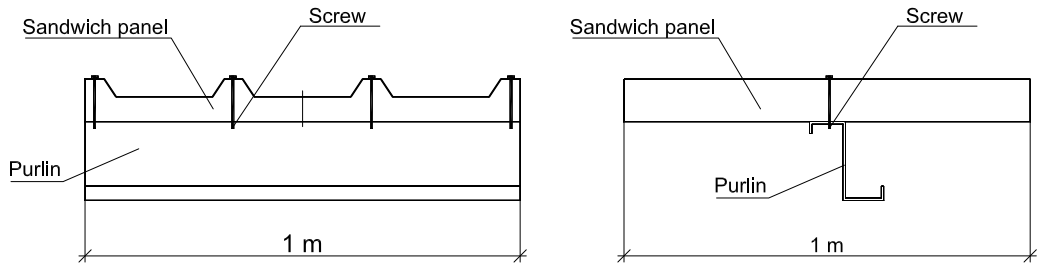


Figure 1. Scheme of screw fastening.

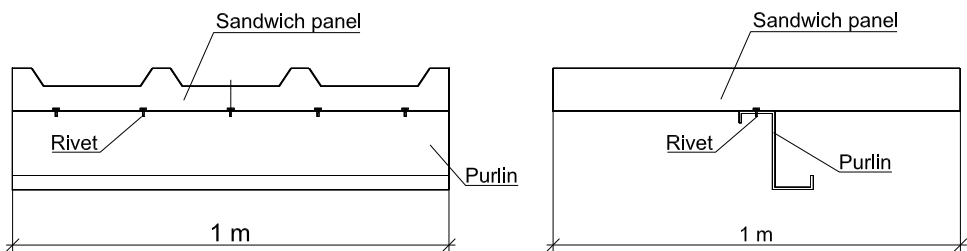


Figure 2. Scheme of rivet fastening.

BACKGROUND

Many researchers have studied similar systems. Ciurej and Piekarczyk [1] carried out numerical calculations using the MSC.Marc program. For the modelling of the purlin, the authors used plate elements. Also, laboratory tests were carried out. The test model was a section of the load-bearing construction of a roof covering being in use for instance in lightweight single-storey buildings. Three purlins Z250 with the length 6 m were applied. Trapezoidal steel sheet was fixed to each purlin. Comparison of experimental and numerical results was done. The analysed beam-sheet structure was effectively modelled as a whole with the use of shell finite elements for steel profiles and sheet roof and brick elements for insulation blankets. The elaborated FEM model of a roof covering is appropriate for simulating the behaviour of real structures of this type.

In the articles [4, 5] stability analysis of thin-walled purlins restrained by sheeting for different beam lengths and type of the cross-section was carried out. Special attention is focused on modelling the restrained purlins in general purpose finite element program ABAQUS. The comparison of results obtained with the use of analytical and numerical models is carried out. The examples illustrate the importance of proper modelling the laterally restrained purlins.

METHODS

The numerical analyses are for the specimens for which test results [3] were available. The investigated model is the one recommended by European standard [2] for design characteristics of testing.

Numerical analyses are done with the use of program NASTRAN. The model (Figure 3) consists of RUUKKI purlin Z200x2, 1 m long, sandwich panel SPC120/80PU and connectors – screws GT6 175-5.5/6.3 mm. Purlins are modelled using PLATE finite elements ($E=210000$ MPa, $\nu=0.33$). Sandwich panel consists of 3 layers – flat and trapezoidal metal sheets (PLATE finite element, thickness 0.5 mm ($E=210000$ MPa, $\nu=0.33$)) and polyurethane core (SOLID finite element, $E=3.5$ MPa, $\nu=0.15$). Connection between purlin and sandwich panel is modelled with the use of RIGID finite element, which connects one row of nodes on the purlin with nodes on the panel (independent node is located on the purlin, connecting degrees of freedom (DOF) are all linear displacements). Screws are modelled as BEAM elements. On the external side of sandwich panel screw-nut is modelled as 4 intersecting beam elements to distribute stresses and to realize more real behaviour of construction.

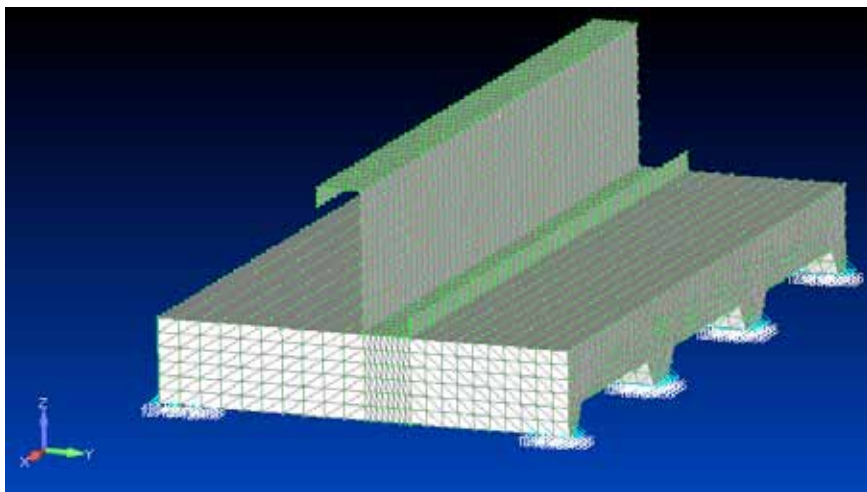


Figure 3. Investigated system.

Only linear analysis has been carried out. The values of force applied to the free flange were obtained from reported tests. The force causes the displacement of the free flange along Y-axis at $h/10$ (h – the height of the purlin). Analyses have been done for different directions of the load (uplift – T1S, T2S, gravity – T3P, T4P), different positions of the purlin and different positions of the screws on the sandwich panel (Figure 4).

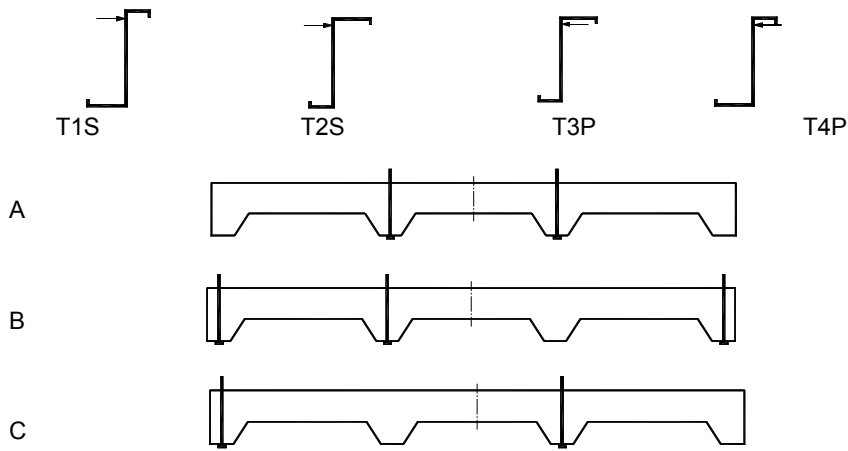


Figure 4. Schemes used in analysis.

To determine the optimal size and number of elements, test numerical analyses were done for different parameters of the mesh for cases T1SA and T4PA. The mesh size of the element along the height of the purlin was equal to 1 cm, 2 cm, 4 cm and 8 cm.

RESULTS

The values of displacements in the direction of load acting in the top point of the purlin web, the axial forces in the screws and the angle of the purlin rotation about its edge are compared in the results for different meshes (Figure 5). This comparison is represented in the Table 1. The results are also represented in graphs (Figures 6, 7, 8).

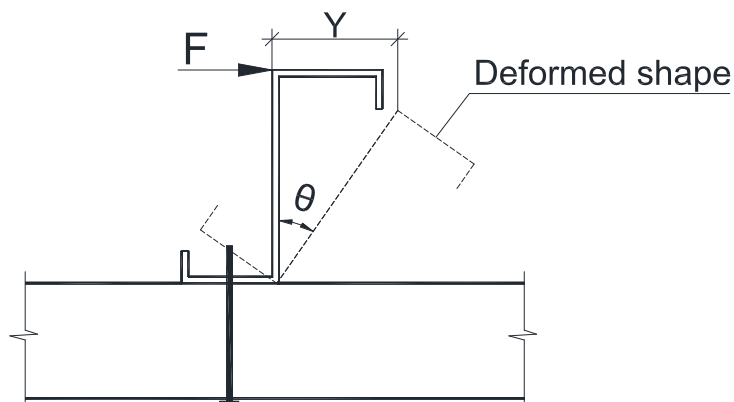
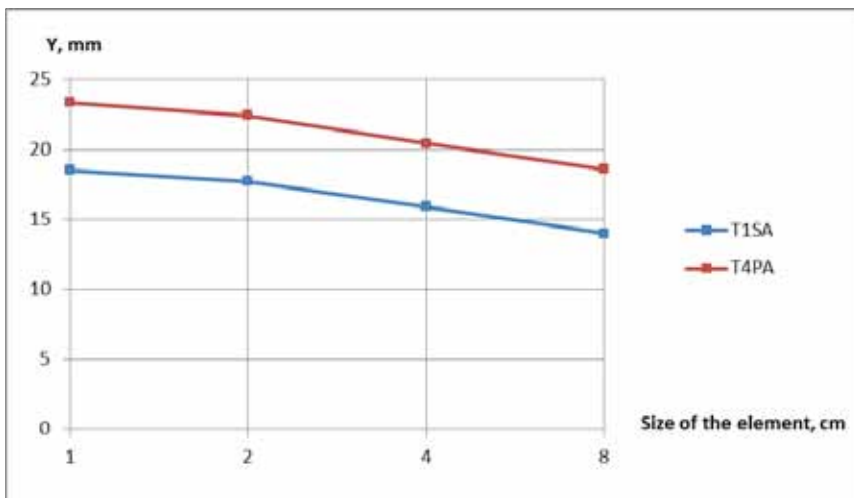
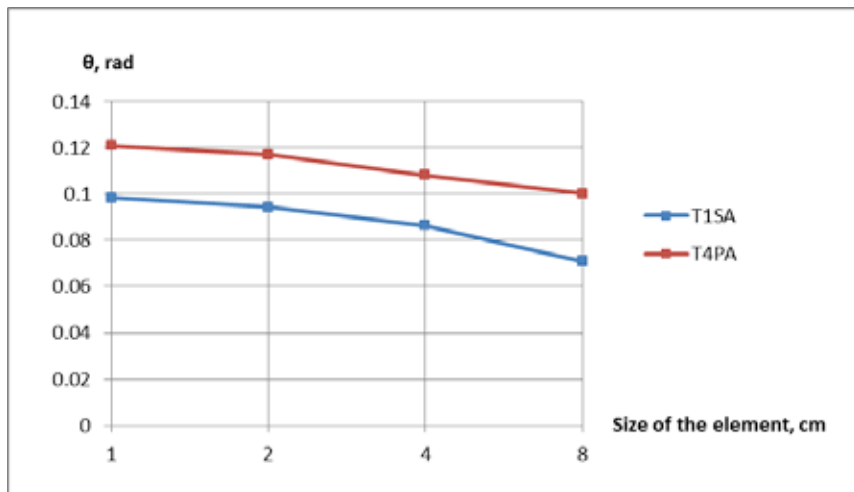


Figure 5. Scheme of purlin showing parameters of deformation.

Table 1. Comparison of the results for different meshes.

Size of the element, cm	Displacement, mm		Axial force in the screws, N		Angle of rotation, rad	
	T1SA	T4PA	T1SA	T4PA	T1SA	T4PA
1	18.5	23.4	18.5	23.4	0.098	0.121
2	17.7	22.4	17.7	22.4	0.094	0.117
4	15.9	20.4	15.9	20.4	0.086	0.108
8	14.0	18.6	14.0	18.6	0.071	0.100

Figure 6. Graph showing the dependence of displacement Y on the size of the element.Figure 7. Graph showing the dependence of angle of rotation θ on the size of the element.

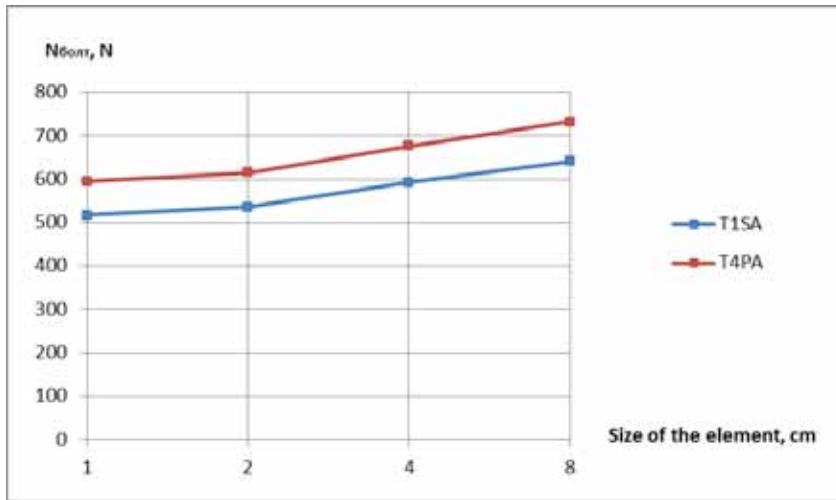


Figure 8. Graph showing the dependence of the axial force in screw N on the size of the element.

As can be seen from the graphs, with the decrease in the element size and corresponding increase in the density of the mesh, the variation of the considered parameters reduces and the results converge to some limit. We can conclude that a size of the element of 2 cm is sufficient. In such a mesh quite accurate results are obtained and the dimension of the problem is still not as large as with the use of 1 cm elements. So we have sufficiently accurate results with reasonable time spent to analyse the FE model. Based on this conclusion, the analyses of all other schemes (T2SA, T2SB, T2SC, T3PA, T3PB, T3PC) have been carried out with these parameters of the mesh.

In the Table 2 the comparison of the experimental [3] and numerical results is represented.

Comparison of the experimental and numerical results shows that the error between NASTRAN and test results does not exceed 25%. Thus, the results, obtained with assumed mesh can be used for further studies and determination of the supporting spring stiffness.

Table 2. Displacement of free flange and error % of numerical analysis as compared with laboratory tests results.

	Scheme	Force, N	Displacement, mm		Error, %
			NASTRAN	Test	
A	T1S	323.96	17.7	20	11.5
	T2S	348.10	20.5	20	2.5
	T3P	308.09	18.6	20	7
	T4P	393.42	22.4	20	12
B	T1S	319.39	17.7	20	11.5
	T2S	307.64	18.5	20	7.5
	T3P	346.38	20.2	20	1
	T4P	344.91	17.4	20	13
C	T1S	233.02	15.9	20	20.5
	T2S	211.2	15.3	20	23.5
	T3P	244.16	18	20	10
	T4P	278.52	19.8	20	1

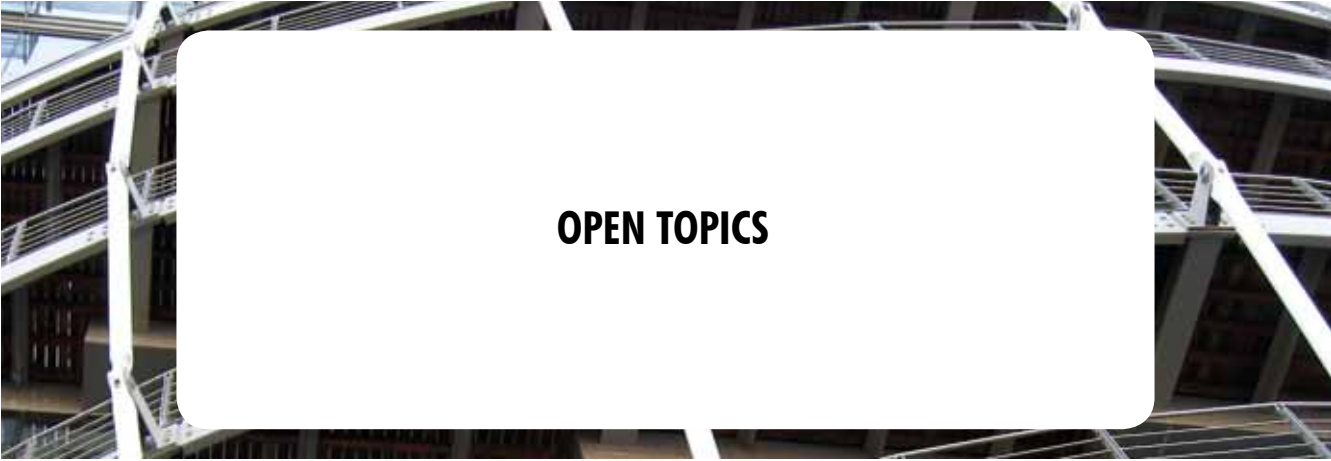
CONCLUSIONS

The compiled numerical model in NASTRAN is valid for studies of the work for this kind of structures. With the use of this numerical model the engineering method of determination of the supporting spring stiffness was developed in Reference [6].

REFERENCES

1. Ciurej H., Piekarczyk M., Pieciorak E. 2010 *Experimental research and integrated FEM modelling for sheet roof covering with thermal insulation* // Mechanics and Mechanical Engineering, Vol. 14, No. 2, pp 183–192.
2. EN 1993-1-3:2004 Eurocode 3: Design of steel structures. Part 1–3: General rules – Supplementary rules for cold-formed members and sheeting.
3. Kujawa M., Werochowski W., Urbańska-Galewska E. 2008 *Restraining of the cold-formed Z-purlins with sandwich panels* – Final report, Gdansk, Poland, 126 p.
4. Rzeszut K., Czajkowski A. 2011 *Laterally braced thin-walled purlins in stability problems* // Proceedings of the 19th International Conference on Computer Methods in Mechanics, Warsaw, Poland, pp 202–203.

5. Rzeszut K., Studzinsky R. 2010 *Stability analyses of thin-walled laterally braced purlins* // The 10th International Conference “Modern Building Materials, Structures and Techniques”, Vilnius, Lithuania, pp 758–762.
6. Tusnina O. 2013 *Design of thin-walled Z-purlins connections with sandwich panels in roof made by rivets* // Design, Fabrication and Economy of Metal Structures, International Conference Proceedings, Miskolc, Hungary, pp 157–163.



OPEN TOPICS

PROBLEMS OF FUNCTIONING AND ELABORATION OF THE MASS HOUSING DEVELOPMENT AREAS OF THE CITIES AND SETTLEMENTS

S.I. Matreninskiy

Candidate of Technical Sciences, Associate Professor

E.M. Chernyshov

**Academician of the Russian Academy of Architectural and Construction Sciences,
Doctor of Technical Sciences, Professor**

V.Y. Mischenko

Doctor of Technical Sciences, Professor

Voronezh State University of Architecture and Civil Engineering, Russia

ABSTRACT

In a number of cities and settlements the existing condition of mass housing development areas, including numerous buildings and constructions, engineering and network infrastructure, road and transport communications etc. demands reconstruction and conformation with modern norms. The purpose of this project is elaboration of the system model of mass housing development areas, and also bases of methodological approach to reorganization of these areas with providing comfortable conditions for residence and life activity of the population.

The suggested approach to functioning and elaboration of the mass housing development area includes 2 levels of specification of description of the given problem. The first level – philosophical or cognitive-theoretic – the verbal description of a plan or a concept, with formation of structure and composition of the hierarchical system with definition of the aim of its development and reorganization – which is to provide favorable conditions for residence and life activity of the society. The second level – introduction of the system and methods of its reorganization in the scientific-research language in the form of models – such as “generation – analysis – choice” for determination of the action variants on reconstruction of territories, as well as variants of technical and technological conditions providing their implementation.

INTRODUCTION

In a number of cities and settlements, the established condition of mass housing development areas, including numerous buildings and constructions, branched engineering and network infrastructure, road and transport communications etc., demands reorganization and conformation in compliance with modern norms and life activity of the population of these areas. Thus, for making effective administrative as well as organizational and technological decisions on maintenance and reorganization of the mass

housing development areas including a great number of various objects, it is necessary to elaborate a system model of these mass housing development areas as well as the bases of methodological approach to reorganization of these areas, providing comfortable conditions for accommodation and life activity of the population of these areas.

Before choosing a certain alternative of modeling of mass housing development areas of the cities and settlements, and also development of methodological bases of decision-making on reorganization of these areas it is necessary to make a thorough analysis of specific features of the concrete city or its part. Such analysis of the reality must be made on the basis of the modern theory and contain not only statistical data, determinative, comparative to normative, dimensional, constructive, ecological, social and other factors, but also include the methodology of making effective administrative and production decisions about reconstruction of mass housing development areas.

Mass housing development area is considered as a component part of the city intended for habitation and life activity of people, according to the modern definition of a city. "A city is one of the types of social and dimensional organizations of population, arising and developing on the basis of concentration of industrial, scientific, cultural, administrative and other functions" (Golyshev et al. 2006). That is why for mass housing development areas as parts of the city or other center of population it is already not enough to be seen only in a spatial refraction as areas of land, set of buildings, constructions and streets. Mass housing development area as a component part of the city is a complex multilevel system with its own laws and peculiarities of existence.

METHODS

Realizing the system approach to existence and development of the city and its component parts, it is reasonable to see the mass housing development area as system complex city planning formation – hereinafter referred to as CPF. In the system analysis for representation of complex systems, one of which is definitely CPF, stratified representation of such systems is normally used (Mesarovich et al. 1973). According to this approach, the system is set by a family of models, each of which describes its behaviour from the point of view of a certain abstracting level.

Originally, in the most general, fundamental understanding, at the semantic, notional level CPF is represented in philosophic or theoretical-cognitive language as a verbal description of a project or conception. Thus, system complex city planning formation (CPF) can be defined as the set of interconnected, controllable, conditioned by existing economic and material and technical potential of the given territory, spatial, architectural and building, engineering decisions of the environment of population groups (society), providing favourable conditions for habitation and life activity

of people. CPF component is implied as its component part, characterizing functional content and purpose of system complex city planning formation.

Introduction of the definition of CPF with formation of its structure is necessary for dynamic evaluation and analysis of different parts and elements of a modern human environment, observing interconnection of CPF components and their interaction with environment, applying system theory and system analysis for solution of the problems of functioning and elaboration of mass housing development areas.

Thus, for further analysis of CPF and determination of possible rational lines of its development considering unavoidable contradictions between separate components it is necessary to represent the system in the language of selected scientific theory – in the form of various kinds of models which help deeper understanding and discovering of the main idea of the system – Figure 1. For this purpose, we make a description of the system in scientific research language of the theory of complex systems synthesis, when CPF is represented as a complex multilevel hierarchical system interacting with the environment under influence of which it is being formed. With that, CPF is defined as the set of interconnected components – architectural and constructional (AC), engineering and network (EN), engineering and transport (ET), territorial and spatial (TS), functioning in environmental conditions for the purpose of providing the required favourable conditions for habitation and life activity of the society on the given mass housing development area – in accordance with Figure 1. In this case, the environment implies existing natural and ecological conditions, generated material and technical potential of the certain territory, existing managing administrative and financial system and the society of the given territory.

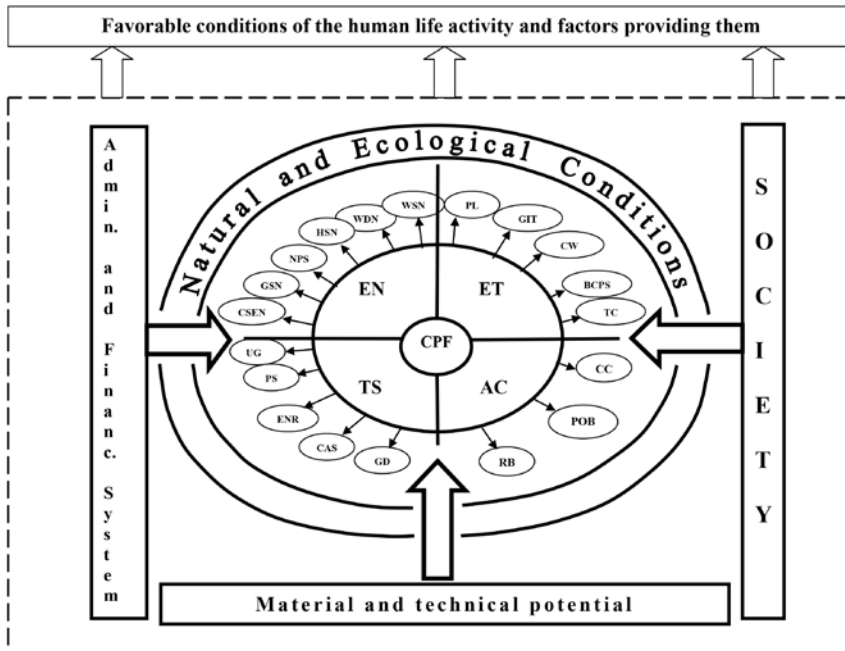


Figure 1. System complex city planning formation – CPF in the form of multilevel hierarchical system interacting with the environment.

RESULTS

Realizing the methods of system approach, the CPF components are considered as subsystems of the First level with their subsequent division into subsystems of the Second level (common objects) which in turn consist of elements – private objects, making in total the subject structure of CPF – according to Figure 2.

Engineering and network component (EN) – pipeline, wire and wireless communications included into the arrangement of residential community involving networks of water supply, water drain, heat supply, gas supply, electric supply, communication and alarm, and also constructions designed for service of engineering networks and cooperation with them. These include, engineering and transport component (ET) – buildings and constructions for service of public and individual transport (depots, garages, parking places, car-washing facilities, auto repair shops), transport communications (roads, bridges, trestles etc.), included into the arrangement of residential community. Other components are, territorial and spatial component (TS) – the set of undeveloped and modified areas of land having particular functionality or being a reserve for beautification and development of the given residential

community. Architectural and constructional component (AC) – the set of residential, public and administrative buildings and constructions (monuments, stadiums, fountains etc.) located in the territory of the given residential community.

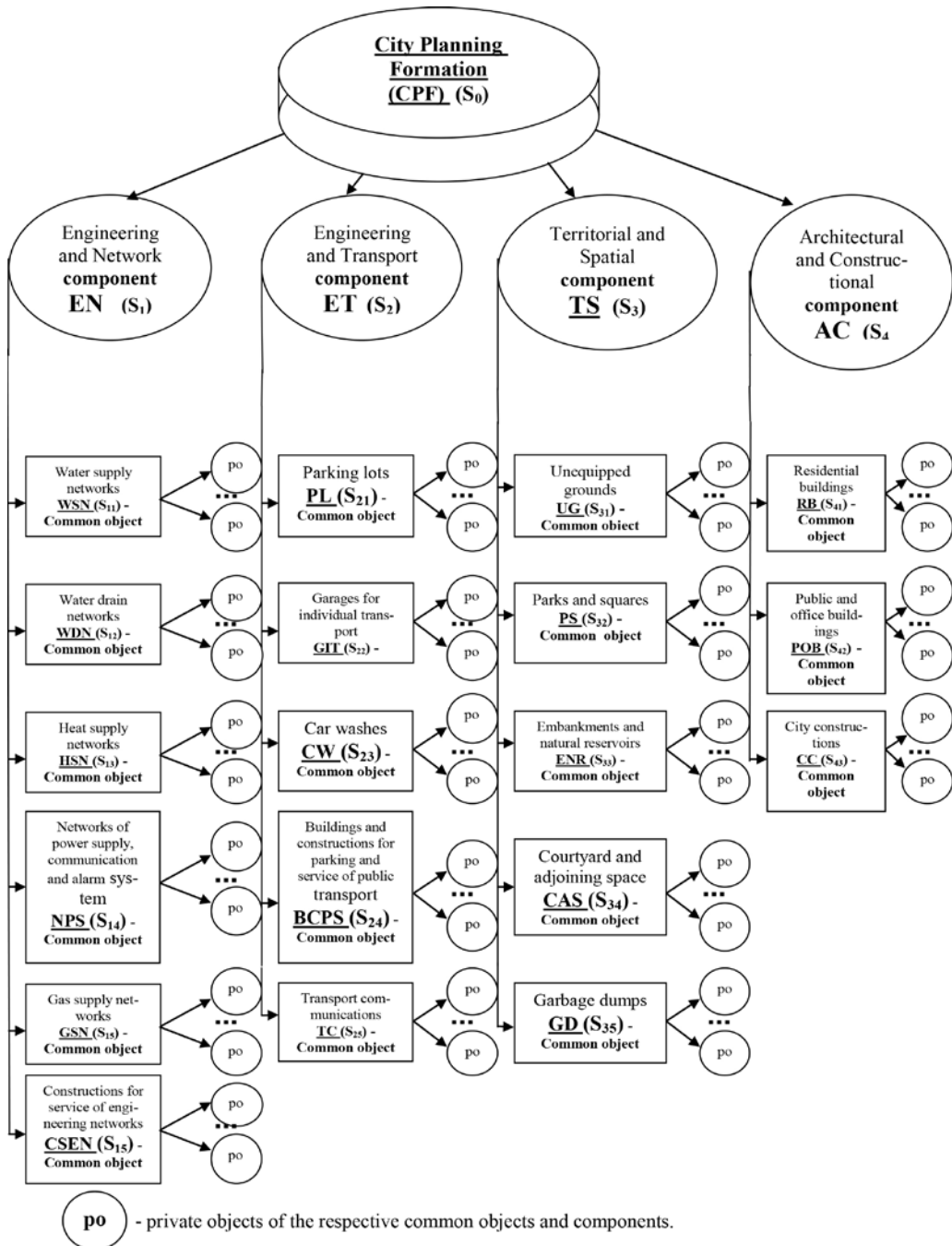


Figure 2. The objective structure of the city planning formation as a system including its components and objects.

As it was already mentioned, one of the most important system design rules is that when designing the system it is required to consider its interaction with “external environment”, but the environment, in its turn, should also be regarded as a system. In our case, the “External environment” system includes the following subsystems: Natural and ecological conditions of CPF – the set of natural components (geographical coordinates, climate, waters, soils etc.) forming natural basis of the given residential community. Material and technical potential of CPF – the set of building materials used in the given region, industrial enterprises producing these materials and goods, building organizations, construction and mounting organizations, branches serving the construction, and also normative basis regulating construction of the CPF objects, their use and maintenance. Administrative and financial system – the set of federal, regional, municipal authorities, regulating the relations among the CPF components as well as the relations between the whole CPF and the environment, and providing financing at the expense of the federal funds, tax and voluntary subscriptions from different enterprises and organizations (industrial, commercial, banking and financial, entertainment, service etc.), including the monetary funds of the population of the given territory for development and reorganization of CPF. CPF society – the total community of people (population) living in the territory of the given residential community or connected with it by a certain kind of activity or way of life, which is expressed by a system of stable social mutual relations.

As it was noted before, the aim of CPF functioning when interacting with environment is creation of favorable conditions for life activity of the society. At the same time it is necessary to consider the permissible level of resource expenditure. This aim as it is formulated is quite difficult to define on the number scale which makes it necessary to introduce the goal achievement efficiency index – or criteria – the factors for evaluation of correspondence between functioning of the system and the given result. With regard to CPF it is reasonable to take as efficiency index such global factors as “comfort” and “resource consuming” which in their turn depend on the particular factors. Interconnection of CPF efficiency indices is shown on Figure 3.

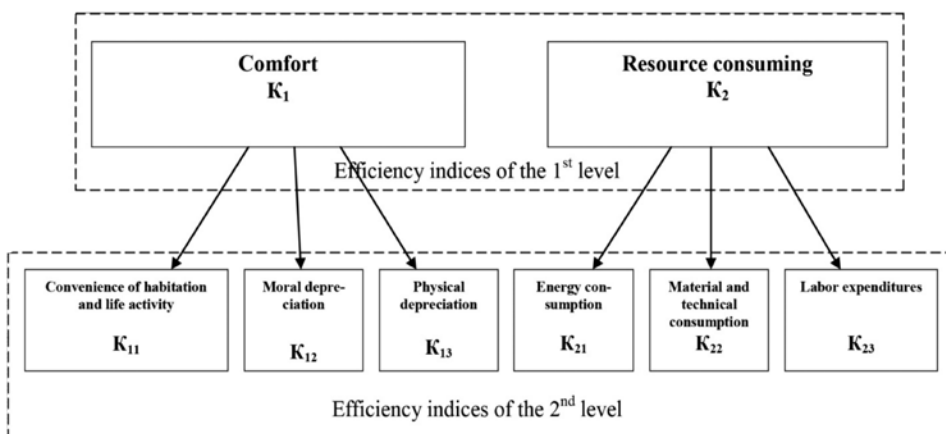


Figure 3. Composition and structure of CPF efficiency indices.

Comfort – is characterized by convenience of the habitation and life activity environment, moral and physical depreciation of this environment. Resource consuming – is characterized by material and technical consumption, energy consumption and labour expenditures, measured in money equivalent, for providing current functioning or rearrangement of the habitation and life activity environment in order to achieve the required level of its comfort.

The convenience of habitation and life activity of the society in the given territory is evaluated by expert method, in accordance with corresponding variants of realization. Moral depreciation – is a gradual (in time) lag of consumer properties of the earlier created urban funds (buildings, engineering equipment, infrastructure etc.) comparing to achievements of the modern operating, architectural and technical level in the given area. Moral depreciation is measured in percentage terms. Determination of moral depreciation consists in calculation of costs for elimination of depreciation, concerning replacement cost of the examined object, in this instance the CPF with all its subsystems. At that, as a variant of CPF with maximal comfort, without moral depreciation it is possible to consider the sketch of architectural and constructional project of mass housing development area developed in accordance with modern achievements of science, technology, ecology, architecture, that is in some way “elite”, close to “ideal” project. Physical depreciation – is a gradual loss of the initial qualities of urban funds (buildings, engineering equipment, infrastructure etc.) in the process of their natural aging and deterioration, with decrease of consumer properties, evaluated by correlation of the cost of objectively necessary repair activities, eliminating damages of the system, construction, element and their replacement cost.

Possible variants of actions concerning further functioning or reconstruction of CPF, including all its material components and subsystems after rating them by corresponding efficiency indices, are as follows:

1. Maintenance of service properties – current repair.
2. Repair of the separate objects, areas and elements.
3. Capital repair.
4. Reconstruction and modernization.
5. Construction of additional objects, areas and elements.
6. Demolition and dismantling of old objects, areas and elements with construction of new ones.

Let us look at the structure and components of the concept “action” with respect to the given variants in accordance with Figure 4.

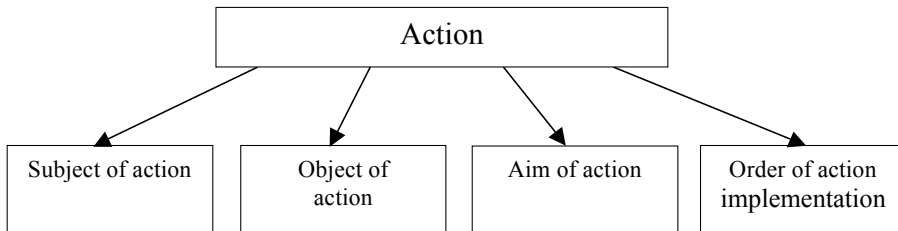


Figure 4. Structure of the concept “action”.

Subject of action are organizations and enterprises directly implementing examination, architectural and building projecting and CPF reconstruction works. Object of action are CPF components which are liable to reorganization – architectural and constructional component (AC), engineering and transport component (ET), territorial and spatial component (TS), engineering and network component (EN) – also including their constituent subsystems and elements. Aim of action is the reorganization of CPF, including its components, with achievement of the established level of comfort at the minimal resource expenses. Order of action implementation is the complex of technical and technological solutions, providing the achievement of the set aim.

Thus, the system of decision-making on reorganization of CPF has 3 levels of specification of description – or strata – according to the terminology accepted in the system analysis as shown in the picture 5 (Mesarovich et al. 1973). Concepts such as subject, object, aim of action are included into the first level of specification of description of decisions – functional stratum, where the decisions (R1) are made on the establishment of the concrete content of these concepts on all the components and subsystems of CPF. On the basis of the first functional stratum, a different variant of actions on reorganization or functioning can be chosen for the different CPF components depending on the established efficiency indices, such as comfort and resource intensity and, in the general case, the quantity of diverse combinations of variants can turn out to be very considerable. For example, for the territorial and spatial component (TS) the variant of actions such as “construction of additional objects, sites and elements” can be accepted, for engineering and network component (EN) it can be “general overhaul”, for engineering and transport component (ET) and architectural and constructional component (AC) – “reconstruction and modernization”.

The next concept – order of action implementation – has two levels of specification of description (two strata) – technical and technological. The second level of specification of description of decisions is technical level, where the general technical decisions (R2) on achievement of the chosen aims are formed. For example, the “reconstruction and modernization” decision on architectural and constructional component, accepted in the

functional stratum, in its turn, in the technical stratum can be realized by the development of design decisions on superstructure of floors, extension of additional sections, change of inner layout, etc.

The third level of specification of description of decisions is technological - that is definition of thorough and detailed design and technological decisions (R3), providing the implementation of technical decisions.

Thus, generally, the values of the global efficiency indices such as “comfort” (K1) and “resource intensity” (K2) depend on the chosen decisions R1, R2, R3. In this case, the problem of CPF synthesis consists in definition of such decisions on the functional, technical and technological strata which provide minimal resource expenses for achievement of the established comfort. Formally the problem is put down as follows. To find

$$(R_1, R_2, R_3) \text{ optimal} = \text{arg min } K_2(R_1, R_2, R_3) \\ \langle R_1, R_2, R_3 \rangle$$

At the restrictions

$$K_1(R_1, R_2, R_3) \geq K \text{ required}$$

$R_1 \in RD_1$ – set of admissible actions.

$R_2 \in RD_2$ – set of admissible technical decisions.

$R_3 \in RD_3$ – set of admissible technological decisions.

At an estimation of CPF condition as a system, its global and private efficiency indices cannot be expressed in the form of analytical dependences on the considered variables (R1, R2, R3), that would allow the forecast of the developments and to introduce recommendations on functioning and reorganization of mass housing development areas on the basis of corresponding mathematical models. To solve the problems of synthesis of complex systems of this kind, nowadays multistage technological schemes of their solution are developed (Mesarovich et al. 1973).

The decision-making process at any stratum is divided into 3 subprocesses: generation of variants, estimation of variants – analysis and choice. These subprocesses are considered as decision-making layers.

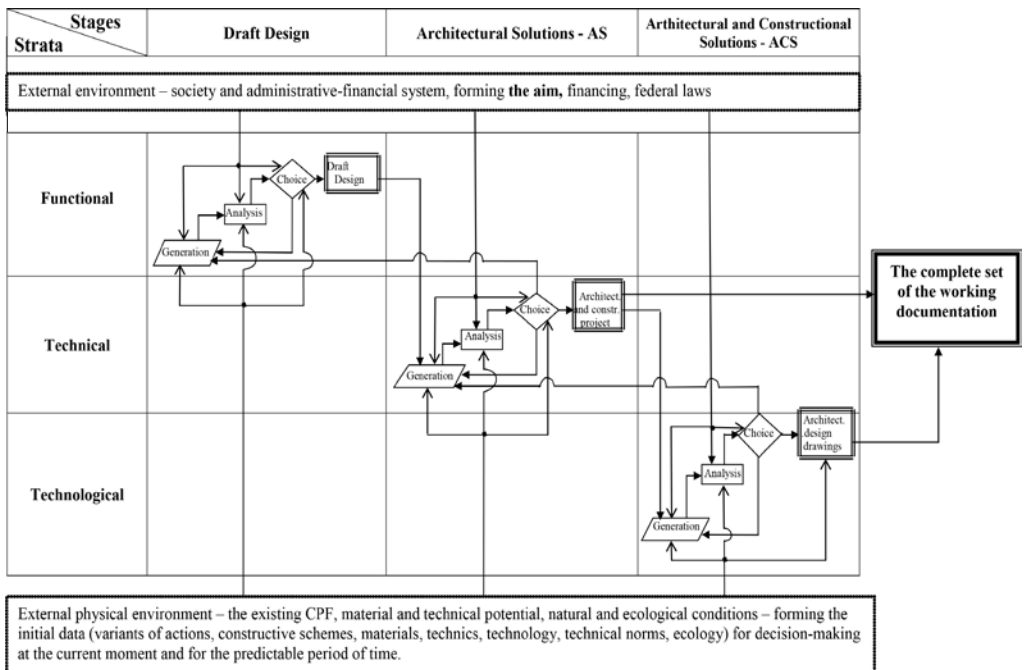


Figure 5. Technological scheme of decision-making on reorganization of mass housing development areas.

On the “generation” layer operations on formation of admissible variants of actions on reorganization of each component and corresponding subsystems of CPF, technical decisions on realization of each chosen action, technological decisions on realization of each chosen technical decision, are realized.

On the “analysis” layer reception of quantitative and qualitative values of the indices characterizing CPF efficiency on a set of chosen admissible variants of actions, and chosen admissible variants of technical and technological decisions, is carried out.

The “choice” layer includes operations of the search of preferences (in the meaning of set criteria) of action variants, technical and technological decisions, which determine rational composition and structure of CPF, and also values of component, subsystem and element characteristics.

The technology of CPF synthesis – as determination of variants of actions and decisions on functional, technical and technological strata – consists in time analysis of the set of formal and heuristic operations on compromise decision-making on substantiation of CPF structure for the purpose of receiving the necessary set of working documentation, regulating its reorganization.

At the first stage – that is the draft design of reorganization of a mass housing development area – the functions (aims) of necessary actions concerning each component and object of CPF are defined.

At the second stage – architectural and building project – technical decisions which are necessary for achieving the generated aims are determined.

At the third stage – concrete working drawings and documentation for direct implementation of reorganization – the detailed constructive and technological decisions, realizing the chosen technical decisions, are defined.

As a result, the technological scheme of decision-making on reorganization of mass housing development areas will look as it appears in the Figure 5.

Thus, the offered methodology allows to form a great number of admissible variants of actions on reorganization of CPF, as well as to estimate the efficiency of each variant by the series of basic indices and to make a reasonable choice of an expedient variant by the accepted criteria.

In Figure 6 there is an example of determining the variants of actions on reorganization of the CPF object – “Residential building” – with specification on 3 strata, in assumption that by the set criterion – minimal resource expenses at the given comfort – the action such as “Reconstruction and modernization”, and technical decisions such as “Superstructure of floors” and “Built-in framework” are chosen.

CONCLUSION

The introduced approach to the functioning and elaboration of mass housing development areas as system complex city planning formations includes two levels of detailed description specification of the given problem.

The first level – philosophical or cognitive-theoretic – the verbal description of a plan or a concept, with formation of structure and composition of the mass housing development areas as system complex city planning formation – CPF, with definition of the aim of its development and reorganization – which is to provide favourable conditions for residence and life activity of the society.

The second level – introduction of CPF system and methods of its reorganization in the scientific-research language in the form of models – such as “generation – analysis – choice” for determination of the action variants on reorganization of CPF, as well as variants of technical and technological decisions responsible for their implementation.

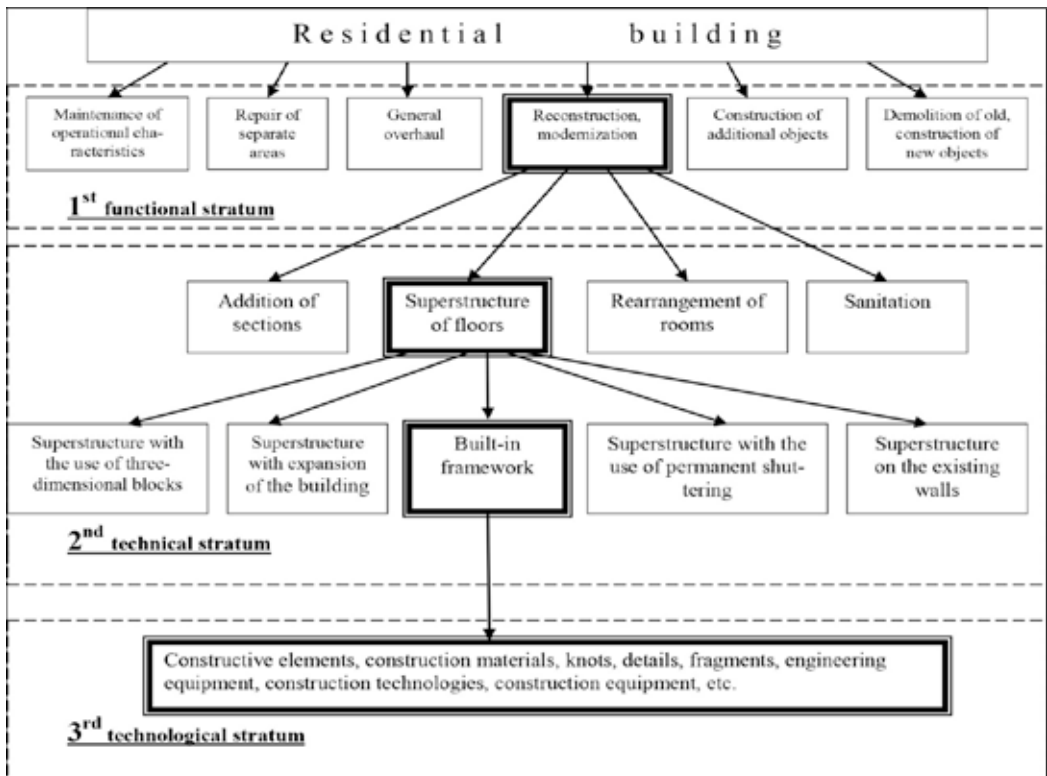


Figure 6. Example of determination of the action variants with specification on 3 strata on reorganization of the CPF object – “Residential building”.

REFERENCES

- Golyshev, A.V., Kolchunov, Vl. I. and Kolchunov, V.I. (2006), *Architectural and Construction Encyclopedia. Reference Dictionary*. Moscow.
- Mesarovich, M., Mako, D. and Takahara, I. (1973), *Theory of hierarchical multilevel systems*. Moscow: Mir.

THE BLUE BOX AND THE TECHNOLOGICAL TRAJECTORIES IN CONTEXT OF UNIVERSITY-BUSINESS COOPERATION (UBC)

Lauri Tenhunen

HAMK University of Applied Science, Hämeenlinna, Finland

Arto Ranta-Eskola

Rautaruukki Oyj, Finland

ABSTRACT

Matthews (1992) presents a concept of “Blue Box” for integrating technology into business strategy. His analysis serves to find and manage the development routes in the inevitable replacement of old technologies by new ones. Matthews also suggests a practical approach, a conceptual Management of Technology (MoT) analysis framework, to enable continuous and intensive discussion and decision-making between business managers and technologists. This represents one of our approaches to university-business cooperation (UBC).

The second approach in this paper is to analyse the UBC possibilities from the point of view of the technological trajectories. A technological trajectory is defined, quite flexible, as the pattern of conventional problem solving activity within a given technological paradigm (Dosi, 1982).

When ideas, markets and professions are institutionalized, a technology development can get ‘stuck’ within one technological trajectory, and organisations as well as individuals are unable to adapt ideas and innovation from outside.

In this article we develop a method for analysing alternative options for UBC.

INTRODUCTION – THE BLUE BOX CONCEPT

Matthews (1992) argues in his analysis that a company’s business strategy and technology strategy cannot successfully be developed in isolation. Cooperation with universities and research institutes is needed and an overall business strategy should be formulated by taking technological considerations into account. He illustrates a conceptual framework within a diagram detailing the central issues together with questions to be asked during the development process. He also outlines further tools and techniques to probe more specific issues which can then be related to the overall framework.

Hakkarainen (2006) describes the original Mathews ideas as follows (Figure 1). The Blue Box covers the interphase development stage where original ideas are gradually developed into commercial solutions (strategic options stage in Picture 1). This stage in technological development would fruitfully be accomplished within UBC.

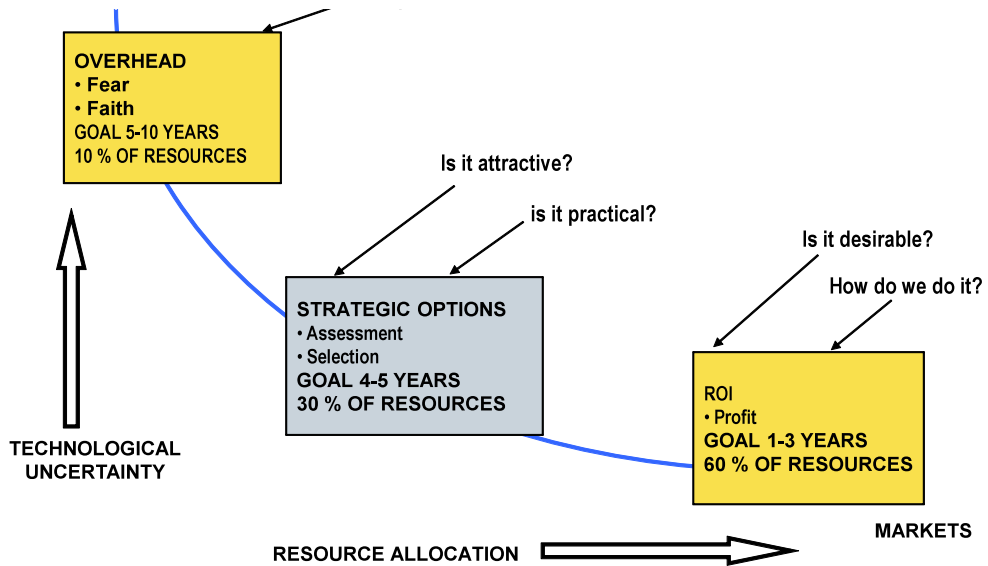


Figure 1. Types of research and development projects (Mathews 1990 and Hakkarainen 2006).

ON TECHNOLOGICAL TRAJECTORIES

Kristinsson-Rao classification

The Kristinsson-Rao classification of technological trajectories is based on industry life cycles. The literature argues that industries go through different stages. Like an organic life form, industries are viewed as going through what is usually described as the four phases of introduction, growth, maturity and decline. Each phase has then its own market structure, and firm characteristics such as innovation rate and type vary with these stages (Kristinsson and Rao 2013).

In life-cycle analyses, the volume of an industry is usually described by either the number of firms (Klepper and Simons, 1997) or the sales volume of an industry (Menhart & Rennhak, 2006). If the sales volume of an industry is the

unit of analysis the industry life cycle is the sum of product life cycles within the industry, as shown in Figure 2.

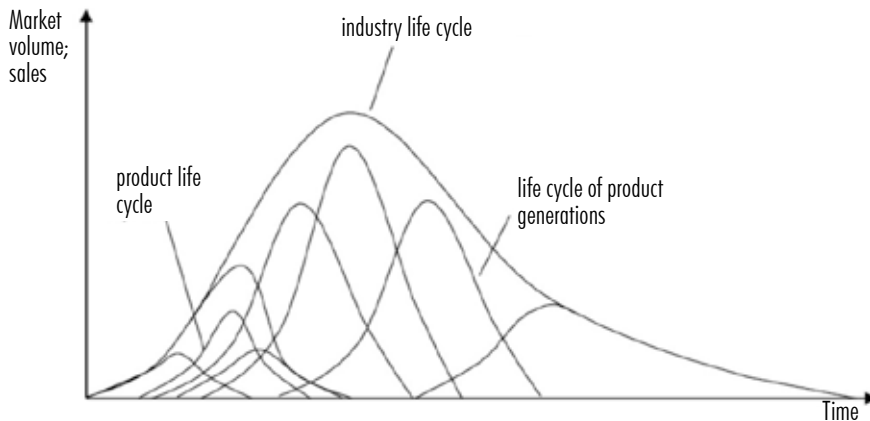


Figure 2. Industry life cycle and product life cycles (Kristinsson & Rao 2013, based on Menhart & Rennhak 2006).

Following the definition of Dosi (1982), a technological paradigm is “a model and a pattern of solution of selected technological problems, based on selected principles derived from natural sciences and on selected material technologies”.

Correspondingly a technological trajectory is defined by Dosi (1982) as “the normal problem solving activity determined by a paradigm, represented by the movement of multi-dimensional trade-offs among the technological variables which the paradigm defines as relevant”.

In other words, even within the same paradigm there is some room for choices, where evolution of the technology depends on the directions taken by the development of the technology, i.e. the technological trajectory.

In many young industries there are two or more alternative technological trajectories competing for dominance. Firms have an interest in seeing that the technological trajectory they are currently most knowledgeable about, would achieve dominance within the industry in longer run. As the industry matures, some technology trajectories are chosen through a socioeconomic process, possibly leading to one trajectory becoming dominant. Several alternate possibilities can emerge from the selection process.

Kristinsson and Rao (2013) have mapped situations where several rival trajectories might achieve roughly equal and stable market share and two similar trajectories might compete over a long period for the dominance while neither achieves it. In Table 1, these and other scenarios are divided

into six phases each representing a different technological environment for the firms in the industry. There is no clear order in which these phases will present themselves; one could easily imagine an industry moving from a dominant technology trajectory to an environment of two rival trajectories vying for dominance. However, in general a trend from ambiguity towards clear dominance might be expected.

Table 1. Emergence of a dominant technology trajectory (Kristinsson and Rao 2013).

Technology Relatedness	Several Competing Trajectories	Dominance Competition	Dominance
Related	A Range of Trajectories	Similar Trajectories	Clear Dominance
Unrelated	Ambiguity	Alternate Trajectories	Dominance

Kristinsson and Rao (2013) have introduced six phases of the development of a dominant trajectory within an industry as follows:

Phase I – Ambiguity

Few pioneer firms. Basic research is done in universities. The possible future technological trajectory is highly uncertain. The range of possible technological trajectories cannot be identified. Other factors such as possible demand, institutional factors and competition are also highly uncertain.

Phase II – A Range of Trajectories

Pioneers in applied research are followed by other organizations. Research programs take place in the area. Gradually the area is populated by several actors each working on their own technological design that often represent totally different technological trajectories.

Phase III – Alternate Trajectories

As the industry matures, stabilizes and the major players become known. Typically two main trajectories turn up. These alternative trajectories are often incompatible and therefore there appears a competition for dominance.

Phase IV – Similar Trajectories

The technological development can be described as having two main outcomes which are related and therefore do not pose so much uncertainty to the firms as in a regime of alternative trajectories.

Phase V – Dominance

One technological trajectory has achieved dominance above all others. More than half of the innovations in the industry belong to this trajectory. The competing trajectories are relegated to minor roles.

Phase VI – Clear Dominance

The majority of the remaining trajectories are related to the dominant one, thus giving a very focused and homogenous R&D space.

Pavitt-Hedge classification

The university-industry innovation cooperation in the Pavitt-Hedge classification of technological trajectories take place mainly in companies which are specialized (e.g. fabricated metals, machinery, instruments, electrical, electronics) or science based (e.g. pharmaceuticals, drugs, chemicals, microelectronics) Table 2.

Table 2. Pavitt's (1984) and Hedge's (2004) sectorial taxonomy and expectations.

	Supplier dominated	Scale intensive	Specialized suppliers	Science based	Information intensive	Primary services
Core sectors	Agriculture, food, wood based, textiles, rubber & plastics	Automotive, transport equipment	Fabricated metals, machinery, instruments, electrical, electronics	Pharmaceuticals, drugs, chemicals, microelectronics	All services	education, transportation, finance, tourism, health
Firm size	Small	Large & Medium	Small	Medium & Large	Small	Small & Medium
Type of innovation	Process	Process	Product	Product & Process	Product & Process	Organisational
Strategy	Cost affectivity	Either cost affectivity (price) or Differentiation (quality)	Differentiation (quality, performance, customization)	Differentiation, Focus strategy (innovation, quality)	Differentiation (quality, quick delivery, customization)	Mixed
External sources of innovation : cooperation	Suppliers and users	Suppliers and users	Universities and users	Universities and users	Users	Financers and users

Comparing the Pavitt-Hedge classification to the Kristinsson-Rao classification, the following hypothesis could be made: The most important role of universities in creating innovations and developing new technology are in the early stages of the industry life cycle, especially in the area of specialized suppliers and science based industries.

Castellacci classification

To analyze technological paradigms, Castellacci (2008) has arranged industries in four sectorial categories and eight sub-groups (Table 3):

1. Advanced knowledge providers
 - Knowledge-intensive business services (e.g. Software; R&D, Engineering, Consultancy)
 - Specialized suppliers manufacturing (e.g. Machinery, Instruments)
2. Mass production goods
 - Science-based manufacturing (e.g. Electronics)
 - Scale-intensive manufacturing (e.g. motor vehicles)

3. Supporting Infrastructure services
 - Network infrastructure services (e.g. Telecommunications, finance)
 - Physical infrastructure services (e.g. Transport, wholesale trade)
4. Personal good and services
 - Supplier dominated goods (e.g. Textiles and wearing)
 - Supplier dominated services (e.g. Hotels and restaurants).

Table 3. Main characteristics of various sectorial groups in the Castellacci taxonomy (Castellacci, 2008).

Sectoral category	Sub-groups within each category	Typical core sectors	Major function and relationship to technological paradigms	Technological regimes	Technological trajectories
Advanced knowledge providers	Knowledge-intensive business services	Software; R&D; Engineering; Consultancy	The supporting knowledge base of the ICT paradigm	Opportunity levels: very high External sources: users and Universities Appropriability: Know-how; copyright Dominant firm size: SMEs	Type of innovation: new services; organisational innovation Innovation expenditures and strategy: R&D; training; cooperations
	Specialised suppliers manufacturing	Machinery; Instruments	The supporting knowledge base of the Fordist paradigm	Opportunity levels: high External sources: users Appropriability: patents, design know-how Dominant firm size: SMEs	Type of innovation: new products Innovation expenditures and strategy: R&D; acquisition of machinery; software purchase
Mass production goods	Science-based manufacturing	Electronics	The carrier industries of the ICT paradigm	Opportunity levels: very high External sources: Universities and users Appropriability: patents, design; copyright Dominant firm size: large	Type of innovation: new products; organizational innovation Innovation expenditures and strategy: R&D; cooperations
	Scale-intensive manufacturing	Motor vehicles	The carrier industries of the Fordist paradigm	Opportunity levels: medium External sources: suppliers and users Appropriability: design; process secrecy Dominant firm size: large	Type of innovation: mixed products and process innovation Innovation expenditures and strategy: R&D; acquisition of machinery
Supporting Infrastructure Services	Network infrastructure services	Tele-communications; Finance	The supporting infrastructure of the ICT paradigm	Opportunity levels: medium External sources: suppliers and users Appropriability: standards; norms; design Dominant firm size: large	Type of innovation: mixed process, service and organizational innovation Innovation expenditures and strategy: R&D; acquisition of software; training
	Physical infrastructure services	Transport; Wholesale trade	The supporting infrastructure of the Fordist paradigm	Opportunity levels: low External sources: suppliers Appropriability: standards; norms; design Dominant firm size: large	Type of innovation: process Innovation expenditures and strategy: acquisition of machinery and software
Personal goods and services	Supplier-dominated goods	Textiles and wearing	They enhance the quality of final products and services by acquiring and embodying technologies related to different paradigms	Opportunity levels: medium External sources: suppliers and end users Appropriability: trademarks; design know-how Dominant firm size: SMEs	Type of innovation: process Innovation expenditures and strategy: acquisition of machinery
	Supplier-dominated services	Hotels and restaurants		Opportunity levels: low External sources: suppliers Appropriability: non-technical means Dominant firm size: SMEs	Type of innovation: process Innovation expenditures and strategy: acquisition of machinery; training

In Table 3, university cooperation turns up only in:

- Knowledge-intensive business services (e.g. Software; R&D, Engineering, Consultancy), where innovations are expected to be organizational or concern new services
- Science-based manufacturing (e.g. Electronics), where innovations are expected to be organizational or concern new products.

Formulating a Model

The types of University-Industry cooperation depend on the degree of the maturity of the industry. See Figure 3.

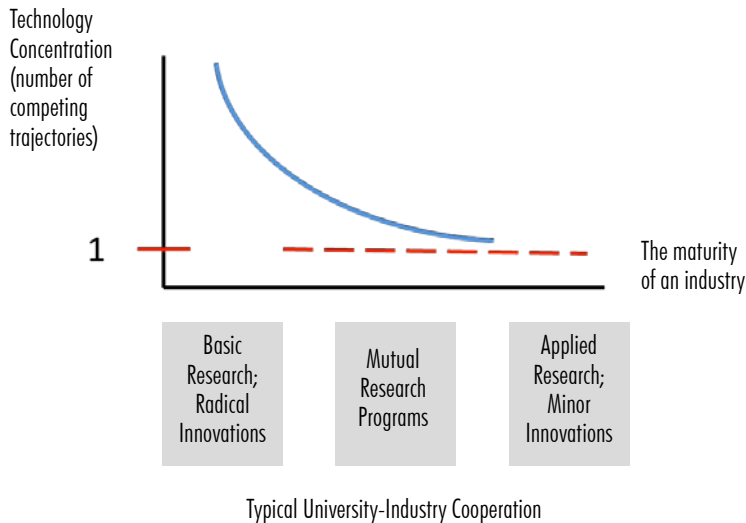


Figure 3. Supplied University Services by Industry Life-Cycle.

On the other hand, some companies are in a continuous stage of quick development (e.g. electronics). The nature of each competing trajectory is supposed to be deep and the stage of basic research and radical innovation possibilities covers a long period. Also companies, whose services are knowledge-based, look for strong partnerships fostering their activities.

These qualitative considerations above give us a possibility to formulate a model to connect types of supplied university R&D services to typical cooperating companies. This is stated in Figure 4.

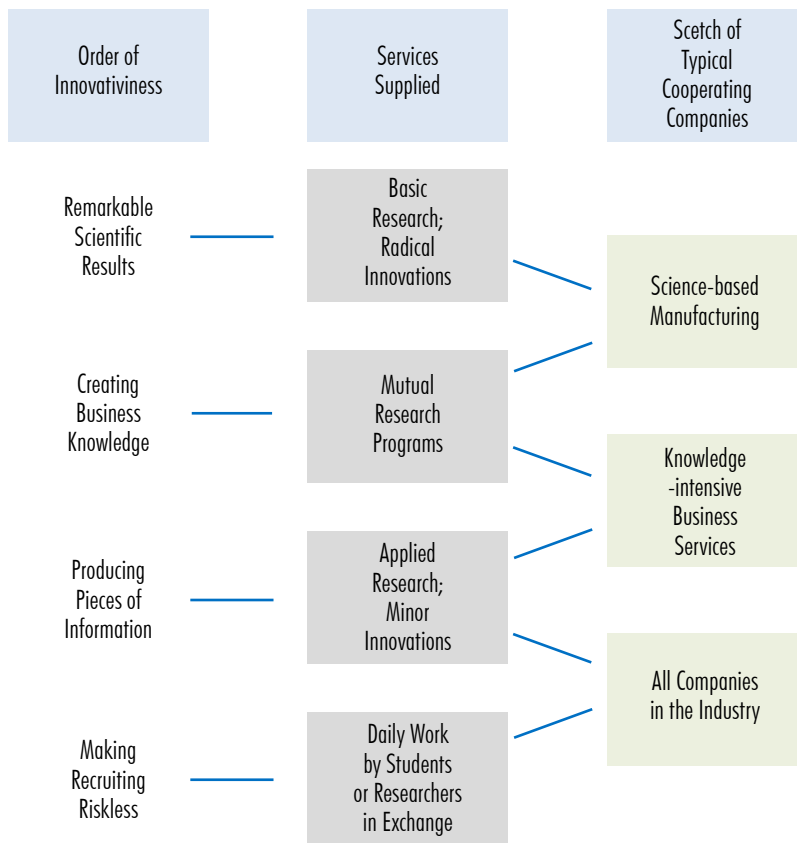


Figure 4. Supplied University R&D Services by Type of Industry.

Consideration of alternative trajectories in company R&D&I

Rautaruukki Oyj (Ruukki) solution, product and production process development (solution and product management or SPM) is a five stage process with go/stop decisions made between the stages, Figure 5. Each product group and key production process has a cross-functional steering group composed of main stakeholders. These groups are responsible for the overall supervision of the development portfolio and for generating ideas for new projects in their area.



Figure 5. Ruukki SPM-process for solution, product and production process development.

The SPM process is very efficient in managing production process and new product development. As the steering groups are composed of persons responsible of e.g. development, sales, marketing, production, quality and production control, they can make fast decisions on launching, freezing or terminating projects and allocating resources to projects with highest economic potential. However, this also represents a problem as there is a risk of adhering exclusively to the existing technology trajectories. Therefore a concurrent development process for radical innovations is included, Figure 6. In this process new disruptive innovations are explored. They are mostly related to new collaboration networks, services or business models than products and solutions. The ideas are developed in this process to concept and application level and then transferred to the normal SPM process. Sometimes a new iteration round is needed if the concept is not tangible enough to be handled by the steering group.

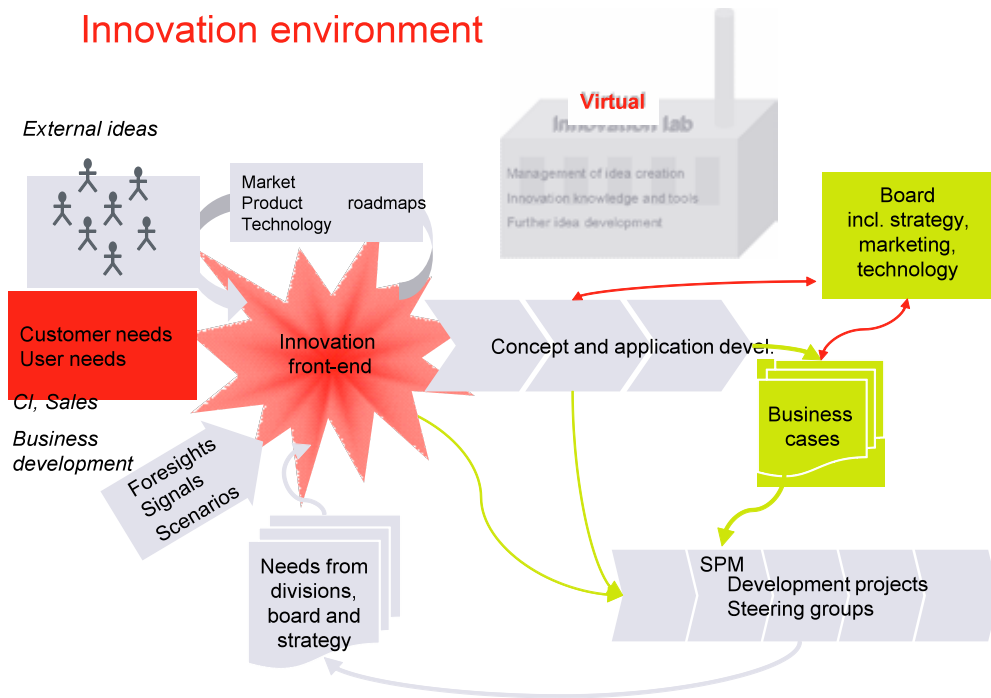


Figure 6. Ruukki innovation environment.

The concept and application development process in Figure 6 is aimed at finding new technological trajectories. It is related mainly to basic research and mutual research programmes depicted in Figure 3. University cooperation and collaboration with other companies play an important role in these activities as a company cannot have enough resources to cover the very large research area needed. When the technology or solution proceeds to the applied research phase, less interaction is possible as the product or solution is approaching launching and competition normally prevents cooperation unless commercialization can be made jointly.

SUMMARY

There exists a risk that companies adhere to their strong historical trajectories. In this article we examine different options for avoiding this pitfall by utilizing several theories of technological trajectories and integration of technology development into business strategy.

In mature stage of industry where the technological trajectories are strong and balanced, it is difficult to find new technical or commercial breakthroughs. Therefore it is important that companies are continuously searching for alternative trajectories and transform them into new businesses. These are most likely to be found in the area of new collaboration networks, services or business models.

Any technological trajectory has a limited lifespan. Thus companies that are not able to renew their technology portfolio are in danger that their business will shrivel. Active search for new trajectories is therefore needed. As the resources of any company are limited and different cooperation networks and e.g. UBC (university-business cooperation) are necessary for renewal of the industry.

REFERENCES

Castellacci, Fulvio (2008). Technological paradigms, regimes and trajectories: Manufacturing and service industries in a new taxonomy of sectoral patterns of innovation. *Research Policy*, 37 (2008), pp. 978–994.

Dosi G. (1982). Technological paradigms and technological trajectories: a suggested interpretation of the determinants and directions of technical change, *Research Policy*, vol. 11, no. 3, June, pp. 147–62.

Hakkarainen, Kari (2006). *Strategic Management of Technology. From Creative Destruction to Superior Resilience*. Acta Wasaensia, Number 162. Industrial Management 11. Universitas Wasaensis 2006.

Hannula, Mika, Ulla Korsman, Eila Pajarre & Marko Seppänen (2003). *A Guide to Academic Writing* [online]. Tampere, Finland. Department of Industrial Engineering and Management, Technical University of Tampere [cited 11.4.2013]. Available: <http://butler.cc.tut.fi/~pesone24/academicwriting.pdf>

Hedge, Deepak (2004). *Innovation and technology trajectories in a developing country context: Evidence from a Survey of Malaysian Firms*. A Thesis. Georgia Institute of Technology, April 2004.

Klepper, S. and K. Simons (1997). Technological extinctions of industrial firms: An inquire into their nature and causes, *Industrial and Corporate Change*, 6, 379–460.

Kristinsson, Kari & Rao, Rekha (2013). The Emergence of Dominant Technology Trajectories in the US Medical Device Industry. First Draft. Aalborg University, DRUID and IKE. Laboratory of Economics and Management, Scuola Superiore S. Anna (Available: www.druid.dk). An unfinished paper.

Matthews, William H. (1990). Kissing Technological Frogs: Managing Technology as a Strategic Resource. *Perspectives for Managers* 5. Lausanne, Switzerland: International Institute for Management Development (IMD).

Matthews, William H. (1992). Conceptual Framework for Integrating Technology into Business Strategy. *Int. J. of Vehicle Design* 13:5/6, 524–532.

Michael Menhart & Carsten Rennhak (2006). Drivers of the Lifecycle – the Example of the German Insurance Industry. Reutlingen Working Papers on Marketing & Management 2006–03. School of International Business, Reutlingen University, 2006.

Pavitt, K. (1984). Sectorial patterns of technical change: towards a taxonomy and a theory. *Research Policy* 13 (1984), pp. 343–373.

SUSTAINABILITY AS A BUSINESS OPPORTUNITY TODAY AND TOMORROW: TRIPLE HELIX PERSPECTIVE

Tarja Meristö
(tarja.meristo@laurea.fi)

Jukka Laitinen
(jukka.laitinen@laurea.fi)

FuturesLabs CoFi
Laurea University of Applied Sciences, Finland

ABSTRACT

In this paper we focus on SMEs from different industries in Baltic Region. The main goal is to recognize the business potential of sustainable development in this region, to wake up the companies to be aware of this potential and finally to design visionary business concepts for number of cases in this field. In the first phase we have designed a tool based on the reporting guidelines of Global Reporting Initiative (GRI). Our tool is meant for companies to recognize their business opportunities and business potential generally throughout the whole value chain as well as new business opportunities across the borders of other industries.

INTRODUCTION

Sustainable development has been used as a word since Bruntland's report 1987 (United Nations 1987). Originally, it meant not only ecological, but also social and economic sustainability. In a broad definition, all the activities throughout the society, including business, have to meet three challenges, not harming the future opportunities of the generation first coming to the planet.

At a regional level, in order to achieve sustainable development in practice, all the Triple Helix dimensions have to be covered, which means actors from public, private and educational sectors (Etzkowitz & Laydesdorff 1995). The role of sustainability in the triple helix context have been inspected earlier (e.g. Yang et al. 2012) but the focus has been in ecological sustainability. In our paper we are focusing on all dimensions of sustainability, i.e. economic, social and ecological sustainability.

In business literature sustainable development means different things, e.g. corporate social responsibility, energy efficiency, lean resource management, human rights policy or eco-efficiency are the expressions to companies' sustainable behaviour in the context of society and environment. From the business perspective, the attitudes of consumers are an important part of sustainable development. The focus from environmental and ecological issues has moved towards more broad definition of sustainability including not only environmental but also healthy and safety aspects of sustainability.

This is called the EHS criteria. Also, World Business Council for Sustainable Development (WBCSD), which is a global association of some 200 international companies, deals with the issues concerning business and sustainable development.

This project is focused on SMEs from different industries in Baltic Region. The main goal is to recognize the business potential of sustainable development in this region, to make the companies aware of this potential and finally to design visionary business concepts for a number of cases in this field. In the first phase, we have designed a tool based on the reporting guidelines of Global Reporting Initiative (GRI). The tool is meant for companies to recognize their business opportunities and business potential generally throughout the whole value chain as well as new business opportunities across the borders of other industries.

SUSTAINABILITY

Sustainability means development with economic, social and ecological balance not only today but for the future generations (United Nations 1987). In business context this means also responsibilities in different time frames, i.e. short, medium and long-term. Economic sustainability includes e.g. economic activity (profitability, turnover), market position (market share) and indirect impacts (e.g. via taxation); ecological sustainability in the company's eyes consists of material use (how much, which kind of), energy use (efficiency, renewables), water footprint, CO₂ footprint, biodiversity and waste management among the others. Social sustainability will cover personnel issues like occupational health and safety and security, but also human rights, corruption, legislation and product responsibilities.

TRIPLE HELIX MODEL

The concept of the Triple Helix of university-industry-government relationships interprets the shift from a dominating industry-government dyad in the Industrial Society to a growing triadic relationship between university-industry-government in the Knowledge Society. The creative renewal arises within each of the three institutional spheres of university, industry and government, as well as at their intersections (Etzkowitz & Leydesdorff 1995). In other words, the Triple Helix is a metaphor for university, industry, and government interacting closely, while each maintains its independent identity. All the Triple Helix actors benefit from some of the capabilities of the other, even as each maintains its primary role and distinct identity (Etzkowitz 2007).

SUSTAINABILITY FROM TRIPLE HELIX PERSPECTIVES

We have combined the Triple Helix context with the sustainability concept which means that all the three dimensions of sustainability have to run through all the actors as a part of triple helix (Figure 1).

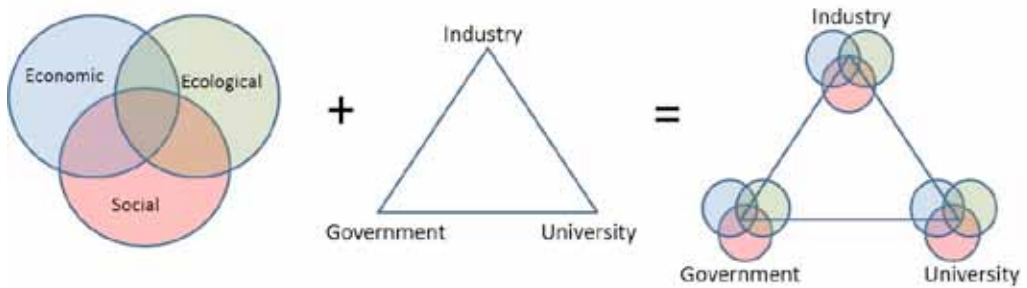


Figure 1. The Triple Helix context combined with the sustainability concept.

In other words, university, government and industry have to adopt sustainability as a living part of their everyday activities. On the university side this means e.g. new study programs focusing on sustainability issues, but as a part of their work, sustainability could and should be a guiding principle. On governmental side the decision-making process will focus on creating new opportunities for sustainable solutions. Government has to be seen as an enabler for new, sustainable business practices. On the industry side, sustainability will also give win-win-situations with 'less is more' solutions, where the company can win, but also the society and nature will be winners even in the long-run.

Developed further, this construction could be a bit more advanced, i.e. in government's corner the social circle (e.g. equality) has more focus than in the others; in industrial corner the economic circle is in the middle and business profit has a bigger role. University perspective will bring Research & Development & Innovation (R&D&I) to the table, and focus on multidisciplinary studies combining e.g. natural and technical sciences to human and commercial perspectives will put attention to ecological issues at many levels (Figure 2).

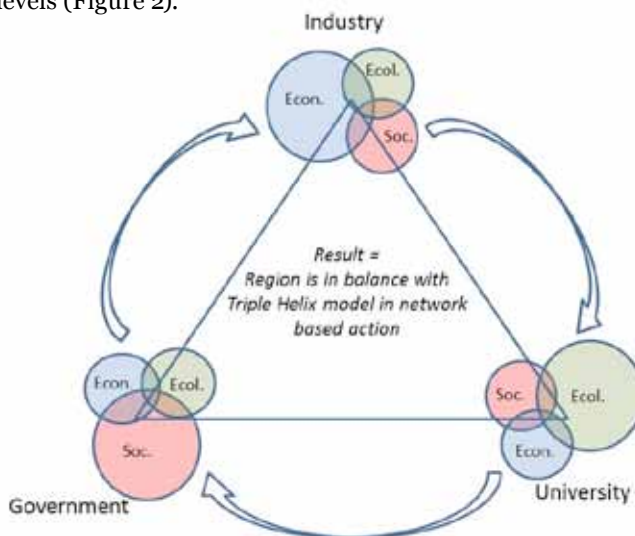


Figure 2. The focus of the sustainability dimensions can vary in triple helix actors. Through networking a balanced sustainability is reached.

SUSTAINABILITY IN CONSTRUCTION INDUSTRY

As an example, in this paper we will focus on construction industry and its problems with sustainability issues. In Finland, construction industry contributes about 10% of annual GNP (Rakennuslehti 2013). Because of northern climate in Finland, housing is an essential part of everyone's budget, i.e. all the sustainable solutions in this side will have a significant impact to the whole society.

Construction is traditionally a local business. It is closely related to cultural tradition, design and materials used. Education for construction industry will also rely on national norms and legislation, including not only individual houses but all the urban planning and community structure with its infrastructure. Therefore, triple helix approach combined with sustainability approach is especially suitable within construction industry and its different phases and activities. On the governmental side, local authorities have impact on infrastructural decisions, but they also decide on social and economic conditions concerning equality and welfare e.g. social housing production. On the industrial side, the material and energy use, waste and footprints as well as labour force with all the economic implications and responsibilities are the key components of sustainability in companies. In the triple helix context, new university programs will focus on sustainability issues, but they also will educate new skills and competences for industry in different sectors including construction industry among the others. The output is, of course, new study programs and students with new skills and competences, but as a part of an education task, new attitudes and values will be spread throughout the society. Also R&D&I project in close co-operation with business people will create new solutions, which are better by nature in terms of sustainability.

Indicators for assessing the sustainability performance of new or existing buildings, related to their design, construction, operation, maintenance, refurbishment and end of life have been defined in ISO 21929-1 standard. The set of indicators provides measures to express the contribution of a building(s) to sustainability and sustainable development. ISO 21929-1:2011 adapts general sustainability principles for buildings and it includes a framework for developing sustainability indicators for use in the assessment of economic, environmental and social impacts of buildings (ISO 21929-1).

Sustainability reporting guidelines to the companies are also offered by the Global Reporting Initiative (GRI) which a non-profit organization that promotes economic, environmental and social sustainability. GRI provides all companies and organizations with a comprehensive sustainability reporting framework that is widely used around the world. Sustainability reporting helps organizations to set goals, measure performance, and manage change in order to make their operations more sustainable (Global Reporting Initiative 2013).

We have developed, as part of a sustainable business opportunities project, a simple tool for companies to recognize their potential in sustainability as well as to wake up their own awareness in this field. The tool consists of

the following parts: company-specific background questions, importance of components of sustainability (economic, social, ecological), the status of sustainable business today and in the future, the channels to get information concerning sustainability as well the future focus area of the company in the future. Testing of the tool and preliminary results from state of the art in construction industry has been applied among top decision makers in Finnish construction industry. Economic sustainability is, in the first place social sustainability, in the second place an ecological sustainability and in the third place among these repliers (Figure 3). Probably construction industry as an energy- and material intensive industry has already worked a lot for ecological sustainability and therefore the other dimensions will rise above that!

None of the repliers said that sustainability does not concern construction business. All the answers were at least on the level of awareness and some of them even at the level of active work today or visioning better future for tomorrow (Figure 4).

Sustainability has been seen for construction industry a part of basic business but also giving new business opportunities and competitive advantage today (Figure 5). In the future, competitive advantage was the most often mentioned reason to develop sustainability as a part of the business. No one said sustainability drive is only empty words without real opportunities.

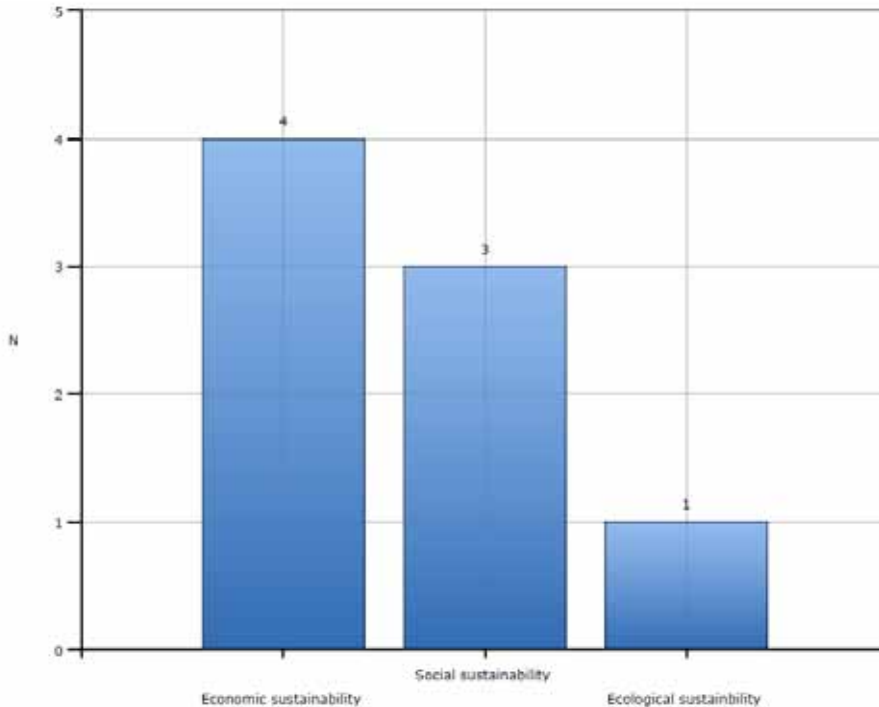


Figure 3. The dimensions of the sustainable development in which the industry should invest.

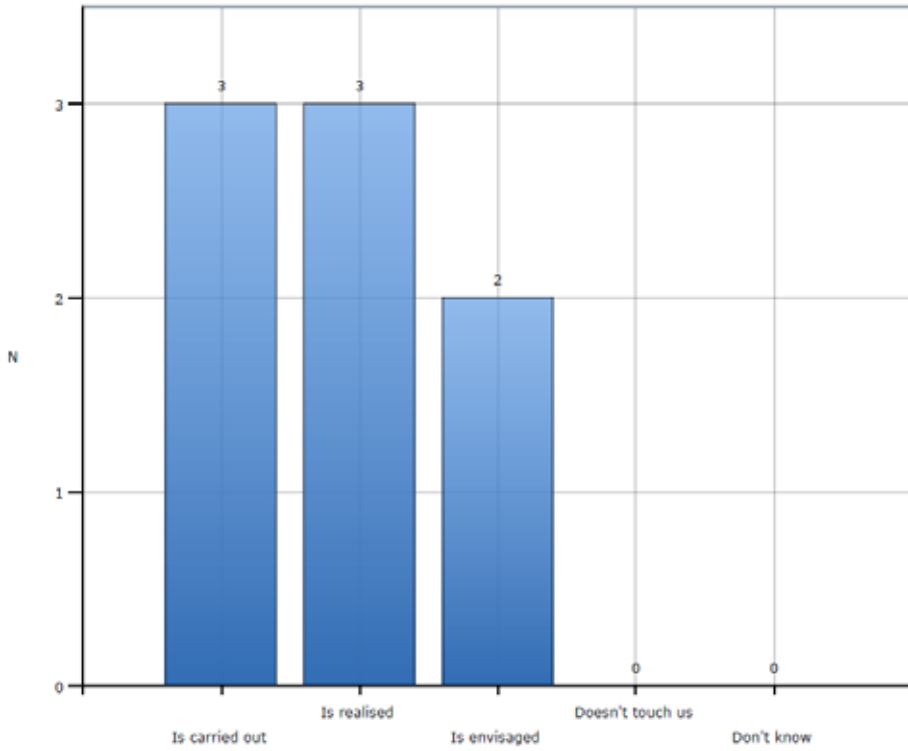


Figure 4. The current role of sustainability in the construction industry.

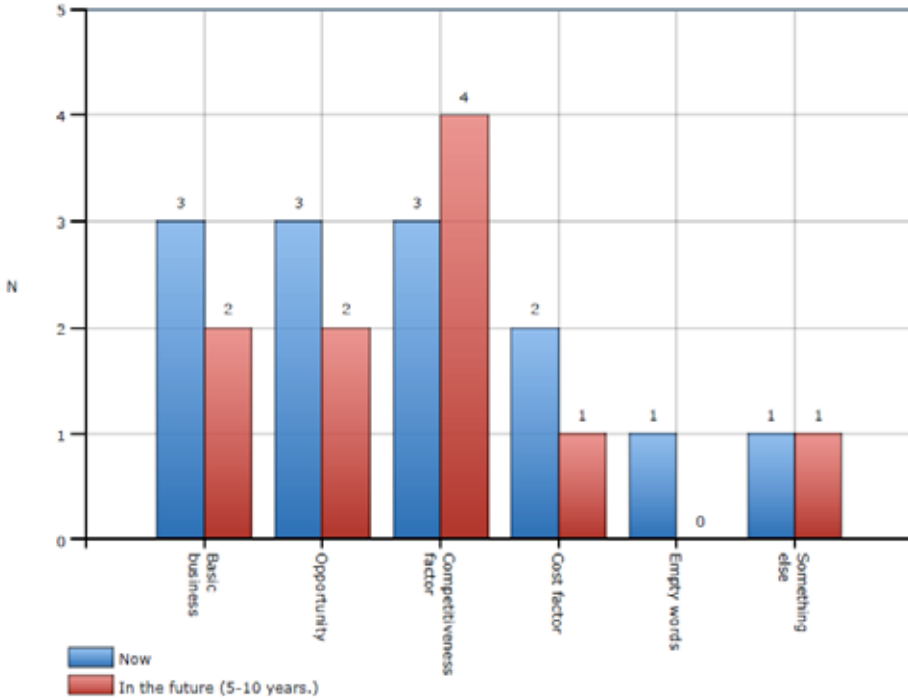


Figure 5. How the sustainability is perceived in the construction industry now and in the future.

Media seems to be the main channel to meet the challenges of sustainable development, but also education and authorities are the actors giving impulses for more active work (Figure 6). Still, money talks and only energy issues and product and service concepts will arise close to that level of economy. Economic activities such as profitability and turnover were perceived the most important issues related to the sustainability in the construction industry (Figure 7). Also energy, products and services and society were seen as essential factors. Surprisingly, the respondents did not note ecological issues such as water, sewage, debris and biodiversity at all. None among human rights, personnel practices or working conditions were seen important.

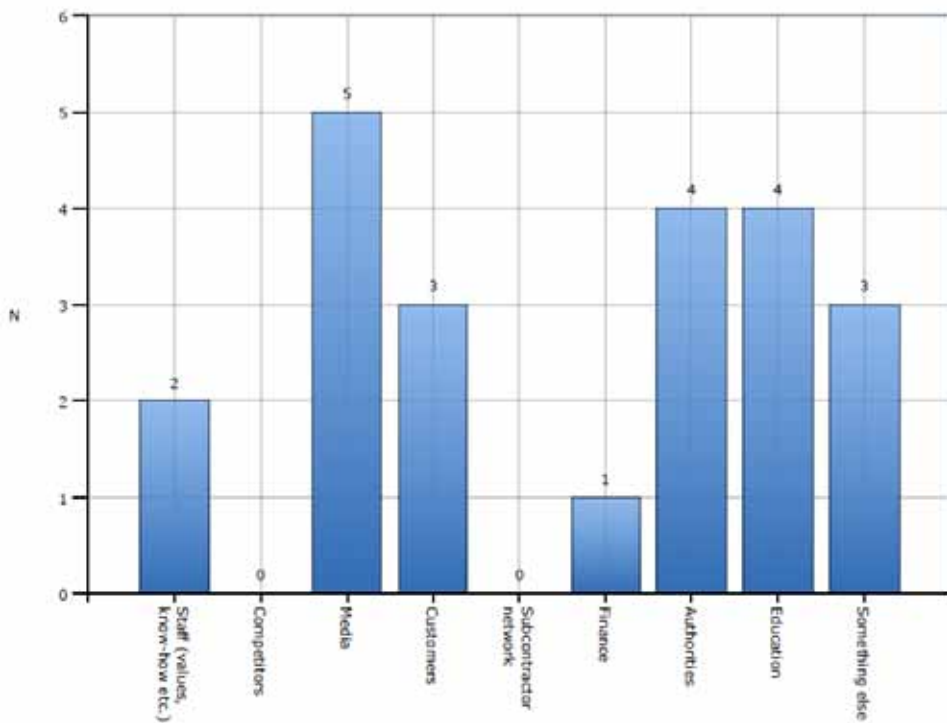


Figure 6. The channel of the sustainable development in the construction industry.

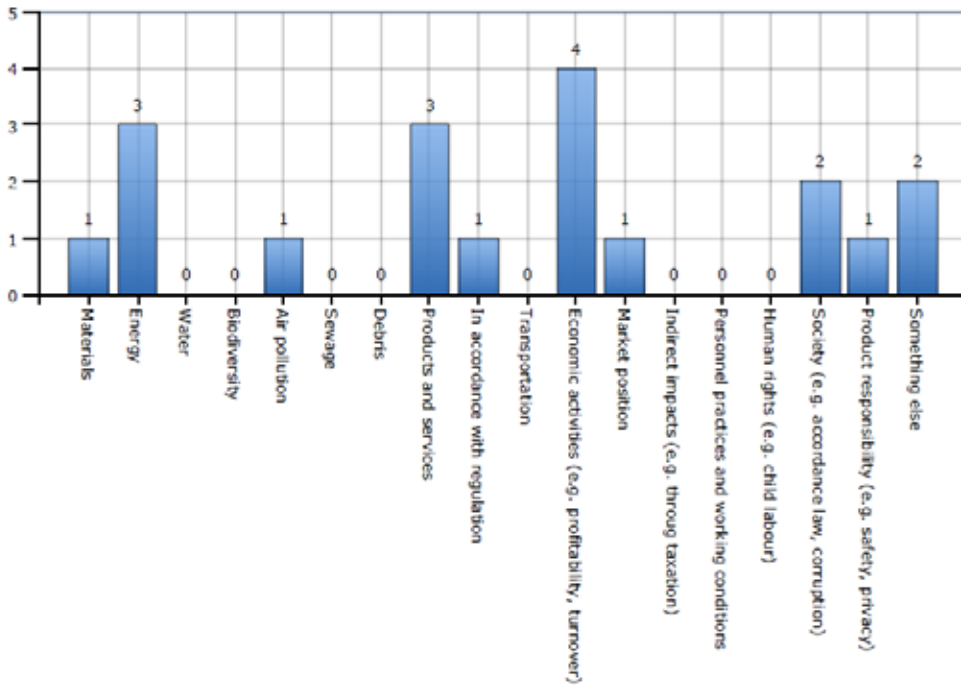


Figure 7. The most important sustainability issues in the construction industry.

Construction industry in this paper has been covered only with opinions of a few experts. In the near future, we will continue the work with in-depth interviews in construction industry companies in Uusimaa County. Also other industrial sectors in the region will be covered and data collected for comparison. Especially from economic viewpoint of sustainability, international interviews in Sweden and in Germany will be carried out with focus on EU's Small Business Act and its opportunities for SMEs. All the interviews will take place in autumn 2013.

CONCLUSION

This paper presents the first results from our work dealing with sustainability and triple helix together. Framework developed in this work seems to be promising. It shows the elements of sustainable development in business context at local and regional level. It also gives alternative perspectives to a balanced development in terms of sustainability. Actor-based model will be replaced by network based model with new features. This gives an opportunity to develop a dynamic model to examine new business opportunities for sustainable growth in the way all the actors can focus on the strengths of their own. This is only a beginning. The research work will continue in autumn with field work (e.g. interviews), but also theoretical framework development will be in progress. Sustainability is one of the most important issues in global

context. Every triple helix hub and every single actor have to be prepared for the future keeping in mind these three dimensions of sustainability, i.e. economic, social and ecological sustainability. Without dynamic balance in this sense there are no business opportunities in the future at all.

REFERENCES:

Etzkowitz, H. (2007) University-Industry-Government: The Triple Helix Model of Innovation. Proceedings of the 51st EOQ Congress, 22–23 May, 2007, Prague, Czech Republic.

Etzkowitz, H., Leydesdorff, L., (1995) The Triple Helix: University – Industry – Government Relations A Laboratory for Knowledge Based Economic Development. *EASST Review* 14 (1), 1995.

Global Reporting Initiative (GRI) (2013) G4 Sustainability Reporting Guidelines. <https://www.globalreporting.org/resource/library/GRIG4-Part1-Reporting-Principles-and-Standard-Disclosures.pdf> (viewed 30.8.2013).

ISO 21929-1 (2011) Sustainability in building construction – Sustainability indicators.

Rakennuslehti (2013) Rakennusmarkkinat Suomessa. (Construction market in Finland) (in Finnish). http://www.rakennuslehti.fi/tietoa/rakennusmarkkinat_suomessa/ (viewed 30.8.2013)

United Nations (1987) Our Common Future – Report of the World Commission on Environment and Development.

Yang, Y., Holgaard, J.E., & Emmen, A. (2012), “What can triple helix frameworks offer to the analysis of eco-innovation dynamics? Theoretical and methodological considerations”. *Science and Public Policy*, Volume 39, Issue 3, pp. 373–385.

WBCSD World Business Council for Sustainable Development <http://www.wbcsd.org/home.aspx> (viewed 30.8.2013).

OPTIMIZATION OF STEEL TOWERS FOR LARGE WIND TURBINES

Anatoly Perelmuter
SCAD Soft Ltd, Kyiv, Ukraine

Vitalina Yurchenko
Kyiv National University of Civil Engineering and Architecture, Kyiv, Ukraine

ABSTRACT

Tall towers of wind-powered generators are relatively new types of steel structures widely applied. At the present time several thousand steel towers for wind-powered generators are manufactured every year in the world. The paper describes a technique for the optimisation of steel towers.

INTRODUCTION

During last decade the typical capacity of the wind-powered generators increased nearly ten times (Perelmuter 2013). Steel towers for wind turbine go up to a height of 100 m and more and the tower cost approaches 15–20% of the construction budget for the whole wind-powered generator. Taking into account the increasing ratio between the cost of the steel tower and the construction budget for the whole wind-powered generator, formulation of an optimization problem for this kind of steel structure is considered as beneficial.

PROBLEM FORMULATION

Optimization problem is formulated as searching of the optimum design of the tower for wind-powered generator, which is designed as a steel conic shell with diameter varied linearly along shell length.

The tower structure was divided into parts along the tower height while using the finite element method for determination of the stress-and-strain state of the tower's conic shell. For each part of the tower a constant thickness and a constant diameter of the middle surface at lower level were considered as characteristic cross-sectional dimensions (Fig. 1).

The main parameters of the steel conic shell tower were considered as design variables, namely: H – the tower's height; D_{\min} – minimum diameter of the middle surface of the tower's conic shell at a height of H (the height of wind wheel above earth's surface level); D_{\max} – maximum diameter of the middle surface of the tower conic shell at the base level; t_i – the thickness of i^{th} part of tower's conic shell, $i = 1 \dots n_s$, where n_s – number of the tower shell parts; D_w – the diameter of the wind wheel.

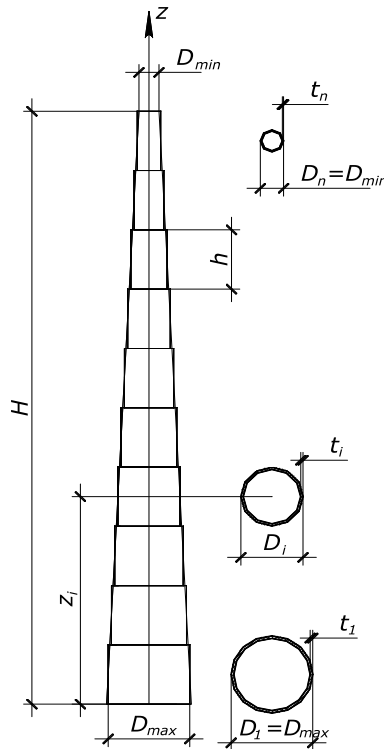


Figure 1. Design variables of the steel conic shell tower.

The load-bearing capacity of the steel tower’s shell structure should be verified for two wind load cases. *The first wind load case* is determined by the maximum possible wind velocity $v_{H,max,1}$ at a height of H above earth’s surface level (at the height of installation of the wind wheel) by which wind wheel’s blades of the wind-powered generator are under operating conditions. The corresponding wind velocity $v_{0,max,1}$ at a height 10 m above the earth’s surface level is calculated as (H in m).

$$v_{0,max,1}(H) = \frac{v_{H,max,1}}{(H/10)^{0,14}} = v_{H,max,1} e^{-0,14(\ln H - \ln 10)}$$

The second wind load case is determined by the maximum possible wind velocity $v_{0,max,2}$ at a height 10 m above the earth’s surface level. This wind velocity characterizes the considered terrain where wind-powered generator will be installed.

The load-bearing capacity of the steel tower’s shell structure should be verified for both the wind load cases mentioned above so long as it is not known

beforehand which of them is more critical. Under the lower wind velocity $v_{0,\max,1}$ ($v_{0,\max,1} < v_{0,\max,2}$) distributed wind load $q_{i,1}(H, z_i, D_i)$ together with concentrated pulling load of the wind turbine $F_x(v_{0,\max,1})$ apply on the steel tower structure. Under the higher wind velocity $v_{0,\max,2}$ the distributed wind load $q_{i,2}(H, z_i, D_i)$ on the tower structure is greater, but the pulling force of the wind turbine is not applied to the tower's top due to rotation of the blades in a feathered position.

Objective Function

The optimization problem of tower for wind turbine with target capacity W^* can be solved by choosing the corresponding diameter D_w of the wind wheel and corresponded wind velocity $v_H(H)$, which depends on the tower height H . It follows from the expression for produced capacity W of the wind-powered generator, which is estimated based on ideal turbine model proposed by N. E. Zhukovskiy and A. Betz's taken into account average annual wind velocity v_0 as:

$$W(v_H(H), D_w) = \frac{16}{27} \cdot \frac{\rho_a v_H^3}{2} \cdot \frac{\pi D_w^2}{4}$$

Naturally, at the same time it is aspired to the minimise the weight of the steel tower. The theoretical weight of the tower conic shell can be calculated as:

$$G(D_i, t_i) = \pi \rho_s h_s \sum_{i=1}^{n_s} t_i D_i$$

where $\rho_s = 7,8 \text{ t/m}^3$ – the steel density.

In the problem formulation, the produced capacity W of the wind-powered generator being equal to the target capacity W^* was considered as additional constraint expressed in the form of inequalities (ε_w – small positive number).

$$W^* - \varepsilon_w \leq W(v_H(H), D_w) \leq W^* + \varepsilon_w$$

System of constraints

Constraints of the ultimate limit state were formulated as verifications that the actual stresses arising in the design cross-section of i^{th} part of tower's conic shell, here $i = 1, \dots, n_s$, caused by k^{th} load case combination, should not exceed the critical stresses of compression (by the local stability):

$$N_i/A_i + M_{i,k}/W_i \leq \sigma_{cr,i}$$

where $\sigma_{cr,i}$ – the critical stress for i^{th} part of the tower's conic shell; N_i – the design axial force in i^{th} part of the tower conic shell; $M_{i,k}$ – the design bending moment for i^{th} part of the tower conic shell subjected to k^{th} load case taking into account concentrated axial load applied at a height H of tower caused by self weight of the rotor; γ_{fmr} , γ_{fmsw} – safety factors for self weight loads caused by the rotor and steel tower conic shell respectively; A_i and W_i – area and second moment of inertia of the cross-section of i^{th} part of the tower conic shell respectively.

RESULTS OF OPTIMIZATION

A number of optimization problems have been formulated with different values of target capacity W^* of the wind-powered generator. These parametric optimization problems have been solved by improved method of projection objective function gradient on the surface of the active constraints using software OptCAD (Peleshko et al. 2009). Initial data are as follows: average annual wind velocity $v_0 = 7$ m/s; maximum possible wind velocities for wind wheel blades and for considered terrain $v_{H,\max,1} = 20$ m/s and $v_{0,\max,2} = 30$ m/s correspondingly; the design steel resistance $R_y = 3,823$ t/sm²; safety factors for wind load $\gamma_{fmsw} = 1,2$, for rotor self weight $\gamma_{fmr} = 1,2$; for tower self weight $\gamma_{fmsw} = 1,05$. Table 1 presents the results of optimization calculations. The correlation between the tower height and the generation capacity is shown in Figure 2.

Table 1. Results of optimization.

W^* , MWt	H , m	G , t	D_{\min} , m	D_{\max} , m	D_w , m
1,0	75,65	39,76	1,881	4,769	65,65
2,0	98,13	90,74	2,520	6,335	88,13
3,0	114,57	147,71	2,975	7,482	104,57
4,0	128,02	209,00	3,347	8,422	118,02
5,0	139,60	273,80	3,667	9,233	129,60
6,0	149,89	341,55	3,951	9,955	139,89
7,0	159,22	411,90	4,209	10,609	149,22

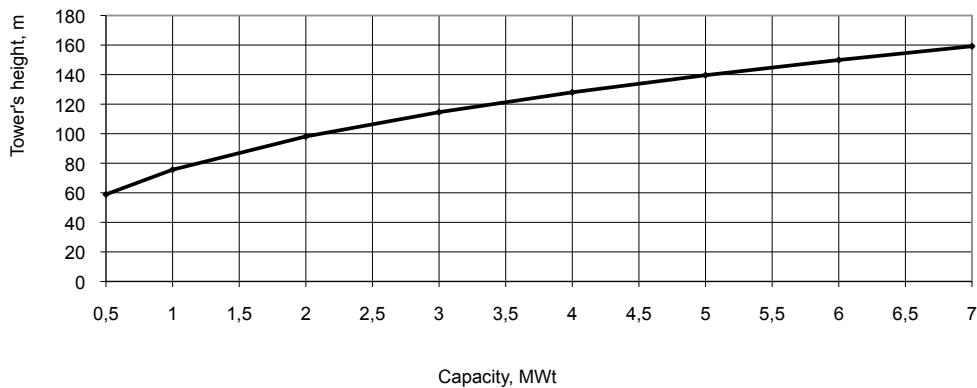


Figure 2. Optimum tower height depending on produced capacity of the generator.

CONCLUSIONS

This paper presents parametric optimization of steel conic shell towers of wind-powered generators. The minimum weight of the steel tower has been considered as the objective function when produced capacity of the wind-powered generators has been fixed at the target level. The tower height, diameters of the middle surface of the tower's conic shell at the base level and at a height of the wind turbine installation, thicknesses of the tower conic shell, and also the diameter of the wind wheel were considered as the design variables. The wind loads applied on steel tower shell have been considered as state variables. The optimization problem, formulated as a non-linear programming task, has been solved by improved gradient method. Optimum designs of the steel conic shell towers for the wind-powered generators with produced capacity of wide range have been defined.

REFERENCES

Перельмутер, А. В. 2013. Башни ветроэнергетических установок мегаваттного класса [The towers of million-kilowatt wind turbines], *Промышленное строительство и инженерные сооружения* [Industrial building and engineering structures], 1.

Peleshko, I.; Yurchenko, V. 2004. An optimum structural computer-aided design using update gradient method, *Proc. of the 8th Int. Conf. "Modern Building Materials, Structures and Techniques"* (Lithuania, Vilnius, May 19–21, 2004): 860–865.

STRUCTURAL BRACING – FORCES AND STIFFNESS

Olli Ilveskoski

HAMK University of Applied Sciences, Hämeenlinna, Finland

INTRODUCTION

The paper deals with the design of structural bracing used in beams, columns, and frame structures. Bracing used in structural systems generally serve two primary functions. They resist secondary loads on structures e.g., wind bracing and increase the strength of individual members by resisting deformation in the weakest direction. For the latter case, structural bracing forces higher modes of deformation by providing resistance to lateral and rotational displacement. This is achieved through axial, shear, and flexural deformations of the bracing member. Diaphragms, for instance, provide restraint through their shear stiffness while diagonal cross-bracing relies on axial stiffness.

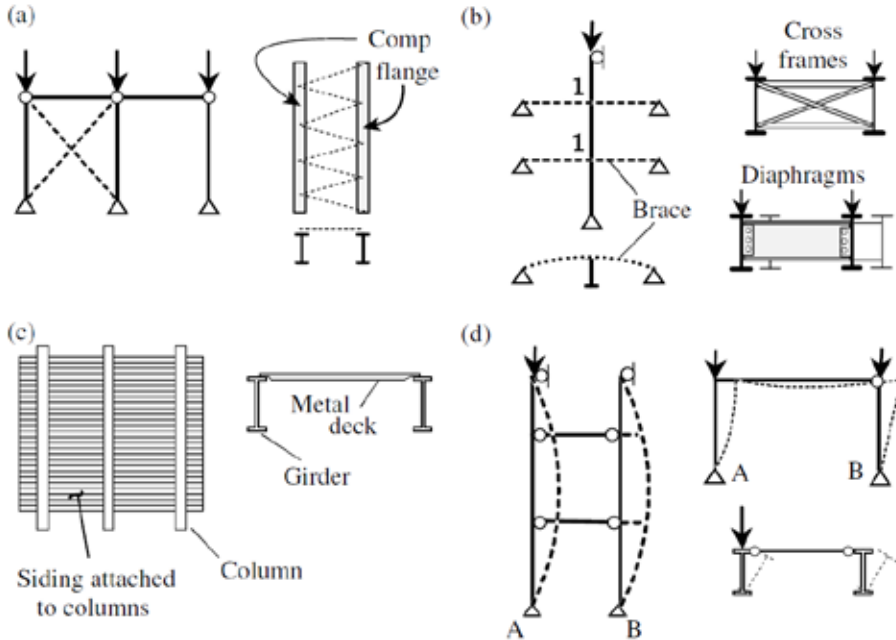
European standards give brief instructions on bracing connection forces and do not inform much about connection stiffness or the use of sandwich panels as stabilizing elements. This short survey is made to check other guidelines and recommendations. Especially the use of self-supporting sandwich panels as stabilizing elements for single steel members such as beams or columns has been recently investigated and Recommendations on the Stabilization of Steel Structures by Sandwich Panels have been published. The possibility to use sandwich panels as stabilizing elements reduces the weight and costs of the frame and creates even the method to design frameless buildings.

Manufactures have big challenges to meet present requirements in standards. The stabilizing elements shall fulfil the requirements shown by the CE-mark of the product. Depending on the case and practice, the manufacturer shall provide the additional information about the stiffness and the resistance of the fastenings or about the shear stiffness and the torsional restraint of the stabilizing system.

BRACING SYSTEMS

Bracing systems used to control instability fall into four general classifications: relative, nodal, continuous, or lean-on. Relative bracing systems, such as diagonal bracing or shear walls, prevent the relative lateral movement of adjacent stories or of adjacent points along the length of a member. Nodal systems control the movement only where they attach to the braced member and do not directly interact with adjacent brace points. Cross-frames or diaphragms between two adjacent beams are considered nodal braces. Continuous systems provide uninterrupted support along the entire length of a member, leaving no unbraced length. Shear walls and roof or floor deck are

examples of continuous bracing systems. Lean-on systems rely on adjacent structural members to provide support. Lean-on bracing links together adjacent structural members such that buckling of one member requires all members in the system to buckle with the same lateral displacement [1].



Types of bracing: (a) relative; (b) nodal; (c) continuous; and (d) lean-on.

Figure 1. Bracing systems [1].

Structural bracing used to increase the strength of members must possess both sufficient strength and stiffness. Simple bracing design rules such as designing a brace to resist 2% of the member compressive force address only the strength criterion. The stiffness of the brace along with the out-of-straightness of the member has a direct effect on the magnitude of the brace force. Design recommendations based on perfectly straight members should not be used directly in design since extremely large brace forces and displacements may result.

Winter developed the concept of a dual strength and stiffness criterion for the design of bracing used to control instability. The required brace strength cannot be uniquely determined, but depends on both the magnitude of the brace stiffness and member initial out-of-straightness. The relationship between these parameters is illustrated for the relative column brace in Figure 2 and can be extended to other types of bracing systems.

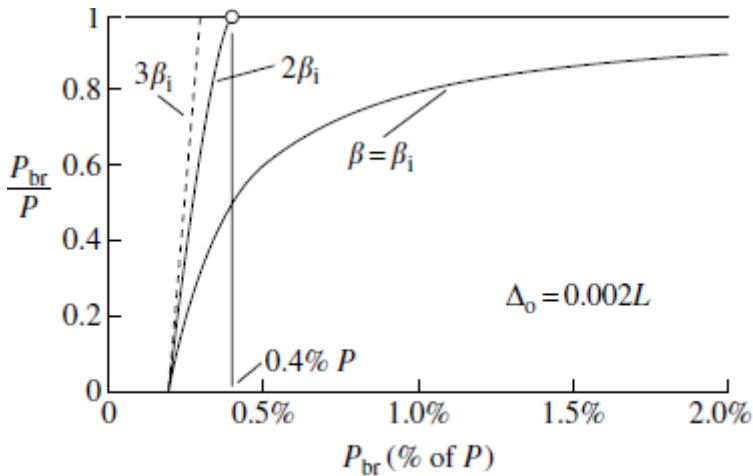


Figure 2. Required brace strength, stiffness and initial member out-of- straightness [1].

In order to reach the Euler buckling load, P_e , the brace must possess a minimum stiffness known as the ideal stiffness, β_i . Figure 2 shows the relationship between the brace stiffness and force. When the ideal stiffness is used ($\beta = \beta_i$), as the column load approaches P_e the sway deflections become very large. Unfortunately, this results in very large brace forces since $P_{br} = \beta \Delta$. At twice the ideal stiffness ($\beta = 2\beta_i$), the brace force equals 0.4% of the column load when $P = P_e$. For practical designs, the deflections and corresponding brace forces are kept small by using brace stiffness greater than the ideal stiffness.

The plots developed in the figure above were based on an assumed initial out-of-straightness equal to $0.002L$. Larger out-of-straightness values linearly increase the magnitude of the brace forces [1]. The connections details used to attach structural bracing members can be of great importance when designing or evaluating the overall performance of a bracing system. If the connections are flexible, the stiffness of the overall bracing system can be significantly less than the stiffness of the bracing member alone. The stiffness of a bracing system can be evaluated as springs in series using

$$\frac{1}{\beta_{sys}} = \frac{1}{\beta_{br}} + \sum \frac{1}{\beta_{conn}}$$

The system stiffness, β_{sys} , will always be less than the smaller of the brace member stiffness, β_{br} , and the connection stiffness values β_{conn} [1].

MEMBER BRACING ACCORDING TO EUROCODE [6]

Eurocode 3 Design of Steel structures – Part 1–1 contains rules to prevent column-beam's lateral – torsional buckling. It includes, e.g. simplified assessment methods for beams with restraints in buildings (6.3.2.4).

$$\bar{\lambda}_f = \frac{k_c L_c}{i_{f,z} \lambda_1} \leq \bar{\lambda}_{c0} \frac{M_{c,Rd}}{M_{y,Ed}} \quad (6.59)$$

More rules can be found about lateral torsional buckling of members with plastic hinges (6.3.5) where significant axial compression in the stable length may be taken from

$$\begin{aligned} L_{stable} &= 35 \varepsilon i_z && \text{for } 0,625 \leq \psi \leq 1 \\ L_{stable} &= (60 - 40\psi) \varepsilon i_z && \text{for } -1 \leq \psi \leq 0,625 \end{aligned} \quad (6.68)$$

and effective restraint should be provided so that at each plastic hinge location, the connection of the compression flange to the resisting element at that point and any intermediate element (e.g. diagonal brace) should be designed to resist a local force equal to 2,5% of $N_{f,Ed}$ transmitted by the flange in its plane and perpendicular to the web plane, without any combination with other loads.

For the design of bracing systems it should be verified that the bracing system is able to resist the effects of local forces Q_m applied at each stabilised member at the plastic hinge locations, where;

$$Q_m = 1,5 \alpha_m \frac{N_{f,Ed}}{100}$$

This verification ensures minimum required stiffness of the bracing system.

Annex BB.3 gives information about stable lengths of segments containing plastic hinges for out-of-plane buckling concerning uniform members made of rolled sections or equivalent welded I-sections (BB.3.1).

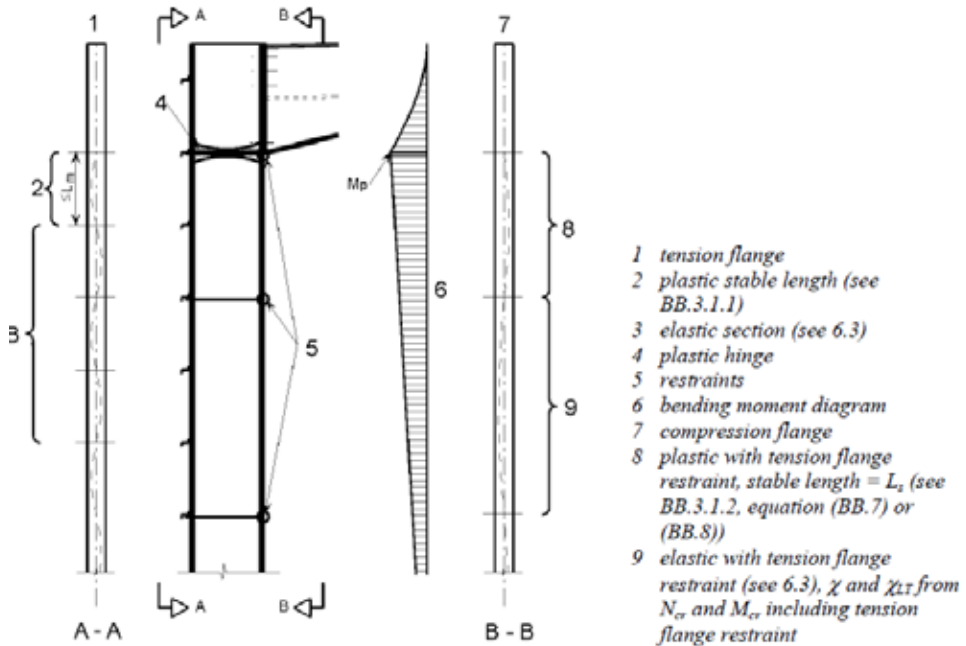


Figure 3. Checks in member without a haunch (BB.3) /6/

The beam at the connection may be regarded as being laterally restrained in the plane of the sheeting if trapezoidal sheeting is connected to a beam and the following condition is met according to EN 1993-1-3

$$S \geq \left(EI_w \frac{\pi^2}{L^2} + GI_t + EI_z \frac{\pi^2}{L^2} 0,25h^2 \right) \frac{70}{h^2} \quad (\text{BB.2})$$

A beam may be considered as sufficiently restraint from torsional deformations [6] if

$$C_{\theta,k} > \frac{M_{pl,k}^2}{EI_z} K_{\theta} K_v$$

Despite the Eurocodes' many rules, designers have to master the theory and the statics in the background to make the right choices. The information about e.g. product properties i.e. diaphragm sandwich walls, connection forces, stiffness and fastening properties would help the design.

To convince oneself it would pay to get familiar with other available material e.g. American Institute of Steel Construction's (AISC) Guidelines Load and Resistance Factor Design Manual 2002, Hedman-Pétursson, E.: Column

buckling with restraint from sandwich wall elements and European Recommendations on the Stabilization of Steel Structures by Sandwich Panels 2013.

MEMBER BRACING ACCORDING TO AISC [1]

The LRFD/AISC design recommendations for relative and nodal column bracing are based on an initial out-of-straightness $\Delta=0.002L$, where L is the column length and a brace stiffness equal to twice the ideal stiffness. AISC/LRFD brace requirements for relative column bracing are

$$\beta_{br} = \frac{2P_u}{\phi L_b}$$

$$P_{br} = 0.004P_u$$

where $\Phi = 0.75$, P_u is the required compressive strength of the column, and L_b is the required brace spacing.

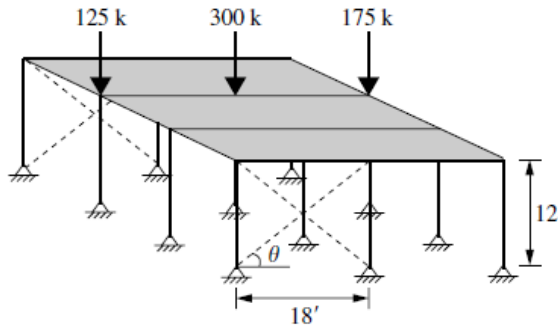


Figure 4. Relative column bracing [1].

AISC/LRFD brace requirements for nodal column bracing are:

$$\beta_{br} = \frac{8P_u}{\phi L_b}$$

$$P_{br} = 0.01P_u$$

where $\Phi = 0.75$, P_u is the required compressive strength of the column, and L_b is the required brace spacing. The formulas are on safe side and can be specified after case by case.

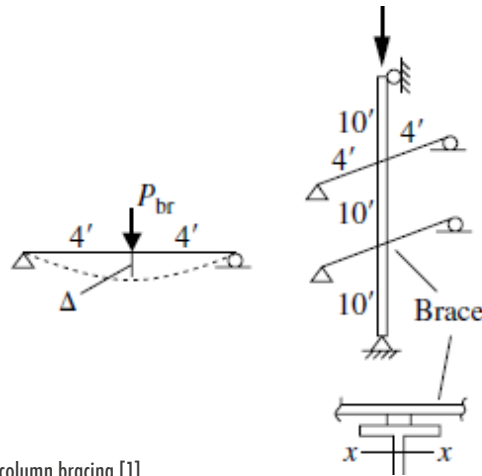


Figure 5. Nodal column bracing [1].

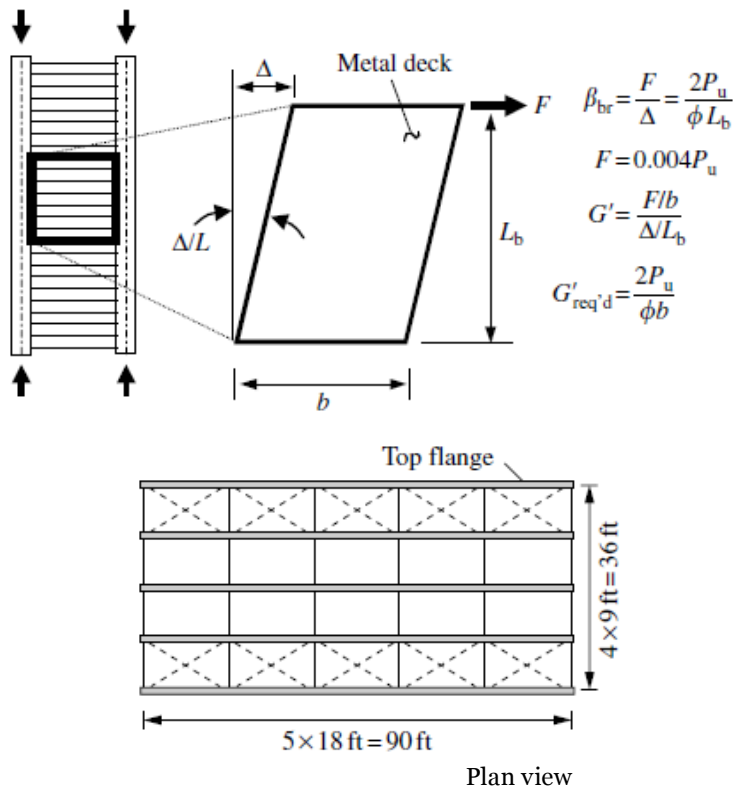


Figure 6. Bracing examples [1].

AISC/LRFD presents as well e.g. continuous metal-deck bracing and lean-on systems and the principles of beam bracing. The LRFD/AISC design recommendations offer formulas for the required bracing forces and the required bracing stiffness of beams and columns. The formulas include an

assumed initial out-of-straightness equal to $L/500$. As expected, the strength criteria are near the simple bracing design rules such as designing a brace to resist 2% of the member compressive force. The stiffness of the brace along with the out of-straightness of the member has a direct effect on the magnitude of the brace force. If the connections are flexible, the stiffness of the overall bracing system can be significantly less than the stiffness of the bracing member alone.

STABILIZATION OF STEEL STRUCTURES BY SANDWICH PANELS [4]

Sandwich panels are commonly used for enclosures of buildings. They are fixed to a substructure and they transfer transverse loads, for example snow and wind, to the substructure. When loaded by in-plane shear forces, sandwich panels have high shear stiffness. Unlike for related building products such as trapezoidal sheeting or cassette profiles, the shear stiffness of sandwich panels is usually not taken into account for the design of the building. The high shear stiffness can be used for different stabilizing effects.

Sandwich panels can restrain the lateral displacement of single components (e.g. beams, columns). Therefore flexural and lateral torsional buckling is prevented. By acting as diaphragm sandwich panels can also be used for global stabilisation of complete building structures and for transferring horizontal loads, e.g. wind loads. To act as a diaphragm sandwich panels have to be connected to the substructure by direct fixings.

The European standard EN 14509 covers the manufacture and design of industrially made self-supporting structural sandwich panels. The use of sandwich panels as stabilizing elements extends the application area outside the scope of EN 14509. Therefore, the extended application area shall be regulated nationally. Sandwich panels used as stabilizing elements have to fulfil the requirements shown by the CE mark of the product.

The European Recommendations on the Stabilization of Steel Structures by Sandwich Panels 2013 gives information about the use of self-supporting sandwich panels as stabilizing elements for single steel members such as beams or columns.

Torsional restraint [4]

The torsional restraint is governed by the stiffness of the connection of the sandwich panel to the supporting structure. Recent research carried out showed that this stiffness significantly depends on the load transferred by the sandwich panel. A design concept for the quantification and calculation of the stabilizing effects on beams under predominantly static loading by sandwich panels was developed within the framework of the EASIE project. Formulae for calculating the parameters of this moment-rotation-relation are given for sandwich panels with three different core materials and connections through the upper or lower crimp.

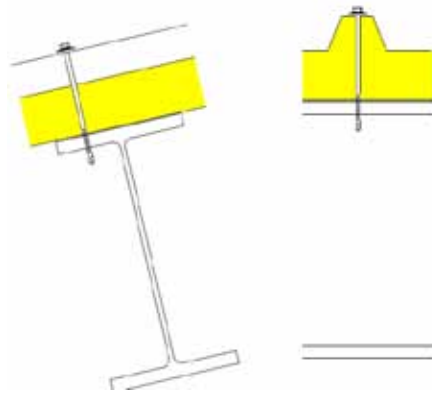


Figure 7. Purlin, sandwich panel and details of fastening [4].

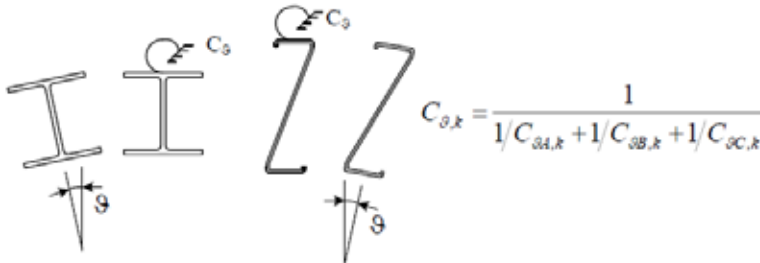


Figure 8. Stabilization: torsional restraint [4].

Limitation of stabilization moment

The torsional restraint given by sandwich panels can be calculated using the mechanical model based on a torsion spring with the spring stiffness $C_{\theta,k}$. This spring stiffness is a combination of the bending stiffness of the attached panel $C_{\theta C,k}$, the stiffness of the connection $C_{\theta A,k}$ and the distortional stiffness $C_{\theta B,k}$ of the beam to be stabilized.

Within the simplified design model introduced [4] using a secant value $C_{\theta A}$, the stabilization moment $m_{\theta A}$ shall be limited to the contact moment m_K . The stabilization moment should be calculated using [4].

$$m_{\theta A} = \frac{1}{C_{\theta A} \cdot \frac{k_c^4 \cdot E \cdot I_z}{M_{Ed}^2} - 1} \cdot C_{\theta A} \cdot \vartheta_0 \leq m_K = q_d \cdot \frac{b}{2}$$

Limitation of the rotation of the stabilized beam

According to the investigations, the rotation has to be limited to $\vartheta \leq 0.08$. The rotation of the stabilized beam can approximately be calculated using [4]:

$$\vartheta = \frac{m_{K,k}}{C_{st}} \leq 0.08$$

Lateral restraint – in-plane shear resistance [4]

Sandwich panels have a high stiffness and strength when loaded in the plane of the panel. This can be used to stabilize the supporting structure of the panels (beams, purlins, columns). The deformation of sandwich panels themselves caused by in-plane shear load may normally be neglected. The flexibility of the fixings usually dominates the shear flexibility. The fixings must be designed for the in-plane shear load. In typical cases, it is not necessary to design the sandwich panels for this additional load, but it is sufficient to design the panels for their primary loading consisting of the distributed snow and wind load and against the forces resulting from the difference of the temperature between the faces. However, this rule resulted from current experiments, which shall not be generalized. The resistance of the individual sandwich panels to in-plane shear load shall be studied in each case. The shear resistance of the individual panels is influenced by imperfections such as incomplete bonding, in addition to material properties and thicknesses.

Sandwich panels are normally connected to the supporting structure at the transverse edges only. They usually do not have connections at the longitudinal edges. This is common practice, especially for wall panels. Each panel acts as an individual element.

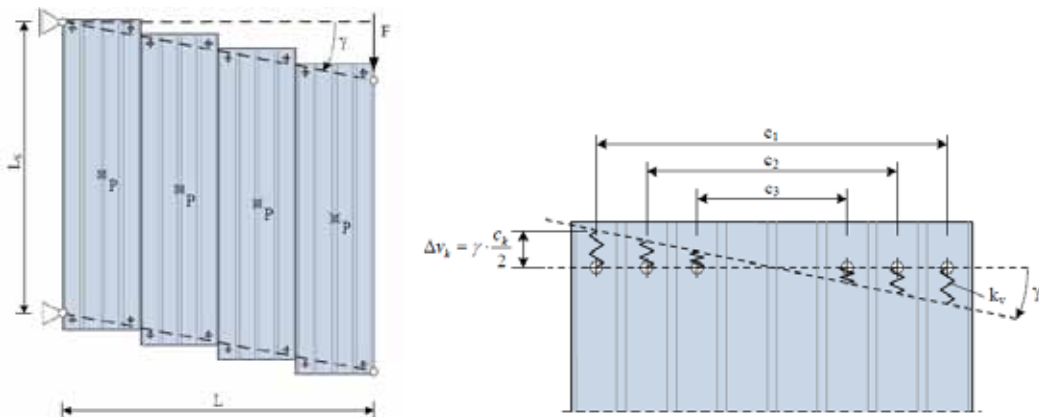


Figure 9. Displacement of shear loaded uni-directionally spanning sandwich panels and fastenings.

For stabilization of each beam the shear stiffness available is

$$S_i = \frac{k_v}{2 \cdot B} \cdot \sum_{k=1}^{n_k} c_k^2 \quad \text{check} \quad S \geq \left(EI_w \frac{\pi^2}{L^2} + GI_T + EI_z \frac{\pi^2}{L^2} 0,25h^2 \right) \frac{70}{h^2}$$

B is the width of a sandwich panel.

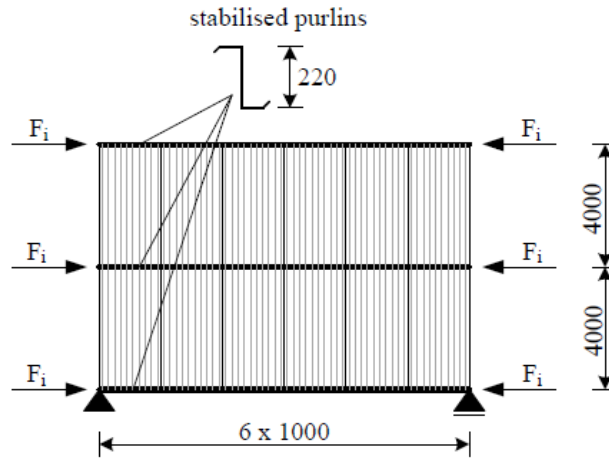


Fig. A.6: System

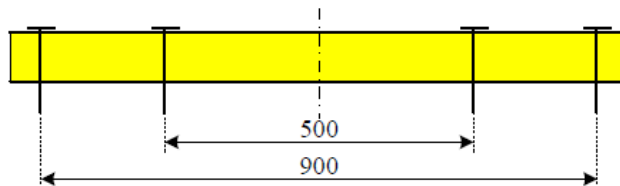


Figure 10. Position of fastenings at the supports of the sandwich panels [4].

For the stabilization of a beam-column with axial force and bending moment

$$F_i = \frac{N_d}{2} + \frac{M_d}{h}$$

/4/

For panels at the ends of the beam-column the moment M_S is approximately [4]:

$$M_{S,\max} = m_{i,\max} \cdot B = F_i \cdot \left(\frac{\pi}{L} \right) \cdot e_0 \cdot \frac{1}{1 - \frac{F_i}{S_i}} \cdot B$$

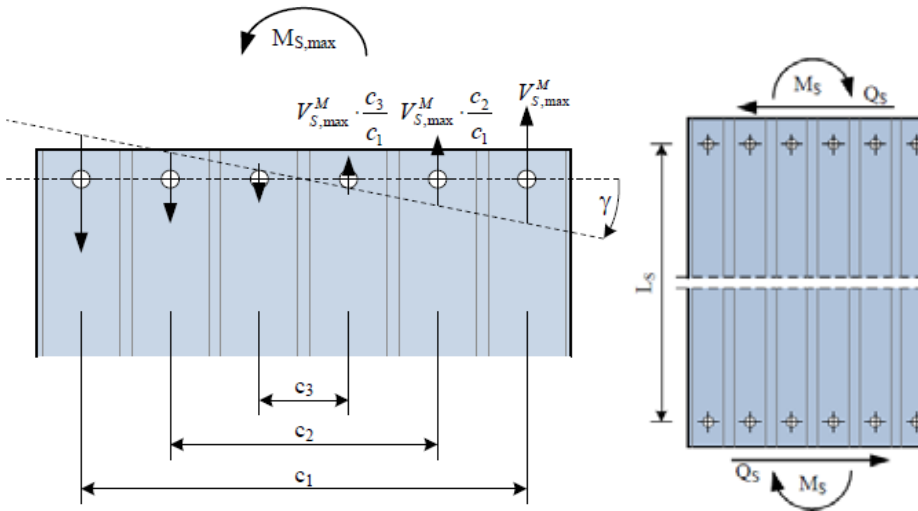


Figure 11. Forces resulting in the moment M_S [4].

The moment M_S results in the shear forces $V_{S,M}$ in the fastenings. These forces act in longitudinal direction of the panel. The highest forces arise in the panel. The force in the highest stressed fastenings is [4]:

$$V_{S,\max}^M = \frac{M_{S,\max}}{\sum \frac{c_k^2}{c_1}} \quad V_{S,\max}^Q = \frac{m \cdot M_{S,\max}}{L_S \cdot n_f}$$

$$V_{S,\max} = \sqrt{(V_{S,\max}^M)^2 + (V_{S,\max}^Q)^2}$$

In addition to the design of the fastenings, the displacements resulting from the stabilization should be limited.

$$\gamma_{\max} = e_0 \cdot \frac{\pi}{L} \cdot \frac{1}{\frac{S_i}{F_i} - 1} \leq \frac{1}{750}$$

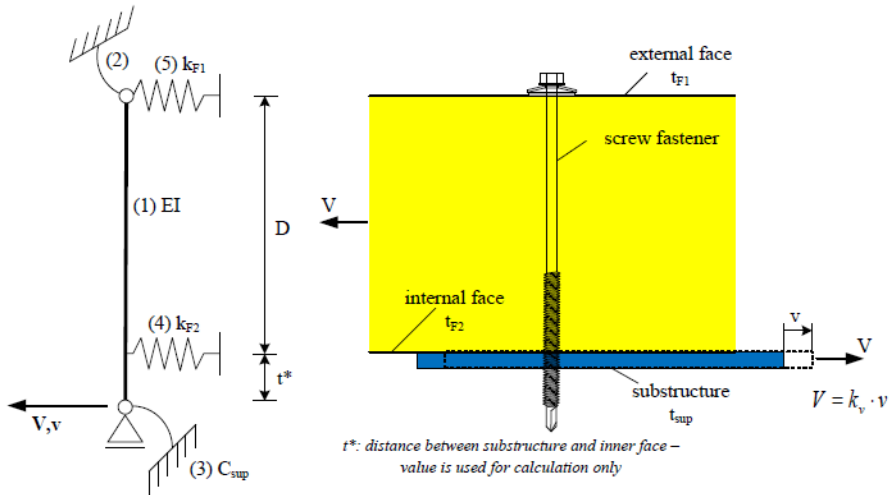


Figure 12. Individual components of a fastening /4/

Stiffness of fastenings

The translational stiffness of a connection with a self-drilling or self-tapping screw fastener can be calculated with [4]:

$$k_v = \frac{1}{\frac{x_F}{k_{F2}} + \frac{t_{cor,sup}^2 + 2 \cdot (1 - x_F) \cdot D \cdot t_{cor,sup}}{4 \cdot C_{sup}} + \frac{3 \cdot (1 - x_F) \cdot D \cdot t_{cor,sup}^2 + t_{cor,sup}^3}{24 \cdot EI}}$$

The fastenings at the longitudinal joints have a wide influence on the stiffness and also on the load bearing capacity of the diaphragm.

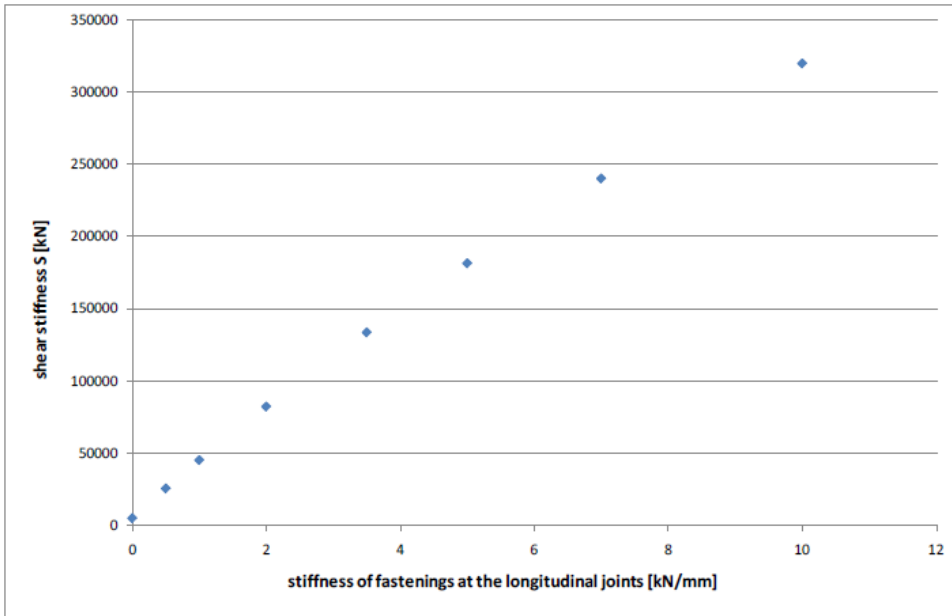


Figure 13. In the diagram, the shear stiffness S resulting from a stiffness of the fastenings between 0 and 10 kN/mm is shown [10].

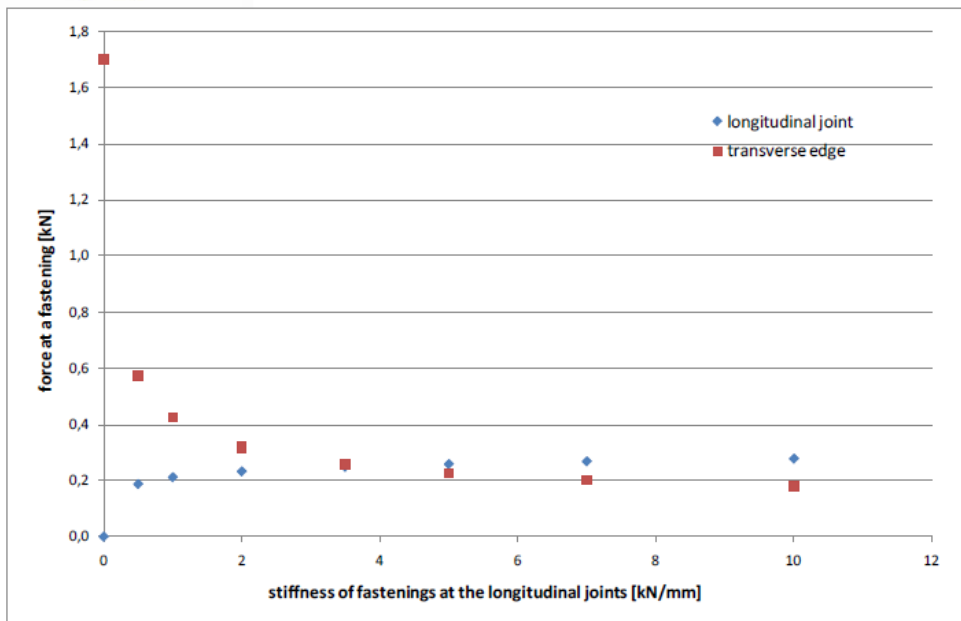


Figure 14. Concerning the forces of the fastenings there is a wide difference between diaphragms with and diaphragms without connections at the longitudinal joints. [10].

Stabilisation of frameless sandwich structures

A new application is to use sandwich panels with flat or lightly profiled faces for frameless buildings. In smaller buildings – such as cooling chambers, climatic chambers and clean rooms – the panels are applied without any load transferring substructure. Because the in-plane shear stiffness of the panels is very much higher than the stiffness of the fastenings, only the fastenings are decisive for load-bearing behaviour and capacity. So the fastenings have to be designed for the forces resulting from transfer of horizontal loads [10].

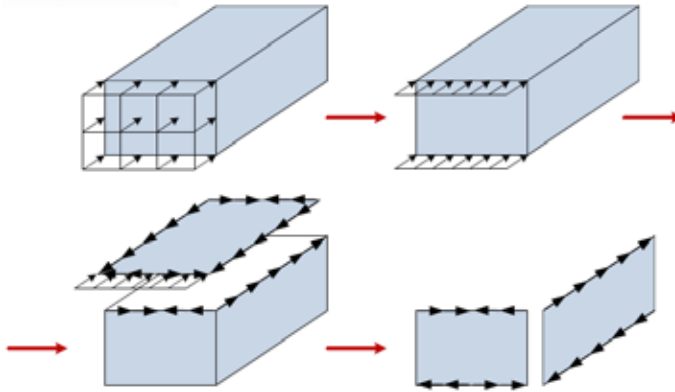


Figure 15. Transfer of horizontal loads in frameless buildings.

Design procedures for sandwich panels subjected to bending moments and transverse forces are given in EN 14509, but there are no general design methods for panels subjected to axial loads or a combination of axial and transverse loads available. A design method for axially loaded sandwich panels has been developed [10].

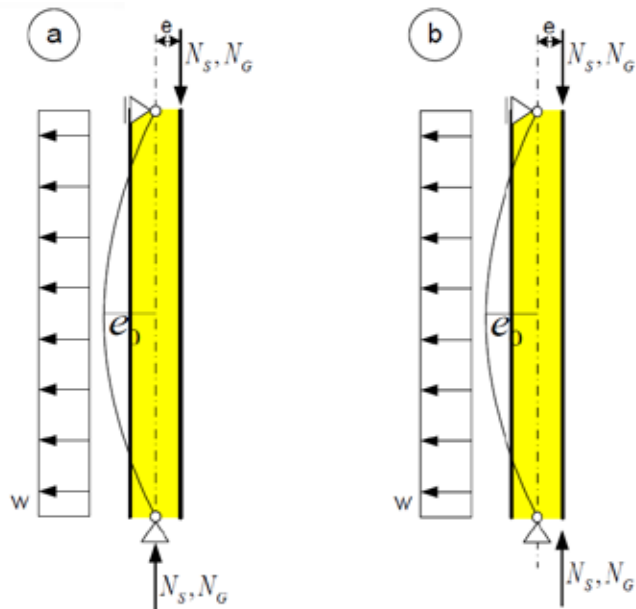


Figure 16. Wall panels with typical loads [10].

Panels loaded by axial load N and bending moment M , can be designed with the formulae [10]:

$$\frac{N_{Ed}}{\chi \cdot N_{Rd}} + k_{yy} \frac{M_{Ed}}{M_{Rd}} \leq 1$$

$$M_{Rd} = \frac{M_w}{\gamma_M} = \frac{D \cdot A_F \cdot \sigma_w}{\gamma_M}$$

$$k_{yy} = C_{my} \cdot \left(1 + 0,8 \cdot \frac{N}{\chi \cdot N_w}\right)$$

COLUMN BUCKLING WITH RESTRAINTS FROM SANDWICH WALL ELEMENT

Eva Hedman-Petursson from Luleå University of Technology has researched in the years 1998–2001 the restraining effect of a sandwich element wall on steel beam-columns. The wall elements give restraint to beam-columns against buckling in the wall plane and that the resistance of the member thereby can be increased. A series of full-scale tests, theoretical modelling and FE-calculations have been performed at the Division of Steel Structures, Luleå University of Technology.

Her doctoral thesis showed that there is a substantial increase in resistance to gain that is worth taking into consideration with the element wall assembled in a conventional way, that is, without connection between the elements. If the wall structure is recognized as a restraint, a brace, and designed accordingly a situation with full support for beam-columns can be offered. The constructive step towards this is to strengthen the horizontal element joints. Consequently, two different cases have been studied; how to benefit from a partial restraint in the design of beam-columns with the wall elements assembled in the conventional way; and how to design the element wall to offer a full lateral support for a beam-column. Design recommendations were given for those two cases [11].

Table 1. Results from full scale testing and FE-simulation.

Test nr.; cross section	Moment lever arm	Axial force			Failure mode
		lab. test	FE-simulation	EC3	
Test 1; IIEA 120	0	413.0 kN	405.3 kN	484.1 kN ¹⁾	flexural buckling
		411.5 kN	398.6 kN		
Test 2; IIEA 120	0.05 m	223.6 kN	212.5 kN	217.0 kN ¹⁾	flexural buckling
		220.1 kN	211.8 kN		
Test 3; IPE 200	0	407.1 kN ²⁾	413.4 kN	415.6 kN ¹⁾	lateral torsional buckling
		414.7 kN ²⁾	408.2 kN		
Test 4; IPE 200	0.25 m	204.4 kN	184.0 kN	191.6 kN ¹⁾	flexural buckling
		199.2 kN	182.7 kN		
Test 5; IPE 200	0	268.3 kN	254.2 kN	125.5 kN ³⁾	partially restrained buckling
		272.5 kN	261.7 kN	412.3 kN ⁴⁾	in weak direction

¹⁾ Full support for the compression flange in calculation of resistance according to EC3, equation 1

²⁾ Testrig failure just before beam-column collapse

³⁾ Unrestrained column capacity, buckling in weak direction

⁴⁾ Fully restrained column, lateral torsional buckling

SUMMARY

In this study bracing systems used to control the instability are presented. The basic theory of a dual strength and stiffness criterion for the design of bracing used to control the instability is studied. Eurocode is reviewed from the bracing point of view. Despite the Eurocodes' many rules, designers have to master the theory and the statics in the background to make the right choices. The information about e.g. product properties of diaphragm sandwich walls, connection forces, stiffness and the fastening properties have to be solved independently.

American Institute of Steel Construction (AISC) Guidelines on Load and Resistance Factor Design Manual 2002, the work of Hedman-Pétursson, E., Column buckling with restraint from sandwich wall elements and European Recommendations on the Stabilization of Steel Structures by Sandwich Panels 2013 were examined to confirm the present bracing practices.

The European standard EN 14509 covers the manufacture and design of industrially made self-supporting structural sandwich panels. The use of sandwich panels as stabilizing elements extends the application area outside the scope of EN 14509. Therefore, the extended application area shall be regulated nationally. The sandwich panels used as stabilizing elements have to fulfil the requirements shown by the CE mark of the product. The European Recommendations on the Stabilization of Steel Structures by Sandwich Panels

2013 gives information about the use of self-supporting sandwich panels as stabilizing elements for single steel members such as beams or columns. A new application is to use sandwich panels with profiled faces for frameless buildings. A design method for axially loaded sandwich panels has been presented.

REFERENCES

- 1 Structural Bracing. Brian Chen Joseph Jura.
- 2 Load and Resistance Factor Design Manual. American Institute of Steel Construction (AISC)
- 3 Column buckling with restraint from sandwich wall elements. Hedman-Pétursson, E.
- 4 European Recommendations on the Stabilization of Steel Structures by Sandwich Panels 2013 CIB
- 5 EN 1990: 2002 + A1:2005 + A1:2005/AC:2010: Eurocode: Basis of structural design.
- 6 EN 1993-1-1:2005 + AC:2009; Eurocode 3: Design of steel structures – Part 1–1:General rules and rules for buildings.
- 7 EN 1993-1-3:2006 + AC:2009; Eurocode 3: Design of steel structures – Part 1–3: General rules – Supplementary rules for cold-formed members and sheeting.
- 8 EN 14509:2006: Self-supporting double skin metal faced insulating panels – Factory made products – Specifications.
- 9 FprEN 14509:2013: Self-supporting double skin metal faced insulating panels – Factory made products – Specifications.
- 10 EASIE Ensuring Advancement in Sandwich Constructions Through Innovation and Exploitation <http://www.easie.eu/>
- 11 Column buckling with restraint from sandwich wall elements Hedman-Pétursson, Eva Doctoral Thesis / 2001-08-30.

INNOVATION IN MECHANICAL FASTENING TECHNOLOGY FOR MAINTENANCE-FREE JOINTS

Hans-Albert Staedler

Alcoa Fastening Systems Industrial Products, Telford, UK

ABSTRACT

The paper describes innovative mechanical bolts which are maintenance free.

INTRODUCTION

Alcoa Fastening Systems have experience of many years in mechanical fastening technologies. Louis Huck (the founder of Huck fasteners) developed in the middle of 1940s the very first lock bolt system. The functionality of lock bolt systems is based on cold forming / extrusion technology. A so-called collar gets cold formed during installation by an anvil (part of a special installation tool) into unique locking grooves of a pin. After the installation the fastener is mechanically locked due to this volume-controlled swaging process. The locking grooves are very often filled with a collar material. This system results in a natural barrier against vibration and loss of tightening. Lock bolt systems create vibration resistant and high fatigue-life joints. Since the very first lock bolts, these systems have been continuously optimized. A major step was, when Alcoa Fastening Systems came to the market with pintail-less lock bolts. These systems not longer have a pintail end with blank and rust effected surface. The installation is faster, smoother and with reduced noise compared with traditional lock bolts and much faster than conventional bolts. Germany's highest construction authority DIBt tested the Bobtail® in accordance with the EN 1993 regulation and approved it as appropriate for generating totally maintenance-free joints when correctly installed and with correlated parts. The Bobtail® delivers also the performance of ISO 12944 C5 M corrosion protection.

Table 1 shows the evolution of lock bolt systems compared with high strength conventional bolts. The table includes the latest innovation product, the Huck 360 (H360®). The H360® bolt thread is similar to a lock bolt system, has mild contours and has no stress concentration areas. In comparison with the lock bolt system, the Huck 360 no longer needs a special installation tool. It is a removable and reusable nut and bolt system (Figure 1) with vibration resistance, high fatigue strength similar and installation flexibility to the equivalent lock bolt. Due to the tightening installation method the tightening range is larger than for the lock bolt system, but smaller than conventional bolt systems. The ductile nut thread and its deformation during the tightening process generate a mechanical lock with a hardened thread of the pin. This makes the Huck360 the highest strength bolting system for connections requiring field service with standard tools.

Table 1. Lock bolt evolution [Source Alcoa Fastening Systems Test Lab. Waco].

	High Strength Bolt & Nut	Traditional Lock Bolt	Advanced Lock Bolt	Huck 360® System
				
Features				
Clamp Load	High	High	High	High
Clamp Variation	±30%	±6%	±6%	±20%
Removability	Yes	Semi-permanent	Semi-permanent	Yes
16mm Tool Weight	< 10 lbs.	20 lbs.	< 10 lbs.	< 10 lbs
Vibration Resistance	Low	High	High	High



Figure 1. Parts of H360® system; //Source: Alcoa fastening Systems test lab Waco//

The free running nut thread quickly spins down and tightens while minimizing damage to coatings. The preloaded H360® thread and conventional bolt/nut thread detail (Figure 2) shows the difference and reason for this high resistance against vibration. The nut thread is designed in a style, which deforms enough material during the tightening process for an efficient locking mechanism. The nut thread is in ductile hardness and allows for removability and reusability. This means, that the system is suitable to solve work piece surface imperfections and/or screw installation strategies for instance in large flange wind turbine towers.

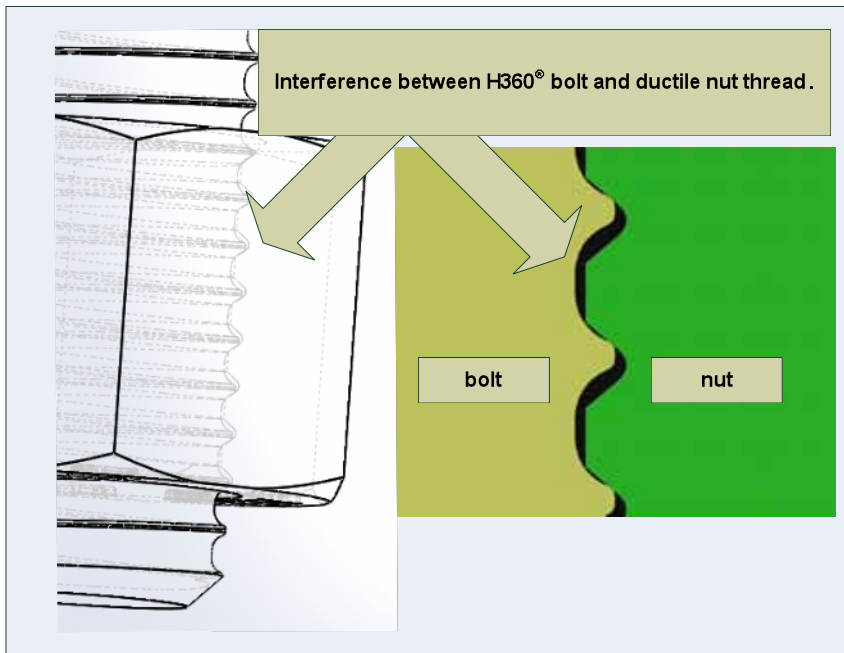


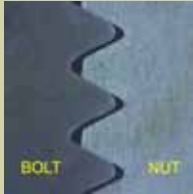
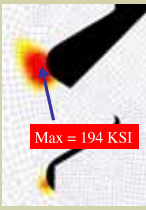
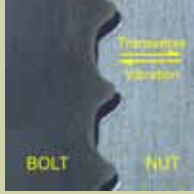
Figure 2. Functionality of H360® system; //Source: Alcoa fastening Systems test lab Waco//

The Alcoa internal test results are shown in Figure 3. The conclusions drawn from the tests are given in Table 2.

Table 2. Summary of Huck 360® features and benefits [Source Alcoa Fastening Systems Test Lab. Waco].

Features	Benefits
Vibration Proof	<ul style="list-style-type: none"> • Reduction in frequency of maintenance • Longer equipment uptime
Free running thread	<ul style="list-style-type: none"> • Fast fit-up • No coating damage • Easy removal • Field serviceable
Shallow low notch factor bolt thread	<ul style="list-style-type: none"> • High fatigue strength • Absorbs high spike loads
Grade8 and Class10.9 tensile and shear strength	<ul style="list-style-type: none"> • Easy upgrade from conventional nuts and bolts
Installed and removed conventional wrenches	<ul style="list-style-type: none"> • Field serviceability

1. Preload thread detail

<div style="border: 1px solid black; padding: 5px; text-align: center; margin-bottom: 10px;">Conventional bolt and nut</div> <div style="display: flex; justify-content: space-between;">  <div style="border: 1px solid black; padding: 5px; width: 60%;"> <p>Thread Flanks can slide. Nut can move relative to bolt.</p> </div> </div> <div style="display: flex; justify-content: space-between; margin-top: 10px;">  <div style="border: 1px solid black; padding: 5px; width: 60%;"> <p>UNC thread</p> <p>194 KSI max stress in thread root radius</p> </div> </div>	<div style="border: 1px solid black; padding: 5px; text-align: center; margin-bottom: 10px;">H360[®] thread</div> <div style="display: flex; justify-content: space-between;">  <div style="border: 1px solid black; padding: 5px; width: 60%;"> <p>Thread Flanks are Locked. Nut cannot move relative to bolt</p> </div> </div> <div style="display: flex; justify-content: space-between; margin-top: 10px;">  <div style="border: 1px solid black; padding: 5px; width: 60%;"> <p>H360[®] thread</p> <p>141 KSI max stress in thread root radius</p> <p style="color: red; font-weight: bold;">27% less stress in thread</p> </div> </div>
---	---

2. Vibration resistance

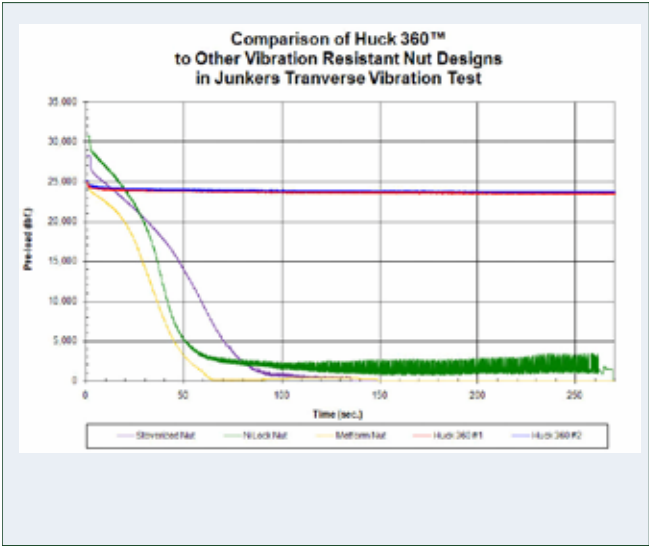


Figure 3. Performance of H360[®] system; //Source: Alcoa fastening Systems Test Lab Waco//

3. Tension- tension Fatigue

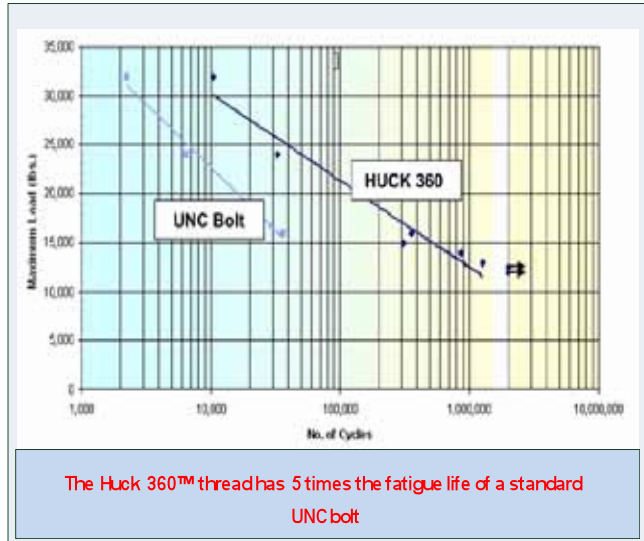


Figure 4 shows all the metric and imperial size diameters which are actually available. In accordance with construction industry needs the diameters are M24, M27, M30 and M42.

An example for usage of H360® system is in the mining industry. Morbark Inc. were having poor insert (tooth) life on a Model 1300 Tub Grinder. Using $\frac{3}{4}$ " stoverized nuts and Grade 8 Bolts. They were losing “upwards of 6 to 8 teeth a day” according to the operator. Using the Huck 360® they were able to save approximately 120 hours over a period of five weeks. During that period of time only 8–10 inserts were lost.



Figure 4. Available H360® system bolts //Source: Alcoa fastening Systems//



Figure 5. Morbark Inc. Grinder with H360®; //Source: Alcoa fastening Systems //

- Other opportunities for using H360 are in
- Steel construction (Figure 6)
- Truck and trailer
- Agriculture, harvest machinery
- Rail and railcar
- Car industry
- Mining
- Construction machines and excavators
- After and repair market where normal screws failed

<p>Structural steel Engineering (Civil Engineering)</p> <p> Storyed Buildings</p> <p> Hall constructions</p> <p>Steel bridge construction</p> <p> Static bridges,</p> <p> Movable bridges</p> <p> Mobile bridges</p> <p>Masts and towers, Solar construction</p> <p> Energy</p> <p> Communication</p> <p>Building and industrial segments</p> <p> Framework</p> <p> Cranes</p> <p> Cooling towers</p> <p> Chimneys</p> <p>Hydro mechanical strutures</p> <p> Channel and harbor construction</p> <p>Special constructions</p> <p> Radio telescope</p> <p> elevators, circus and exhibition constructions</p>	
--	--

Figure 6. H360® in Steel construction.

For all applications in construction market an approval is necessary. In Germany, the approach is through DIBt approval. DIBt is the German authority for the fulfilment of technical tasks in the field of public law. This authority sets National Technical approvals. The DIBt is member of EOTA (European Organization for Technical Approvals).

The actual status is of this approach is:

1. The approach has been generated and the DIBt decided the accredited test laboratory and the assessor.
2. The test program has been developed and approved. The test program includes the tests in accordance with categories A, B, C, D and E in accordance with DIN EN 1993-1-8. The clear advantage is supposed for high strength and friction controlled connections (category B, C and E after DIN EN 1993-1-8).
3. Preliminary and first tests with M27 diameter have been done and results look good.

Preliminary test for bolt diameter M 27

The aim of these preliminary tests was to get a first impression from an independent third party about the service which can be provided with H360® bolt system. These preliminary results are the basis for the official test program, which will start at the end of 2013. All test specifications have been developed by Fraunhofer AGP Rostock and in accordance with DIBt requirements. Specimen for tests material was S355. The Preload (clamp force) sensor is from company Kistler.

1. Characteristic preload and preload loss $F_{p,C}$ measured with Piezo system (Figure 7)
2. Slip resistance at serviceability and ultimate $F_{v,Rk}$.
3. Cyclic load tests for identifying of self-loosening effects in friction controlled joints.
4. Preload after multiple retightening processes.

Table 3. Categories of bolted connections [Source: EN1993-1-8].

Category	Criteria	Remarks
Shear connections		
A bearing type	$F_{v,Ed} \leq F_{v,Rd}$ $F_{v,Ed} \leq F_{b,Rd}$	No preloading required. Bolt classes from 4.6 to 10.9 may be used.
B slip-resistant at serviceability	$F_{v,Ed,ser} \leq F_{v,Rd,ser}$ $F_{v,Ed} \leq F_{v,Rd}$ $F_{v,Ed} \leq F_{b,Rd}$	Preloaded 8.8 or 10.9 bolts should be used. For slip resistance at serviceability see 3.9.
C slip-resistant at ultimate	$F_{v,Ed} \leq F_{v,Rd}$ $F_{v,Ed} \leq F_{b,Rd}$ $F_{v,Ed} \leq N_{net,Rd}$	Preloaded 8.8 or 10.9 bolts should be used. For slip resistance at ultimate see 3.9. $N_{net,Rd}$ see EN 1993-1-1
Tension connections		
D non-preloaded	$F_{t,Ed} \leq F_{t,Rd}$ $F_{t,Ed} \leq B_{p,Rd}$	No preloading required. Bolt classes from 4.6 to 10.9 may be used. $B_{p,Rd}$ see Table 3.4.
E preloaded	$F_{t,Ed} \leq F_{t,Rd}$ $F_{t,Ed} \leq B_{p,Rd}$	Preloaded 8.8 or 10.9 bolts should be used. $B_{p,Rd}$ see Table 3.4.
The design tensile force $F_{t,Ed}$ should include any force due to prying action, see 3.11. Bolts subjected to both shear force and tensile force should also satisfy the criteria given in Table 3.4.		

Test results of characteristic preload and preload loss $F_{p,C}$

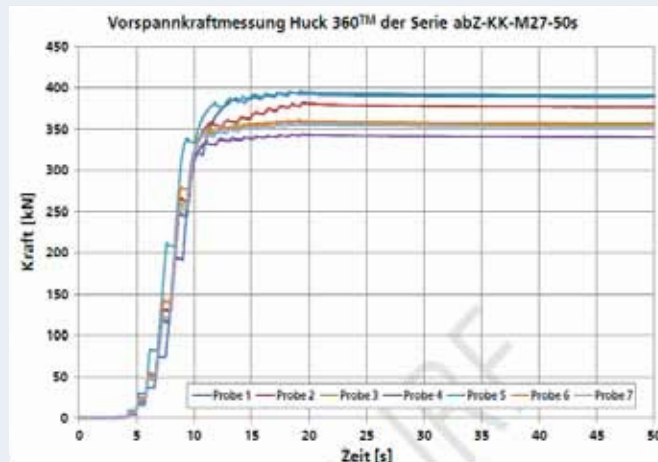
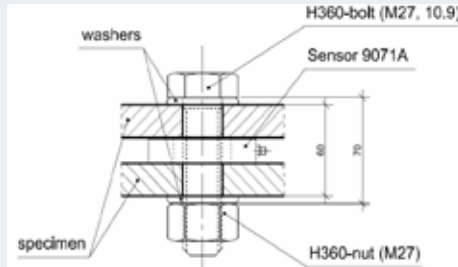
The range of installed preload is arises from the tightening installation method. The loss of preload is very close to a lock bolt system and shows the minimal setting effects in the installed system. The reason for this is the impact of bolt and nut thread style. The determination of preload loss $F_{p,C}$ has been identified for each one bolt after 24, 48 and 96 hours. Therefore, a sensor has been placed into the preloaded connection. After 24, 48, or 96 hours the nut has been removed with an automatic screwdriver. The disconnection of the joint is synchronous with the discharge of the sensor. This supplies a negative signal voltage, which is equivalent to the preload at the point of time before disconnecting. A continuous determination of preload is impossible with this test method. For the long time preload loss different tests methods are necessary.

Test results about slip resistance $F_{v,Rk}$

These tests have been done on double shear specimen S355J2+N material with a hole tolerance $\Delta d = 2,0$ mm. The holes in diameter 29mm have been drilled. Style and size of specimen deliver bolt failure as criterion. The bolts have been equipped with hardened washers. The test speed was 1mm/min until bolt failure. To get specimen surface friction coefficient $\mu \geq 0,5$, Zinc-Silicate in accordance with DIN 18800-7 has been used. The bolt failure occurred as expected. The A linear inductive displacement transducer picks up the relative and absolute expansion between outer and middle work piece.

Displacement has been measured up to 200 µm. The servo-hydraulic machine software delivered machine force and transfer displacement.

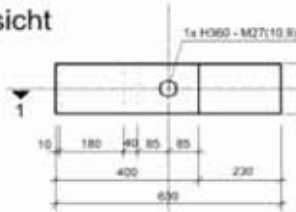
Test spec



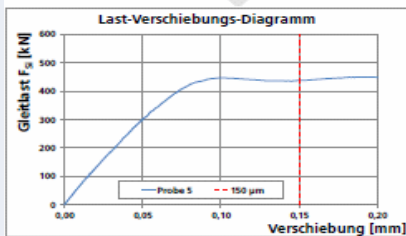
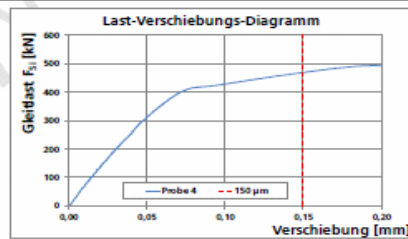
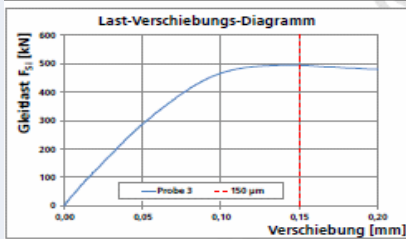
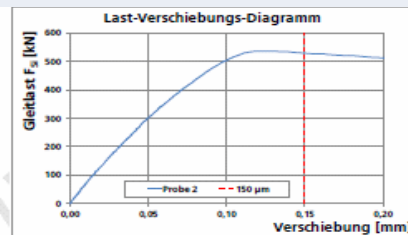
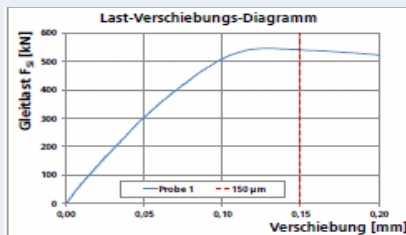
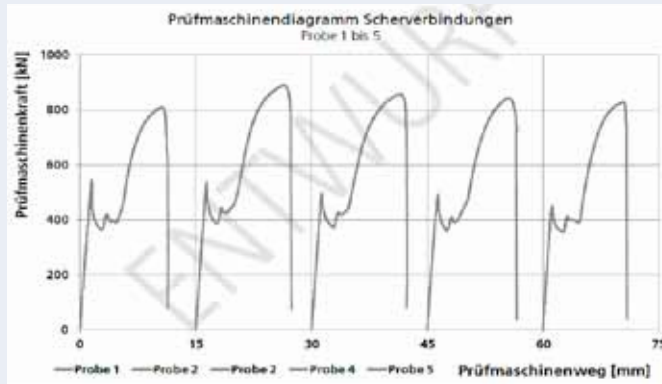
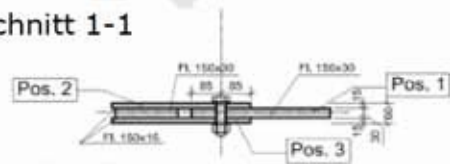
Versuch Nr.	Messzeit	Vorspannkraft nach Wegnahme Anziehwerkzeug $F_{p,c}$	Vorspannkraft nach Haltezeit $F_{p,c,time}$	Abfall der Vorspannkraft $\Delta F_{p,c}$	
abZ-KK-M27-50s-1	50 s	389 kN			
abZ-KK-M27-50s-2		377 kN			
abZ-KK-M27-50s-3		356 kN			
abZ-KK-M27-50s-4		340 kN			
abZ-KK-M27-50s-5		391 kN			
abZ-KK-M27-50s-6		357 kN			
abZ-KK-M27-50s-7		353 kN			
abZ-KK-M27-24h-1	24 h	389 kN	380 kN	9 kN	2,31%
abZ-KK-M27-48h-1	48 h	405 kN	390 kN	15 kN	3,70%
abZ-KK-M27-96h-1	96 h	361 kN	348 kN	13 kN	3,60%
Mittelwert		371,8 kN	Preliminary Clamp loss after 24 hrs 2,31 bis 3,70 %		
Standardabweichung		21,2 kN			
Variationskoeffizient		5,7 %			
k_n (DIN EN1090 [14], Tab. D.1)		1,92			
charakt. Vorspannkraft $F_{p,c}$ [kN]		331,1 kN			

Figure 7. Draft of test results "Preload and preload loss after 24 hours"; //Source: Fraunhofer AGP Test Laboratory Rostock, "Prüfbericht Nr. P-FhAGP – V1109-03", Rostock 2012 //

Draufsicht



Schnitt 1-1



Probe-Nr.	$F_{g,150 \mu m}$ [kN]	$F_{g,max}$ [kN]	$SF_{g,max}$ [μm]
1	542,30	547,50	127
2	530,66	537,49	121
3	494,74	495,54	143
4	468,70	468,70	150
5	438,22	447,59	101
m_x	494,92	499,36	128,40
s_x	43,083	43,03	19,28
V_x [%]	8,70	8,62	15,02

Machine load diagrams (left) and load displacement diagrams (right) (EN1090-2 annex G)

Materialkennwerte:		Verbindung:			Verbindungsmittel	
Bauteilwerkstoff: S355J2+N Oberfläche: Zink-Silicat-System ($\mu \geq 0,50$) Dicke Mittellasche: 30 mm Dicke Außenlaschen: 15 mm + 15 mm		Anzahl Bolzen: 1 Anzahl Scherfugen: 2			Nenn Durchmesser: 27,0 mm Bolzen: M360H-DT27X120DL Mutter: M360NH-R27DL Anziehdrehmoment: 1250 Nm	
Versuchs Nr.	Schichtdicke [μm]	für die Verbindung			für 1 VM und 1 SF	
		Gleitlast F_{Sl} [kN]	Bruchkraft [kN]	Versagens- art	$F_{s,Rk1}$ [kN]	$F_{v,Rk1}$ [kN]
abZ-S-1-H360-M27-1	84,1 - 250,0	547,50	809,6	Abscheren	271,2	404,8
abZ-S-1-H360-M27-2	86,2 - 172,5	537,49	889,9	Abscheren	265,3	445,0
abZ-S-1-H360-M27-3	32,5 - 190,5	495,54	857,6	Abscheren	247,4	428,8
abZ-S-1-H360-M27-4	52,5 - 241,5	468,70	843,9	Abscheren	234,4	422,0
abZ-S-1-H360-M27-5	78,1 - 222,0	447,59	829,7	Abscheren	219,1	414,8
Mittelwert					247,5	423,1 kN
Standardabweichung					21,5	15,1 kN
Variationskoeffizient					8,71 %	3,57%
k_s (DIN EN1090 [14], Tab. D.1)					2,33	2,33
charakteristische Tragfähigkeiten R_s [kN]					197,3 kN	387,8 kN

Figure 8. Draft test results for shear and slip resistance; //Source: Fraunhofer AGP Test Laboratory Rostock, "Prüfbericht Nr. P-FhAGP – V1109-03", Rostock 2012 /

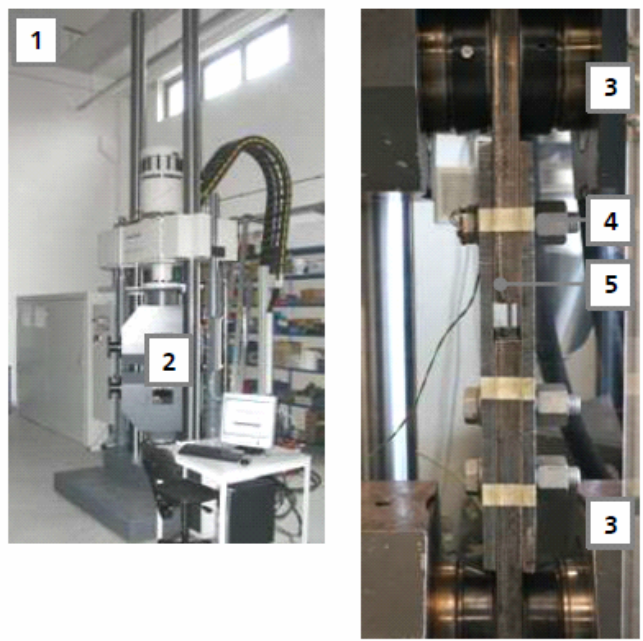
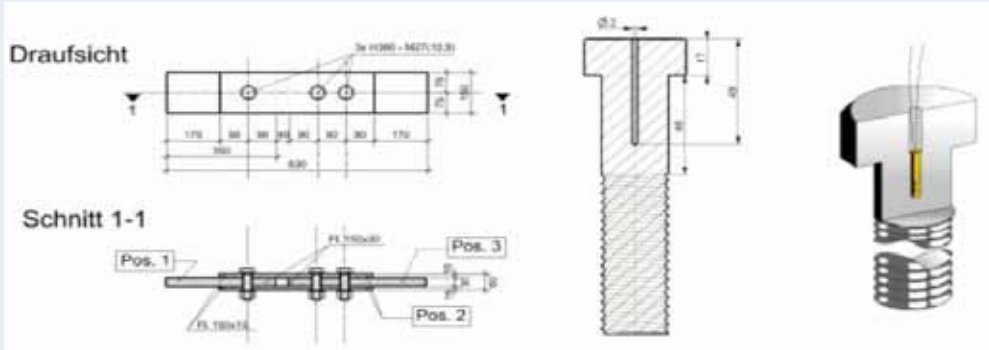
Cyclic load tests to determine self-loosening effects in friction controlled connections

Friction controlled joints are preferred in reverse and /or cyclic loaded connections. Keeping the preload is essential for long service life. Conventional bolt and nut connections tend to unscrew with time. This effect reduces the fatigue life of the joints. To determine these effects for H360 system the following preliminary test has been done.

Specimen used in double shear S355J2-N plates, dry, no rust and uncoated.
Hole diameter 29mm with tolerance $\Delta d = 2,0$ mm, drilled.
Hardened washers have been used.

Bolts have been equipped with strain gauges which have been calibrated in force range 50 up to 400 kN. Therefore, a force can be assigned for each signal voltage. For statistical reasons 3 specimens were pre-tested. The testing came out with individual sliding match 113 kN, 153 kN and 182 kN, the average was 149 kN. Further details are described in test report, revision 2 of Fraunhofer AGP Rostock.

Test specimen



- 1 Servo- hydraulic test machine
 - 2 Test house laboratory
 - 3 Tooling to fit specimen
 - 4 Strain gauged bolt
 - 5 workpiece package
- Test parameter
 $R = -1,0/5\text{Hz}$
 room temperature

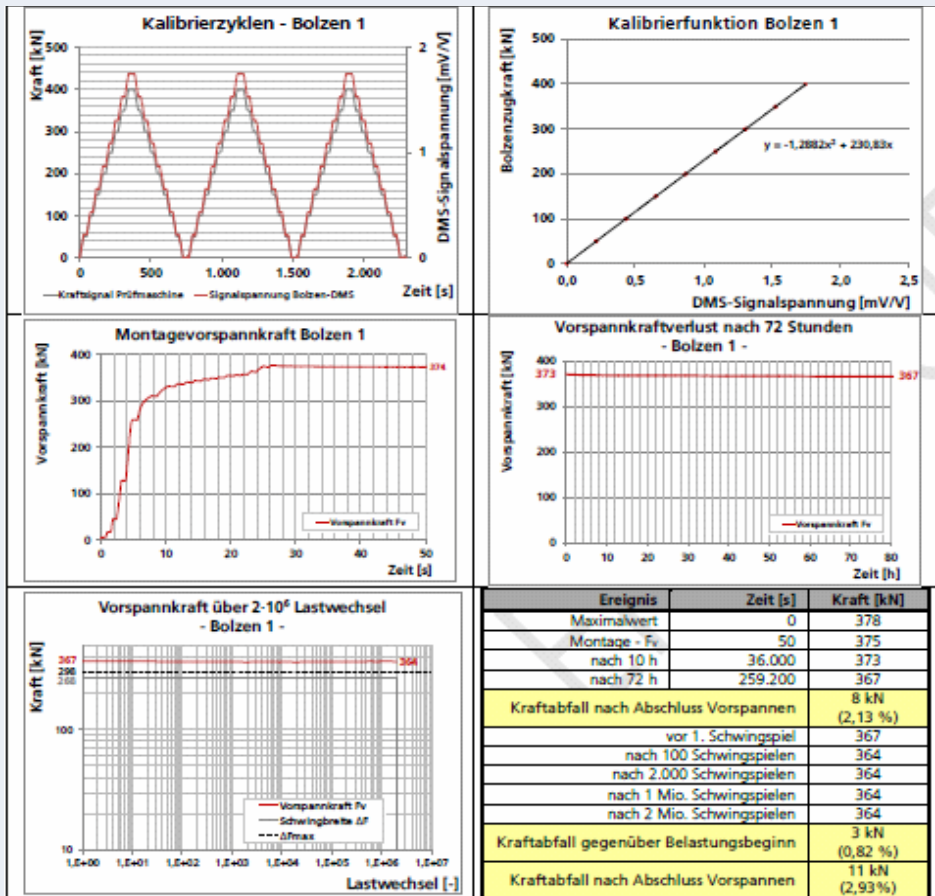
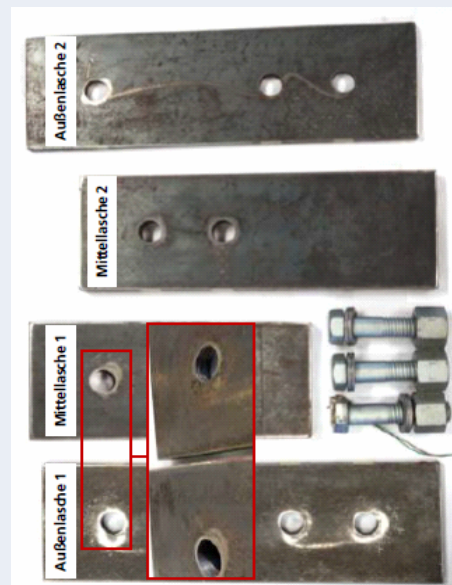


Figure 9. Draft of test results “self-loosening effects under cyclic load”; /Source: Fraunhofer AGP test laboratory Rostock, “Prüfbericht Nr. P-FhAGP – V1109-03”, Rostock 2012.



Ability of retightening of H360 system

This first step of the test about the performance of H360 system for remove and reuse does demonstrate the ability for instance to solve work piece imperfections in large flange application.

The results below in picture 10 show the accuracy of preload after 5 time complete retightening process. The process was by torque control and similar for both systems in terms of usage of installation tool and test conditions.

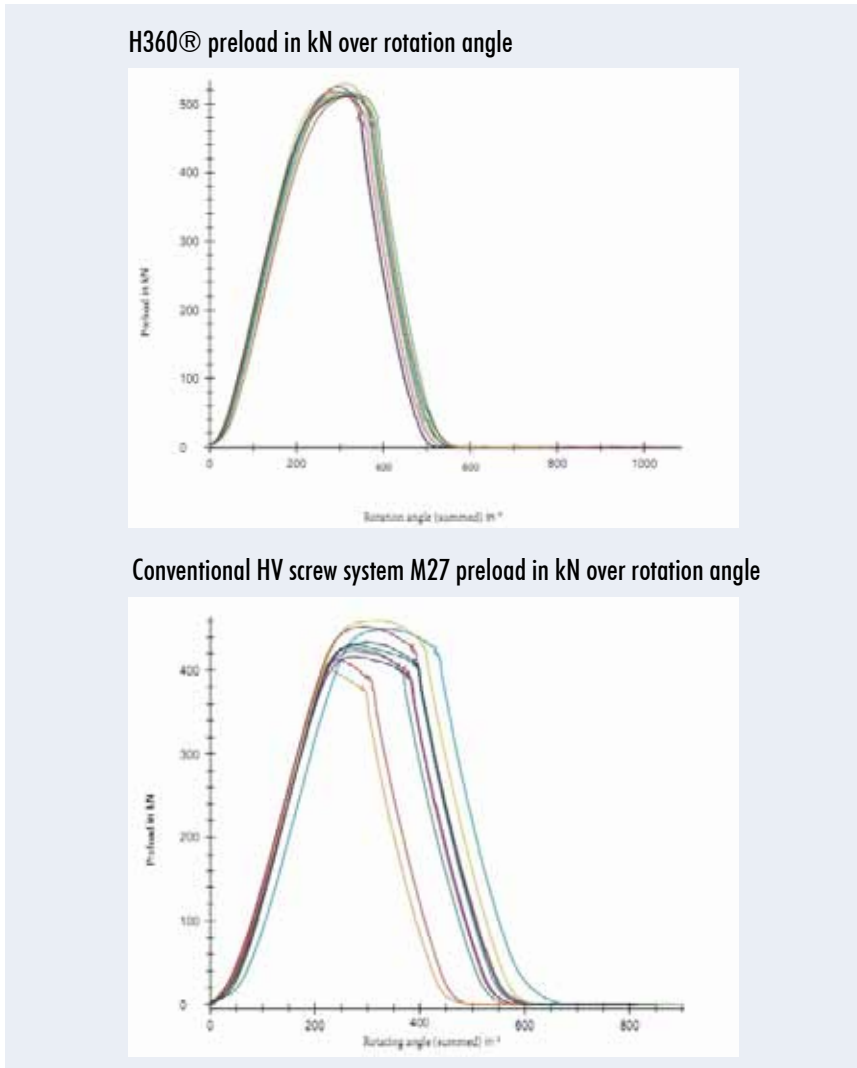


Figure 10. Draft of test results "retightening of H360®"; /Source: Fraunhofer AGP test laboratory Rostock, 2012.

CONCLUSIONS

Overall the H360® system is already in many applications in rail, mining and construction in the United States and other countries and now on the approach to get the DIBT approval. The aim is the ability to generate maintenance free joints.

FLANGELESS CONNECTIONS IN STEEL TUBULAR WIND TOWERS

Christine Heistermann¹

Anh Tuan Tran¹

Milan Veljkovic¹

Carlos Rebelo²

¹ Luleå University of Technology
Department of Civil, Environmental and Natural Resources Engineering
Division of Structural and Construction Engineering
Research Group of Steel Structures
Sweden

² University of Coimbra
Department of Civil Engineering
Institute for Sustainability and Innovation in Structural Engineering
Steel and Mixed Construction Technologies
Portugal

ABSTRACT

Extensive research is currently being conducted on the improvement on the use of renewable energy. One field is the use of wind energy, where the tower construction is one of the main issues. This paper deals with new ideas and ongoing research in this area. To raise the height of steel tubular towers, fatigue as the design limit and constraints due to transportation issues have to be overcome. Changes in the cross-section are considered as one of the possible solutions. This work presents an extensive finite element study dealing with different ways to improve shell stability, which become the limiting criteria if a friction connection substitutes the common flange connection between two tower segments. The use of circular and polygonal cross-sections is briefly described and will be investigated in an experimental programme.

INTRODUCTION

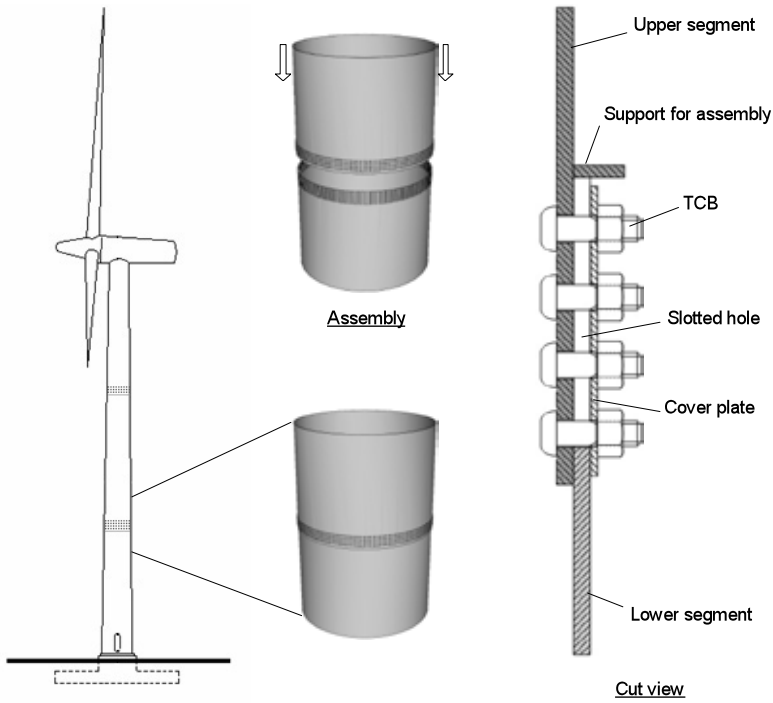
Wind is one of the most important sources of renewable energy. One of its main advantages is very low CO₂-emission while it generates power (Burton et al. 2001) within a very short payback time. Wind power stations convert kinetic energy from wind into electrical energy. During the last years, wind energy had an increase of about 25%. The installed capacity for wind power all over the world increased from 6 GW in 1996 up to 121 GW in 2008, of which about 60% are produced in OECD-Europe. In September 2012 the installed wind power capacity in the European Union hit the milestone of 100 GW, which equals the output of 39 nuclear power plants (EWEA 2012a). This continuing trend requires growing production.

The European Wind Initiative (EWI) aims for making wind energy produced onshore the most competitive energy source by 2020. Until 2030 offshore wind energy shall follow (EWEA 2012b, 2013a, 2013b, Fichaux et al. 2011). To improve the wind energy industry's competitiveness, technologies for turbines and components, grid integration and management methods will be focused on. In addition, the design and layout of wind farms as well as the manufacturing process and structural concept is receiving attention as the trend of building higher towers is continuing. Therefore, the project "High-strength tower in steel for wind turbines (HISTWIN)" and the dissemination of knowledge gained in it fills an important gap in promoting the design of wind towers, which has been seen as the exclusive work of highly specialized offices. The competitiveness of steel tubular towers as support for wind turbines improves by using an innovative solution for the assembling joint: a friction connection with long open slotted holes (Veljkovic et al. 2012). Thereby, one of the most common design criteria of the traditional towers, the fatigue resistance of the flange connection, is overcome and the design of the shell stability becomes an interesting issue. This opens the possibility to use higher strength steel grades if the tower shell is properly designed.

Other advantages of this type of connection are

- Simpler design,
- Reduction of construction time accompanied by a decrease of costs for construction,
- Lower production and maintenance costs,
- Improvement of work conditions, as the bolts can be installed and maintained always from inside the tower.

Hence, steel tubular towers with friction connections hold the potential to outclass traditional flange connection towers, which has been proven clearly within the scope of the HISTWIN project (Veljkovic et al. 2012). To connect the tubular segments of steel towers in a flangeless way is one of the main objectives of this project. The substitution of the expensive and fatigue-susceptible flange connections with friction connections with long open slotted holes is illustrated in Figure 1. The specimen shown represents one of the 1:2 scale prototypes developed within the framework of the projects.



a) Main concept of the friction connection



b) Feasibility test

Figure 1. The HISTWIN connection, friction connection for "the flangeless wind tower".

In this type of connection, the two tower segments easily slide over each other. Long open slots are cut into the lower segment, whereas the upper one contains normal clearance holes, in which the bolts can be preinstalled and will be used for angular alignment during positioning of the upper tower segment. Due to long open slots the lower tower part is quite flexible and therefore less sensitive to assembling tolerances. During the tightening process of the bolts, these flexible “fingers” will move towards the stiffer outer tower segment.

Instead of single washers, cover plates per bolt column are used. They hold the bolts in position during assembly and distribute the bolt force uniformly afterwards. The overlapping part of the connection also improves the shell bending stiffness.

The resistance of a friction connection mainly depends on the slip behaviour of the joint, which is directly related to the clamping force of the engaged bolts as well as the surface conditions of the clamped plates. The performance of various bolt types has been tested. To predict the behaviour of the connection, long- and short-term tests were performed. From these tests, a function for the loss of pretension in the bolts could be established and the correction factor k_s , which considers the hole geometry, and the correction factor μ taking into account the slip could be obtained and improved.

Additional tests compared the behaviour of the common flange connection to the one of the new type of friction connection and show that the bolts keep their forces more constantly in the friction connection. The friction connection behaves completely elastically until it reaches its ultimate resistance, which is higher than that of the common flange connection, and fails in a ductile way.

From the fatigue tests, it was found that the ultimate fatigue resistance for friction connections according to EN 1993-1-9 is very conservative (Eurocode3, 1-9). In reality it was found to be more than twice as high as the fatigue resistance for the common flange connection.

DESIGN OF FRICTION CONNECTIONS

High strength friction grip connections, or simply friction connections, work by clamping together the plates of the joint with the help of high strength friction grip bolts. These bolts are usually of grade 10.9 or even higher. Load applied on the plates is lead across the connection by friction. For design of a friction connection the general rules of, for example, Eurocode 3 part 1-8 can be followed (Eurocode3, 1-8):

$$F_{s,Rd} = \frac{k_s \cdot n \cdot \mu}{\gamma_{M3}} \cdot F_{p,C} \quad (1)$$

Where $F_{s,Rd}$ is the static design resistance of the joint,
 k_s is the coefficient depending on the type of hole,
 n is the number of friction surfaces,
 m is the slip factor,
 γ_{M3} is the partial coefficient, usually 1.25,
 $F_{p,C}$ is the pretension force for the sum of all bolts in the joint.

The slip resistance of the connection can be regarded as ultimate limit state. Of course, fatigue of the connection has to be checked as well. The friction connection in steel tubular towers can be regarded as detail category 90 (Veljkovic et al. 2012; Eurocode3, 1–9).

The design for a friction connection can be carried out segment wise, so that it is not necessary to take the complete cross-section of the tubular tower into account but only a segment, which corresponds to the distance between two rows of bolts. It is important that although the lap joint becomes unsymmetrical by this simplification, it can still be regarded as constraint in three dimensions by the complete tower cross-section. Obviously, the serviceability limit state needs also to be checked, but it is not regarded as critical for the design of a tubular tower.

ONGOING RESEARCH: HISTWIN 2

The substitution of the common flange connection by the use of friction connections with long open slotted holes changes the design driving criteria of the tower. The fatigue resistance of the flanges is no longer the main constraint. Instead, the stability of the steel tube limits the resistance and thereby the height of the structure. Also, transportation to the construction site raises questions, as it defines the maximum diameter of the tower. Since on-site welding is not an option, the tubes have to be transported to the construction place as one piece of full cross section. To overcome this problem, a modularized tower is suggested, in which the parts of the tubular cross section are bolted to each other. Herein, friction connections will join the tower segments even in vertical direction, see Figure 2. Ongoing research is aimed at studying the behavior of circular and polygonal cross sections.

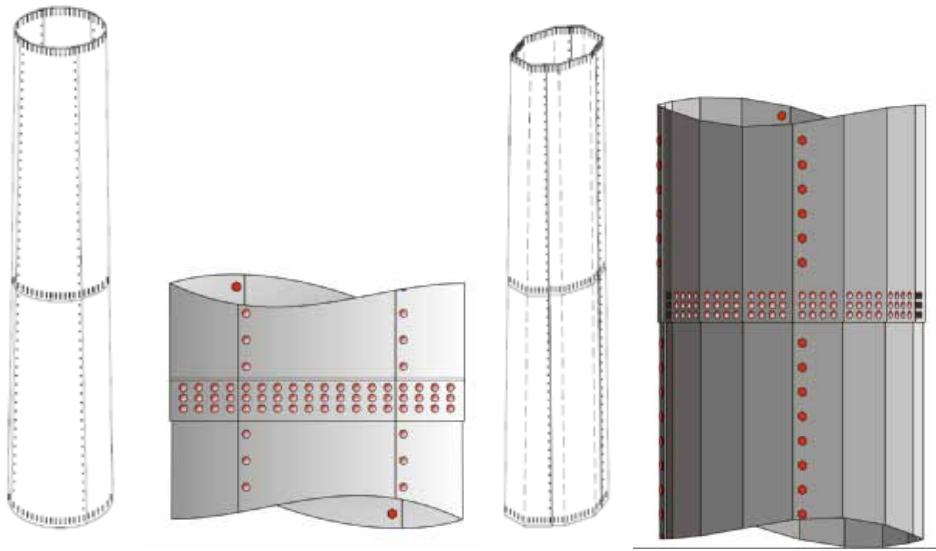


Figure 2. Circular vs. polygonal tubular cross section of the steel modular tower, two segments of modularized tower are shown.

As the door opening forms a hole in the tower structure, this represents one of the weakest parts of the construction. Therefore, the shell around the hole has to be stiffened to transfer the applied load. There are two alternatives, which have been considered in a finite element analysis at LTU: a) to increase the thickness of the shell structure surrounding the door opening or b) to implement a stiffener.

FINITE ELEMENT STUDY

An extensive finite element study was carried out in order to investigate the influence of a door opening in the lowest tower segment (Tran et al. 2013). A height of the lowest tower segment of 6.7 m, a diameter of 4.15 m at the bottom and 3.919 m at the top and a wall thickness of 37 mm were considered. A parametric study showed that for a door opening of 750 mm a stiffener with a 37 mm thickness would be sufficient to obtain the same resistance as in a tower segment without opening. Raising the steel grade from the common S355 to S500 or even S650 reduces the thickness of the stiffener by 22% and 38%, respectively. Figure 3 shows that the different steel grades reach the same moment resistance. But the reduced thickness has to be taken into account. The study also showed that the position of the door opening within the cross-section does not affect the ultimate strength of the tower significantly.

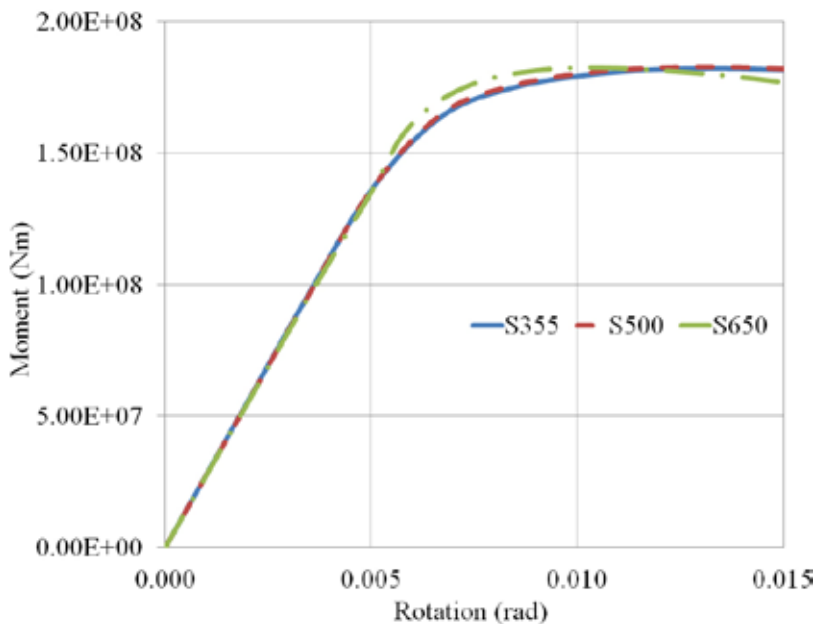


Figure 3. Comparison of various steel grades to stiffen the door opening.

EXPERIMENTS

Experiments are planned to be performed at LTU in order to investigate the effects of using high strength steel, cold forming bend in manufacture and opening. Coupon tests will be carried out and considered as input data of numerical models. Coupon specimens will be cut off from original plate specimens. The positions of coupon specimens will reflect effects of cold formed corner on the strength of material. Figure 4 shows positions of coupon specimens in circular and polygonal plate specimens.



Figure 4. Positions of coupon specimens.

Figure 5 shows a coupon test being performed at LTU. A 100 kN Dartec machine is used for these tests. Displacement of the coupon specimens is measured by an Epsilon Extensometer with a 25 mm of gage length and travel in tension and in compression of 12.5 mm and 6.25 mm, respectively.



Figure 5. Set up of coupon tests.

36 L-specimens with different angles and different thicknesses will be tested in order to investigate the effects of different angles in corners of the polygonal tower. Figure 6 shows L-specimens with angles: 90° , 100° , 120° , 140° , 160° and 170° . 4 mm and 6 mm plate thicknesses are considered. The length of L specimens is 600 mm.

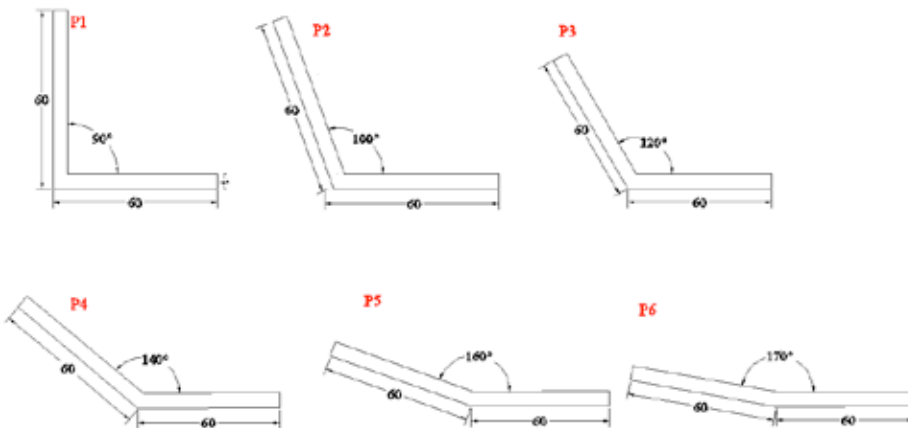


Figure 6. L-specimens with different angles.

In addition, there are 32 specimens with opening and without opening made of different steel grades, see Table 1.

Two types of cross sections are polygonal and circular. Figure 7 shows plate specimens with opening and without opening.

Figure 8 shows a compression test with a circular downscale specimen without opening. The experiments are performed using an Instron system with a maximum load of 4500 kN.

Table 1. List of plate specimens.

Name of specimens	Material	Length (mm)	Thickness (mm)	Number of specimens
Test-1	650MC	1000	6	4
Test-2	650MC	1000	6	4
Test-3	650MC	1000	6	4
Test-4	650MC	1000	6	4
Test-5	650MC	1000	4	4
Test-6	650MC	1000	4	4
Test-7	650MC	1000	4	4
Test-8	650MC	1000	4	4



Figure 7. Plate specimens with opening and without opening.



Figure 8. Compression test of plate specimen.

The failure modes obtained in the experiment and by FEA are rather similar as it is shown in Figure 9. It should be emphasized that material used in numerical simulation is S650. The properties of this material are defined in Tran et al. (2013).

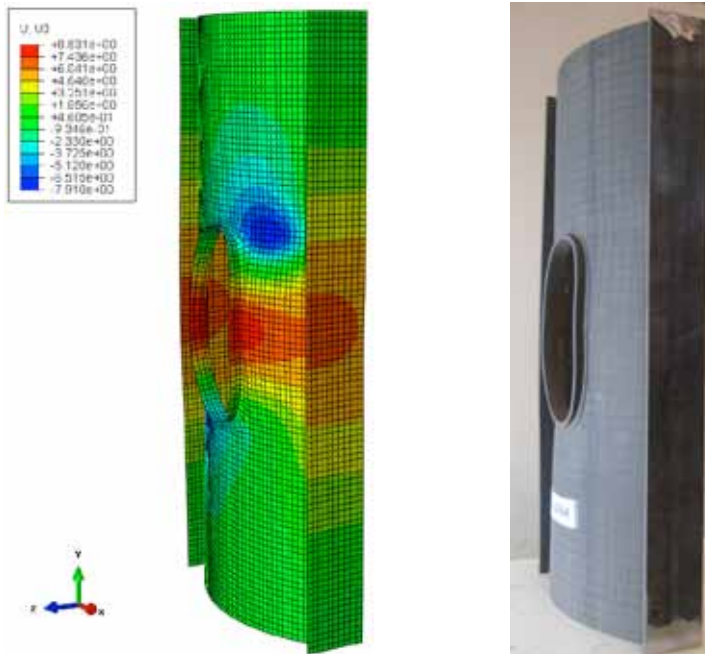


Figure 9. Deformation of opening circular plate specimen with 6 mm thickness.

Preliminary results for the ultimate loads are presented in Table 2. Differences between results range from 1.1% to 7.6%.

Table 2. Preliminary initial results of ultimate load.

	Ultimate load (kN)		
	According to EC3	According to experiment	Difference %
Test-Cir-1	3292	3255	1.1
Test-Cir-D-1	2672	2484	7.6
Test-Pol-1	3177	3258	2.5
Test-Pol-D-1	2567	2444	5.0

CONCLUSIONS

From the findings described above, the following can be concluded when using friction connections in tubular steel wind towers:

1. Fatigue endurance of the towers with the friction connections increases.
2. Shell stability may often be the main design criterion.
3. The use of higher steel grades than the common S355 may be justified from the structural point of view.
4. The use of higher steel grades for the segment with the door opening leads to less material.

ACKNOWLEDGEMENTS

The authors gratefully acknowledge the financial support by the European Research Fund of Coal and Steel, Grant-Agreement No. RFSR-CT-2010-00031, and the Centrum for High-performance Steel (CHS) at Luleå University of Technology, Sweden.

REFERENCES

- (Burton et al. 2001) Burton T, Sharpe D, Jenkins N and Bossanyi E: *Wind energy handbook*, Chichester: Wiley, 2001.
- (Eurocode3, 1-6) EN-1993-1-6 *Design of Steel Structures*, Part 1–6: *Strength and stability of shell structures*, Brussels, Belgium, European Committee for Standardization, 2007.

(Eurocode3, 1–8) EN-1993-1-8 Design of Steel Structures, Part 1–8: *Design of joints*, Brussels, Belgium, European Committee for Standardization, 2005.

(Eurocode3, 1–9) EN-1993-1-9 *Design of Steel Structures*, Part 1–9: Fatigue strength, Brussels, Belgium, European Committee for Standardization, 2004.

(EWEA 2012a) EWEA: *United in tough times – The European Wind Energy Association*, Annual report 2012.

(EWEA 2012b) EWEA: *Green Growth – The impact of wind energy on jobs and the economy*, April 2012.

(EWEA 2013a) EWEA: *The European Wind Initiative – Wind Power Research and Development to 2020*, 2013.

(EWEA 2013b) EWEA: *Wind in power – 2012 European statistics*, February 2013.

(Fichaux 2011) Fichaux N, Beurskens J, Hjuler P, Wilkes J, Frandsen S, Dalsgaard Sørensen J, Eecen P, Malamatenios C, Arteaga Gomez J, Hemmelmann J, van Kuik G, Bulder B, Rasmussen F, Janssen B, Fischer T, Vossanyi E, Courtney M, Giebhardt J, Barthelmie R, Holmstrøm O: *UpWind – Design limits and solutions for very large wind turbines*, EWEA, March 2011.

(Germ.Lloyd 2004) Germanischer Lloyd Wind Energy: *Guideline for the certification of wind turbines*, Edition 2003 with supplement 2004.

(RFCS 2013) Success Stories of the Research Fund for Coal & Steel, http://cordis.europa.eu/coal-steel-rtd/stories_en.html, last updated 2013-01-22.

(Tran et al. 2013) Tran A T, Veljkovic M, Rebelo C, da Silva L: *Resistance of door openings in towers for wind turbines*, 3rd South-East European Conference on Computational Mechanics, Kos Island, Greece, 12–14 June 2013.

(Veljkovic et al. 2012) Veljkovic M, Heistermann C, Husson W, Limam M, Feldmann M, Naumes J, Pak D, Faber T, Klose M, Fruhner K.-U, Krutschinna L, Baniotopoulos C, Lavasas I, Pontes A, Ribeiro E, Hadden M, Sousa R, da Silva L, Rebelo C, Simoes R, Henriques J, Matos R, Nuutinen J, Kinnunen H: *High-strength tower in steel for wind turbines (HISTWIN)*, final report, RFCS-CT-2006-00031, 2012.



Leverage from
the EU
2007-2013



This book covers the papers presented in the annual Metnet Seminar in October 2013 held at Luleå University of Technology. The seminar continued the METNET tradition of presenting scientific and development papers of high calibre.

METNET seminars deal with technical aspects of metal construction as well as issues of concern to industry on management, planning and sustainability of projects.

Metnet cooperation promotes regional innovation environments and strengthens knowledge structures, especially in the European regions represented by its members. At the annual seminars, the participating partner organization represents its regional innovation environment but simultaneously is a partner of a larger and stronger international innovation world created by active cooperation between the institutes and enterprises.

PRINTED

ISBN 978-951-784-641-7
ISSN 1795-4231
HAMKin julkaisu 1/2014

ELECTRONIC

ISBN 978-951-784-642-4 (PDF)
ISSN 1795-424X
HAMKin e-julkaisu 1/2014

HAMK
UNIVERSITY OF APPLIED SCIENCES